FABRICATION AND CHARACTERIZATION OF LOW CRYSTALLINE CURCUMIN LOADED LIPID NANOPARTICLES

By

YUECHAO DU

A Thesis submitted to the

Graduate School-New Brunswick

Rutgers, The State University of New Jersey

in partial fulfillment of the requirements

for the degree of

Master of Science

Graduate Program in Food Science

written under the direction of

Professor Paul Takhistov

and approved by

_____

_____

_____

_____

New Brunswick, New Jersey

May, 2011

ABSTRACT OF THE THESIS

FABRICATION AND CHARACTERIZATION OF LOW CRYSTALLINE CURCUMIN LOADED LIPID NANOPARTICLES

By YUECHAO DU

Thesis Director:

Professor Paul Takhistov

Preventable chronic diseases such as cardiovascular disease, cancer account for nearly 70% of the death in the States annually. Research attributes these diseases to oxidation stress induced by free radicals. Recently, it is shown that risk of chronic diseases can be minimized by increasing intake of antioxidant. The increasing public health awareness has lead to intense need for functional food enriched with powerful antioxidants. Recent research reveals that polyphenolic compounds such as quecertin,curcumin possess great anti-oxidation and anti-cancer potential. However, enriching food with these antioxidants has been limited, because these compounds usually have poor solubility and chemically unstable.

Solid lipid nanoparticles offer promising approach to deliver these hydrophobic compounds. However, it has been noted that solid lipid nanoparticles have limited loading capacity due to high crystallinity of lipid crystals. In addition, fast polymorphic transition of lipid leads to aggregation and burst release of encapsulated compound. To overcome these limitations, Nanostructured lipid carriers composed of solid lipids and liquid lipids are developed. Until recently, little research has been done on SLN and NLC for food application.

In this research, food grade materials are used to fabricate SLN and NLC via ultrasonication. Curcumin, a polyphenolic antioxidant is chosen to be model compound to be encapsulated. The surface morphology of SLN and NLC are studied by dynamic light scattering and transmission electron microscope. Structure and molecular interaction of lipid nanoparticles are explored by Raman spectroscope. Differential scanning calorimetry and X-ray diffraction technique are applied to provide more insight information about crystallinity and the effect of different components on polymorphic transition of lipid nanoparticles. Research results show curcumin is encapsulated in spherical lipid nanoparticles. The encapsulation greatly improves the chemical stability of curcumin under extreme alkaline condition. Curcumin loaded SLN shows structure of curcumin enriched core with lipid shell. The average size of SLN is between 200-500nm. However, aggregation takes place shortly during storage. NLC has lower crystallinity than SLN. Lipid polymorphic transition in NLC is retarded by the addition of methyl stearate, oleic acid. In addition, smaller particles are formed in methyl stearate NLC and oleic acid NLC.

ACKNOWLEDGEMENTS

I would like to offer my sincere appreciation to my advisor, Dr. Paul Takhistov, for his intellectual support and acute scientific insight that guides me throughout graduate study.

I appreciate Dr. Kit L.Yam for being a wonderful graduate director,

I am grateful to Dr. Henryk Daun for his broad knowledge and informative insights.

I thank Dr. Lee Simon and Dr. Thomas J. Emge for their help in TEM and XRD study.

I thank my friend Yangyang Jin for her kindness and support during my study. My labmates: Phong, Abhishek, Marlena and Natalia for their help in general and wish them best of luck in their pursuing.

I thank graduate school of Rutgers University for handling my thesis.

I am privileged to have studied and worked in this distinguished food science department.

I greatly appreciate to my parents and grandmother who make support my study in the States unconditionally.

Last but not least important, I appreciate anyone who have been kind and helpful to me during my graduate study.

TABLE OF CONTENTS

ABSTRACT OF THE THESIS ii

ACKNOWLEDGEMENTS iv

TABLE OF CONTENTS v

LIST OF TABLES ix

LIST OF ILLUSTRATIONS x

Chapter 1 Introduction 1

Chapter 2 Literature review 5

Solid lipid nanoparticles 5

Loading capacity of lipophilic compounds 6

Improve stability of liable compound 8

Release of encapsulated compounds 8

Enhancement in bioavailability of poorly absorbed compounds 12

Production of solid lipid nanoaparticles 13

Structure of Solid lipid nanoparticles 16

Physical stability of Solid lipid nanoparticles 17

Challenges of solid lipid nanoparticles 19

Low drug loading capacity 19

Burst release of encapsulated compounds 20

Poor stability at high concentration 20

Lipid nanostructured carriers 20

Structure of lipid nanostructured carriers: reduce in crystallinity and slower polymorphic transition 21

Improved loading capacity 22
Improved long term stability at high concentration 23
Perspective and challenges for food application 24
Conclusion 28
Hypotheses and objectives of the research projects 28
Chapter 3 Method and Materials 30
Materials for SLN and NLC fabrication 30
Materials for SLN fabrication 30
Materials for NLC fabrication 31
Methods 33
Fabrication of monostearin solid lipid nanoparticles and nanostructured lipid carries 33
Characterization of lipid nanoparticles 34
X-ray diffraction (XRD) 34
Differential scanning calorimeter (DSC) 35
Dynamic light scattering (DLS) 36
Transmission electron microscopy (TEM) 37
Raman spectroscopy 37
Protective effect of lipid carrier in high pH environment 38
Chapter 4 Characterization of solid lipid nanoparticles and nanostructured lipid carriers 39
Introduction to curcumin loaded solid lipid nanoparticles 39
Characterization of solid lipid nanoparticles 40
Dynamic light scattering study 40

TEM study of monostearin SLN 41
Raman spectroscopy study 42
Confirm the encapsulation of curcumin in monostearin SLN 44
Exploring the structure of monostearin SLN 44
The protective effect of curcumin in alkaline condition 46
Differential scanning calorimetry study 48
Presence of multiple polymorphic form and depression of melting point 49
Crystallinity of monostearin SLN 50
X-ray diffraction study 51
Effect of cooling rate on monostearin crystallization 51
Polymorphic change of monostearin SLN during solidification 53
Low crystallinity of curcumin 55
Discussion 55
Surface enhancement of Raman signal 55
Prediction of polymorphic by Raman spectroscopy 58
Curcumin encapsulation and structural organization of fabricated SLN 62
Conclusion 64
Introduction to curcumin loaded nanostructured lipid carriers 65
Characterization of nanostructured lipid carriers 65
Dynamic light scattering study 65
TEM study of NLC 75
Raman spectroscopy study 77
Encapsulation of curcumin in lipid nanoparticle 77

Chain mobility: 3000 cm^{-1} to 2800 cm^{-1} 81
Molecule arrangement: 1500 cm^{-1} to 1300 cm^{-1} 83
Alkyl chain conformation: 1300 cm^{-1}-1000 cm^{-1} 89
Differential scanning calorimetry study 91
Effect of curcumin 93
Effect of methyl stearate 96
Effect of oleic acid 97
Effect of poly ethylene glycol stearate 98
X-ray diffraction study 98
Effect of average cooling rate 99
Effect of methyl stearate 100
Effect of oleic acid 101
Effect of poly ethylene glycol stearate 102
Discussion 103
Effect methyl stearate on crystallization of monostearin (bulk phase) 104
Effect of curcumin 106
Effect of methyl stearate 107
Effect of oleic acid 109
Effect of polyethylene glycol 111
Conclusion 111
References 113

LIST OF TABLES

Table 1 Bioactive compounds and related health effect. Adapt from..... 25

Table 2 Formulations for SLN and NLC 32

Table 3 Raman assignment to molecular vibration..... 42

Table 4 DSC results 51

Table 5 XRD finger print of different types of crystals..... 52

Table 6 Hydrodynamic diameters of different NLC..... 66

Table 7 Raman assignment to molecular vibration..... 80

Table 8 I(2880 cm^{-1})/I(2340 cm^{-1}) The ratio is an indicator of chain mobility. Higher value indicates the lower chain mobility 82

LIST OF ILLUSTRATIONS

Figure 1 Schematic graph of SLN and NLC at high concentration. 24

Figure 2 Different digestion time lengths for solid and liquid lipid 27

Figure 3 Size distribution of control SLN and curcumin loaded SLN 40

Figure 4 TEM photos of curcumin loaded solid nanoparticles 42

Figure 5 Spectra of bulk phase materials 42

Figure 6 Macro-models used to investigate effect of the lipid outer layer on the subsurface Raman signal 44

Figure 7 Spectra of curcumin/monostearin mixture and curcumin loaded SLN 45

Figure 8 Comparison between curcumin loaded SLN and sandwich structure model 46

Figure 9 Degradation of curcumin 47

Figure 10 Spectra of curcumin loaded SLN and bulk phase curcumin dispersed in 0.01 mol/L NaOH solution for 5hours 48

Figure 11 Thermograms of control SLN and curcumin loaded SLN (endothermic up). 50

Figure 12 Diffractograms of re-cyrstallized bulk phase monostearin and bulk phase monostearin before re-crystallization 53

Figure 13 Diffractograms of control SLN, curcumin loaded SLN and re-crystallized bulk phase monostearin 54

Figure 14 Diffractograms of bulk phase curcumin and curcumin loaded SLN 55

Figure 15 Raman spectra of SLN dispersion on glass substrate 56

Figure 16 Raman spectra of SLN precipitate on glass substrate 57

Figure 17 Raman spectra of SLN dispersion on aluminum substrate 57

Figure 18 CH_2 scissoring vibration of α form (re-crystallized monostearin) and β (bulk phase monostearin) 59

Figure 19 C=O stretching of α form (re-crystallized monostearin) and β form (bulk phase monostearin) 60

Figure 20 CH_2 scissoring vibration of curcumin loaded SLN and control SLN. 61

Figure 21 C=O stretching of curcumin loaded SLN and control SLN 61

Figure 22. Proposed mechanism of SLN formation and encapsulation of curcumin 64

Figure 23 Effect of methyl stearate on size distribution in aqueous environment..... 67

Figure 24 Effect of oleic acid on size distribution. 68

Figure 25 Effect of poly ethylene glycol (PEG) on size distribution 69

Figure 26 Size distributions of curcumin loaded NLC with differnt proportion of methyl stearate. 71

Figure 27 Size distribution of curcumin loaded NLC with different proportion of oleic acid. 73

Figure 28 Size distribution of curcumin loaded NLC with different proportion of PEG. 74

Figure 29 TEM photo of curcumin loaded NLC composed of 60% methyl stearate 75

Figure 30 TEM photo of curcumin loaded NLC composed of 20% oleic acid 76

Figure 31 TEM photo of curcumin loaded NLC composed of 10% PEG 77

Figure 32 Typical spectra of curcumin in NLC. Curcumin specific peaks at 1184 cm^{-1},1250 cm^{-1},1601 cm^{-1} and 1627 cm^{-1} 78

Figure 33 Spectra of bulk phase materials. 80

Figure 34 Scissoring vibration of monostearin and methyl stearate 84

Figure 35 Shift of peak at 1440cm^{-1} 1440 cm^{-1} with increasing proportion of methyl stearate 85
Figure 36 Change of peak shape in NLC with oleic acid 86
Figure 37 Change in Carbonyl stretching peak. The bulk phase material of monostearin and methyl stearate gave rise to peaks at 1731 cm^{-1} and 1740 cm^{-1} respectively. 89
Figure 38 Change of overall spectra with increasing amount of oleic acid..... 91
Figure 39 Thermograms of curcumin loaded NLC and control NLC 94
Figure 40 Thermograms of curcumin loaded NLC with different proportion of methyl stearate 95
Figure 41 Thermograms of curcumin loaded NLC with different proportion of oleic acid. 97
Figure 42 Thermograms of curcumin loaded NLC with different proportion of PEG. 98
Figure 43 Diffractogram of re-crystallized methyl stearate..... 100
Figure 44 Diffractogram of curcumin loaded NLC composed of 60% methyl stearate. 101
Figure 45 Diffractogram of curcumin loaded NLC composed of 20% oleic acid..... 102
Figure 46 Diffractogram of re-crystallized PEG 103
Figure 47 Diffractogram of curcumin loaded NLC composed of 10% PEG..... 103
Figure 48 Chemical formulas of methyl stearate and monostearin 104
Figure 49 Effect of methyl stearate on the melting behavior of monostearin. 104
Figure 50 Effect of methyl stearate on the crystallization behavior of monostearin. 105
Figure 51 Schematic graph of metyl stearate weakens the interaction between monostearin molecules 109

Figure 52 Schematic graph of oleic acid blocks the interaction between monostearin molecules 110

Chapter 1 Introduction

Functional food and beverage refers to food and beverage with added ingredient to provide extra health benefits beyond its basic nutrition value. The market for functional beverage along in the U.S is estimated to be 9.6 billion dollars. The sales figure is expected to growing to 97 billion in 5 years. Although the sales for many functional beverages such as functional juice and enhanced water (6.9% decrease in 2009) reduced in 2009 due to economic recession, many segments of function beverage has kept growing. AriZona, for example, has kept growing by developing new tea products(ANON. 2010).

Despite of the promising market in functional beverages, developing of functional beverages are facing increased challenges. Numeral reports and surveys have found that most consumers are skeptical about the claim that functional beverage could provide sufficient amount of nutrient to bring any health beneficial effect. At least for now, few products have been subjected to clinical study. With FDA becoming more active in evaluating claim for functional drinks, it is expected that future development of functional beverage will be more challenging.

Market research shows that increasing awareness of health diet has been one of the market drivers for the growth functional beverage. Majority of consumers choose functional beverages enriched with antioxidants, vitamins for boosting immunity digestion. As for functional food, the major ingredients that consumers are looking for are antioxidants, calcium and unsaturated fatty acid.

The investigation by Centers for Disease Control and Prevention shows that chronic diseases – such as heart disease, stroke, cancer, diabetes are the most costly yet preventable health problem. It was found that these chronic diseases are the leading causes of death in the States. They are responsible for 70% of the death in the United States each year. Among chronic diseases, cardiovascular disease, cancer account for 50% of all death(ANON.)

Research reviews (Steinmetz and Potter 1996; Kris-Etherton, Hecker et al. 2002; Willcox, Ash et al. 2004) of results of numeral epidemiological studies on the relationship between the consumption of plant products to chronic diseases have shown the risk of chronic diseases, such as cardiovascular diseases and cancers, are inversely associated with consumption of vegetables and fruits. Some researchers attribute chronic diseases to oxidative damage to cells (Willcox, Ash et al. 2004; Valko, Rhodes et al. 2006). The effect of antioxidants such as phenolic compounds, vitamins on the risk of chronic diseases has been studied and reviewed (Hertog, Feskens et al. 1993; Kushi, Folsom et al. 1996; Steinmetz and Potter 1996). Result shows risk of cardiovascular diseases is inversely related to the intake of different antioxidants such as vimtamin E and flavonoid.

It has been found that polyphenolic compound such as flavonoids are abundant in plant products such as apple, orange etc. They are the metabolic product of plants. Flavoniods can be further divided into 7 categories according to their structural difference (Chi-Tang Ho). Earlier research has shown that these phenolic substances are metal chelators and possess remarkable ability of scavenging free radicals. In the review by (Paul Knekt, Jorma Kumpulainen et al. 2002) an inverse relationship between flavonoids intake and diabetes. In addition to diabetes, flavonoids also play important role in lowing risk of cancer. More

recently, Different studies have shown that polyphenolic compounds other than flavonoids such as EGCG, curcumin, quercetin are even more potent in anti-inflammation and anticancer. A considerable amount of reports have been published on the remarkable ability of suppressing growth of tumor, leading to apoptosis in cancer cells (Shimizu, Deguchi et al. 2005; Bengmark 2006; Hwang, Ha et al. 2007; Lee, Szczepanski et al. 2008).

Despite of the promising potential, enriching food with these polyphenolic compounds has been proved to be challenges. Polyphenolic compounds such as curcumin and quercetin, has poor water solubility. Phase separation will occur if added in large amount. Polyphenolic compounds can react with other compounds in beverage and form undesirable haze(Siebert, Carrasco et al. 1996) , What is more, Polyphenolic compounds such as EGCG has poor stability(Ishii, Mori et al.) under ambient environment conditions such light and oxygen. What is worse, health beneficial effect is greatly limited by the low bioavailability. Polyphenolic compounds are poorly absorbed through GI tract due to their hydrophobic nature, even after absorbed, they are usually chemically modified which leads to fast excretion, hardly any free form of polyphenol can be found in plasma(Scalbert, Morand et al. 2002).

Different delivery systems aimed at improving the stability and bioavailability of these antioxidants for pharmaceutical and food application have been developed: polymeric nanoparticles, liposomes and emulsions. However, for food application, food grade materials are required. This limits the choices of materials for carriers.

In early 90s, solid lipid nanoparticles were developed. Within short time, it generated broad attention. First, Many lipids are derived from animal and therefore have very good

biocompatibility. Second, solid lipid nanoparticles not only possess the advantage of nanoemulsion, but also being able to improve the physical stability of encapsulated drug against degradation. Third, solid lipid nanoparticles can be produced using commercially available method. Nanostructured lipid carriers were developed after solid lipid nanoparticles. It is reported that NLC has out performance of SLN in many aspects drug loading capacity, physical stability etc.

The research on solid lipid nanoparticles and nanostructured lipid carriers for food application is still in initial stages. Several research reviews have listed lipid nanoparticles as potential delivery system for future functional beverage and food (McClements and Li ; Weiss, Takhistov et al. 2006).

Chapter 2 Literature review

Solid lipid nanoparticles

Solid lipid nanoparticles is a colloidal deliver system made from solid (under room temperature)lipid, (Wissing, Kayser et al. 2004). Diameter of solid lipid nanoparticles by photo correlation spectroscopy is between 50 and 100nm. SLN can, unlike polymeric nanoparticles, can be produced by conveniently by different methods, such as high pressure homogenization. The obtained solid lipid nanoparticles can be stabilized by surfactant such as lecithin, Tween 80, Pluronic 68 or the combination of different surfactant (Muller, Maer et al. 2000; Muller, Radtke et al. 2002; Pardeike, Hommoss et al. 2009). .

Solid lipid nanoparticles are invented in early 90s. It is the latest development of lipid based colloidal delivery system after nanoemulsion, liposome. Nanoemulsions are made from lipids that are liquid under room temperature. It quickly generated broad public attention and within few years. The first safe emulsion for parental nutrition delivery was invented by Wretlind, which marks the beginning of emulsion as colloidal delivery for lipophilic drugs. After years of research some of them are successively commercialized, Diprivan(1980). Research review reported that applying oil in water emulsions were able to reduce injection dosage and thereby minimize side effect. O/W emulsion was designed and applied for drug delivery. Products such as Diazemuls and Diazepam-Lipuro were developed and put into market (Muller, Maer et al. 2000). Despite of the advantages, major limitations of these emulsions are also obvious: poor physical stability of drug containing

emulsion. Encapsulation of drugs is able to cause agglomeration, drug expulsion and poor ability to offer protection to liable compounds.

Another lipid based carrier developed earlier is liposome, which normally composed of phospholipid. It is invented as early as 1965 with focus on cosmetic market (Muller, Maer et al. 2000). After one decade of research, several products such as lung surfactant for pulmonary instillation were put into market. However, the total number of successful product is rather limited when compared to emulsion. Major obstacle is lack of commercially available production method. In another word, liposome product is only feasible in lab scale.

For polymeric nanoparticles, it has been under intensive research for 50 years. However, this delivery system is well commercialized like lipid based delivery system. Similar to the problem encountered by liposome, polymeric particles is difficult to be produced in large quantity. What is worse, it has been reported that polymeric particle has poor tolerability. It is believe that polymeric lipid nanoparticles are able to penetrate through cell membrane and leads to cytotoxic effect when degrades inside cell (Muller, Maer et al. 2000).

Loading capacity of lipophilic compounds

In pharmaceutical industry where solid lipid nanoparticles first developed, Drug loaded SLN has been developed and its surface property can also be modified to fit delivery route and achieve intelligent targeting.

Recent research has found the loading capacity and entrapment efficiency of solid lipid nanoparticles to be promising. The loading capacity is defined as the ratio between drug and lipid phase. The entrapment efficiency is defined as the ratio between encapsulated

drug and total drug added into the system. In research by (Nayak, Tiyaboonchai et al.), curcuminoids-loaded SLN for parenteral administration was fabricated via hot emulsification method. The result showed the entrapment efficiency and drug loading capacity to be in the range of 80–94% and 1.62–3.27% respectively. In another experiment done by(Ying, Cui et al.), doxorubicin-loaded SLN modified with chitosan oligosaccharide showed a high drug loading (about 20%) . SLN loaded with doxorubicin were prepared by solvent emulsification-diffusion method The entrapment efficiency and drug loading capacity were 67.5 % and 2.0%(Subedi, Kang et al. 2009), For ubidecarenone, the maximum loading capacities of up to 50% are reported. For tetracaine andetomidate capacities of 10–20% are reported. In some cases the solid lipid nanoparticles have great advantage over tradition emulsion and offers promising alternative for drug delivery. One of successful example is paclitaxel delivery. Paclitaxel is a powerful anti-cancer drug. However, clinic application has been limited due to its low solubility in water and many solvents that have been proved for parenteral administration. The only available carrier composed of Cremphor EL and dehydrated alcohol. This delivery system has been proved to be problematic: 1. Carriers have short shelf life, 2. Components of carriers cause hypersensitivity reactions. Encapsulation using oil in water emulsion using soybean oil showed a poor result for paclitaxel is not compatible with oil (0.3mg/ml). (Lee, Lim et al. 2007) tries solid lipid nanoparticles, the result showed that paclitaxel can be incorporated to 7w/w% in solid lipid. Depending on the lipids and surfactant, the loading capacity can vary greatly. (Xie, Zhu et al.) fabricated Enrofloxacin-loaded SLN with different lipids and surfactant. The results of encapsulation efficiency and drug loading capacity varied with lipids, to be detail, in the order of stearic

acid > palmitic acid > tetradecanoic acid. It should be mentioned that loading capacity of solid lipid nanoparticles are determined by multiple factors, it should be evaluated on case by case basis.

Improve stability of liable compound

Research about solid lipid nanoparticles showed improved stability of encapsulated compound against chemical degradation. In research by (Jee, Lim et al. 2006), all-*trans* retinol was encapsulated into SLN. The obtained SLN is irradiated with 60W bulb. The result showed improvement of stability. In addition, with small amount of antioxidant, the stability is further improved by 43% compared SLN without antioxidant. One of the reasons that contributed to the improvement in stability is due to solid matrix. The compound located in the solid core is isolated from outer environment. Unlike emulsion, the solid matrix significantly reduced mobility of encapsulated molecules and migration of chemical from outside environment. However, lipids and surfactants must be chosen carefully if chemical stability can be improved. In other words, lipids themselves must not react with materials, In Muller review, this information is emphasized. In retinol SLN research, acidic lipid failed displaying any protection effect. In addition to lipids, particle size also played a role in stabilizing retinon, research was conducted on SLN with same component but different sizes. SLN with smallest size was shown to have highest stabilization effect. Research attributed this size –stability effect to large interfacial area for retinol accommodation.

Release of encapsulated compounds

In addition to improve chemical stability of liable compound, the release rate of these compounds from SLN can be manipulating according to the need. Compared to emulsion, SLN has much more flexibility in modulating release pattern of encapsulated compound. As mentioned above, when encapsulated into solid core, encapsulated compound has much lower diffusion rate, therefore prolonged release can be achieved. On the other hand, fast polymorphic transition of SLN will lead to burst release. Different release patterns are useful to serve different needs: For particles that travel through circulation system, prolonged release is desired, (Subedi, Kang et al. 2009) Fabricated Doxorubicin solid lipid nanoparticles with mean diameter of 199nm using glyceryl caprate and dimethyl sulfoxide via solvent emulsification method. Prolonged release of doxorubicin was observed.In another research by (Xie, Zhu et al.),, Enrofloxacin-loaded solid lipid nanoparticles (SLN) were fabricated using tetradecanoic acid, palmitic acid, stearic acid respectively. Kinetic study within 24 h showed that three formulations were significantly different. tetradecanoic acid-SLN had the highest release rate where as stearic acid-SLN had the slowest. In addition to drug delivery, prolonged release is also desired for topical application. (Jenning, Schaer-Korting et al. 2000) Vitamin A loaded SLN was fabricated and release profile was studied. (Jenning, Schaer-Korting et al. 2000), the release kinetic of vitamin A was studied by Franz diffusion cells in a period of 24 hours. It was found that slow release in the first 6 hours and accelerated release faster than nanoemulsion after the first 6 hours. What is more, SLN can be conveniently incorporated into cream and exhibits controlled release pattern of vitamin A. For topic application, prolonged release is feasible for applying high efficient but highly irritating when used in high concentration. In research reviewed by Muller, solid lipid nanoparticles were fabricated to develop new sun

screen. The tradition sun screen involves the use of titanium dioxide particles as part of the sunscreen however, these particles in the range of nanometer are able to penetrate skin causing allergy. It was found that highly crystalline solid lipid nanoparticles were also able to block UV rays. What is more, it was also found that functional ingredient loaded SLN showed synergistic protection effect. When compared to emulsion, a 50 % decrease of release rate over 6 hours were reported. SLN technology has also been used in cosmetic industry. In the review by Muller, In terms of release time, perfume incorporated SLN when compared to nanoemulsion of same surfactant, showed an addition 8 hours longer release time.

Considerable amount of research effort have been spent on elucidating release mechanism of solid lipid nanoparticles. Recently X-ray and DSC study of different SLN have shown that polymorphic transition of lipids molecules is a critical factor affecting the release of pattern of lipid nanoparticles.

The polymorphic transition of lipid is defined as the ability to forming different cell structure in crystals due to different molecular conformations and packing patterns (Nissim Garti 2001). For lipid, there are three polymorphic forms: α, β' and β. A fourth type form sub-α is found for monoglyceride (Lutton and Jackson 1948). The major difference between these polymorphic forms is the molecular distance. For instance, α form (unstable) is characterized by hexagonal structure whose molecular distance is the largest whereas β form (most stable) is triclinic packing that the tightest packing pattern. The study of polymorphic transition has been a major focus, since it has profound impact on food, chemical industry. X-ray and DSC are the standardized methods for their high accuracy (Nissim Garti 2001). The polymorphic transition in solid lipid nanoparticles has

been explored in different research (Bunjes, Westesen et al. 1996) (Lukowski, Kasbohm et al. 2000), and has been claimed to be related to drug loading capacity and release pattern. When hot nanoemulsion is cooled down, oil droplet is forced to become solid. During this process, lipid molecule is able to re-arrange in different way according to the cooling gradient and presence of impurity. The crystallization occurs when nucleus exceeds critical size ($\frac{dG}{dr} = 0$). The critical size is

$$r_{critical} = \frac{2\gamma V}{\Delta u} \quad (1)$$

($\gamma = surface\ energy, V = volume\ of\ a\ molecule\ inside\ nucleus, \Delta u = chemical\ potential$) There two types of crystallization occurs: homogenous and heterogeneous. The critical crystal sizes are the same, However, the critical Gibbs energy is different, For heterogeneous nucleation:

$$\Delta G_{hetero} = \Delta G_{homo}\left[\frac{1}{2} - \frac{3}{4}\cos\alpha + \frac{1}{4}(\cos\alpha)^3\right] \quad (2)$$

α is the contact angle of two substance. It is easy to see that Gibbs energy for heterogeneous nucleation (ΔG_{hetero}) is usually lower than that of homogeneous

Nucleation (ΔG_{homo}). In term of nucleation rate, the presence of very small amount of

impurity usually increases the rate since it decreases the supersaturation requirement (Nissim Garti 2001). In lipid nanoparticles heterogeneous can be dominant. Therefore, fast surface nucleation can be expected.

The formation of different form is governed by their thermodynamic stability and external conditions detailed information can be found in (Nissim Garti 2001). It should be noted

that polymorphic form with the largest Gibbs energy is form first and depends on external conditions, transfer to more stable form. For some lipids, it is possible that two forms appeared at the same time is the crystallization process is melt-mediated transformation. As for external environment, fast cooling rate 5℃/min favors the formation of α, whereas slow cooling rate 0.1-1℃/min facilitates the formation of more stable form. In addition, the presence of impurity is detected to be able to induce fast polymorphic transition from α to β. This transition reduces the number of imperfect crystals that are critical to accommodate foreign molecules and therefore pushed out encapsulated compound. Depending on the transition rate, different release pattern can be expected. In another aspect, it is important to release that other factors, such as solubility of drug in lipid can also affected the release pattern(Bunjes, Westesen et al. 1996). In addition, polymorphic transition from α to β also leads to change in particle shape from sphere to needle like shape leading to accelerated particle growth. Numerals result has strengthened the relationship between polymorphic transition and the release of drug from solid lipid nanoparticles. Vitamin A loaded SLN exhibits slow release in first 6 hours and accelerated release from 12-24 hours (Jenning, Schaer-Korting et al. 2000). In further exploration it is found that a good correlation of polymorphic transition to accelerated release where β′ transformed to β. More example is can be found in the review of (Sagalowicz and Leser ; Bunjes and Unruh 2007)

Enhancement in bioavailability of poorly absorbed compounds

Bioavailability is the proportion of a compound that is available for utilization in metabolic process. Recent bioavailability researches on solid lipid nanoparticles showed very positive results. For example, quercetin, a kind of flavonoid, has been proved to possess

high nutrient and pharmacological, such as anti-cancer, anti-inflammation etc. However, due to the highly hydrophobic nature, quercetin has very low bioavailability. As reported by (Gugler, Leschik et al. 1975) the bioavailability of quecertin in men is around 1%. (Shaikh, Ankola et al. 2009) By applying solid lipid nanoparticle technology, a relative bioavailability of quecertin to its suspension is increased 5 folds. In another works about curcuminoinds for parental administration, curcumin SLN showed pharmacodynamic activity 2-fold increase in pharmacodynamic activity against malarial activity when compared to free curcuminoids (Nayak, Tiyaboonchai et al.). In pharmaceutics research, SLN is found to be able to enhance the efficiency of certain drugs by targeting specific organ/cells. For long circulating particles, poly ethyleneglycol and folate modified the particles were able to minimize depletion due to immune response and increases accumulation in tumor (Jain, Agarwal et al.) while reducing the accessibility to normal cell. Others found specific component helped to improve the delivery of specific drugs to tumor. It is found that the uptake of SLN is concentration depended. The cellular uptake of SLN is also closely related to the melting point of lipids, chain length and particles size (Yuan, Miao et al. 2008).

Production of solid lipid nanoaparticles

Solid lipid nanoparticles are composed of lipids which are solid under room temperature. Lipids such as tri, di, monoglyceride, mixture of middle chains fats, Other commercial grape lipids such as Compritol 888 and Preciol 5(Radomska-Soukharev 2007) are also used as fabrication materials. In addition to handful of choices of non-toxic lipids

excipients, surfactants that are able to stabilize SLN are also abundant due to recent development in surfactant science.

Recent reviews mentioned that multiple researches had reported low toxicity of solid lipid nanoparticles. In addition to low toxicity, when compared to liquid lipid, it is able to offer better protection of incorporated compounds and performing controlled release. With more research groups focusing on SLN established globally, Solid lipid nanoparticles are revealing its potential as excellent delivery systems for multiple area including food and drug.

Solid lipid nanoparticles can be produced in large scale like emulsion with GRAS lipids. Different method has been sued to produce solid lipid nanoparticles. Hot emulsification is one of the most widely used fabrication methods(Mehnert and Muller 2001). For this technique, drugs or bioactives are premixed with lipids. The temperature is then brought up to 5℃ -10℃ above the temperature of lipid with highest melting point. The melt lipid drug mixture is mixed with surfactant solution at the same temperature. The adsorption of surfactant at oil and water interface will reduce the energy barrier to create new surfaces and stabilized nanoemulsion. External energy is then applied to produce nanoemulsion. The hot nanoemulsion is cooled to force melt lipids become solid. Particle size is directly related to energy dissipation and nature of the surfactant during this process. Lots of work has been done to elucidate and predict oil droplet size. External energy is needed because of the existence of Laplace pressure(Walstra 1993)

$$P_L = \gamma\left(\frac{1}{R_1}+\frac{1}{R_2}\right) \quad (3)$$

R_1 ,R_2 refer to the principal radii of curvature. γ is the interfacial tension of oil and water interface. It is assumed that the formed droplet is in spherical shape, therefore, $R_1 = R_2$.

Equation (1) becomes $P_L = \frac{2\gamma}{R}$. For a droplet in nano range, the Laplace pressure is 1-2 atm, therefore, a large external pressure is needed to deform a large particles. To decrease the interfacial tension, surfactant can be added. The adsorption rate and amount are also important factors. Detailed discussion can be seen in (Walstra 1993)

The external pressure can be provided by different method. High pressure homogenization can provided the pressure when the oil and water is forced to pass through valves by applying large pressure gradient. Mathmetic model for high pressure homogenization has been done (Hakansson, Tragadh et al. 2009). The production of solid lipid nanoparticles by high pressure homogenization is feasible to large scale production since high pressure homogenizer has already been commercialized. In addition, with 2%-10% of surfactant, the particle size was claimed to remained the same for over 1 year under 4 ℃ (Casoli, Vacca et al. ; Shegokar, Singh et al.)

In addition to high pressure homogenization, ultrasonication is also capable of providing external pressure and reducing droplet size to nanoscale. The are number of theories with regards to sonication, It is claimed that cavitation is likely to control break up of droplet, in addition to cavitation, the generation of interfacial capillary waves also affected the particle size. However, capillary force only affected particles larger than the wave length. Under normal condition, it is still cavitation to be crucial factor. The Ultrasounds when applied in sufficient high intensity, vapor bubbles will form at the interface. After reaching critical size, the bubbles will collapse and generate high shear force in the vicinity. In addition to shear force generated by the collapsing bubbles, dynamic pressure by sonoprobe also generate high speed liquid movement. Different models based on

Kolmogorov theory of minimum drop size has been developed for oil droplet prediction. Detailed information could be found in the work by (Tal-Figiel 2007).

Solvent emulsification-evaporation method is also developed in lab. In this method, water immiscible organic solvents such as chloroform, toluene, are used to dissolve lipids and drug. When temperature is raised, the organic solvent will be evaporated leaving the lipids and drug form nanoparticles. The advantage of this method is avoiding high temperature therefore suitable for heat sensitive compounds. The size distribution is narrow and the mean particle size is small (apox.100nm). However, limitations of this method are also obvious. In the review by Wissing, (Wissing, Kayser et al. 2004)it was reported: 1. The residues solvent in the final product: it is found that toluene residues as 20-100ppm in final SLN dispersion ; 2. The final concentration of SLN is low due to the dilute organic solvent used in the procedure.

Structure of Solid lipid nanoparticles

After the hot nanoemulsion is formed, it is cooled to force the formation of solid lipid. During this process, different structure will be formed. There are three types of structures of solid lipid nanoparticles: Drug dispersed evenly across the volume of solid lipid nanoparticles is formed if the drug has very good miscibility with lipids. Because of the partition of drug in lipid and in aqueous phase during solidification process, Drug-enriched shell with lipid core and drug-enriched core with lipid shell can be formed. According to (Muller, Mader et al. 2000) Due to existence of surfactant, drug solubility in aqueous environment is therefore increases. When temperature continues to drop, the drug will tend to get back to lipid, however, the oil droplet has solidified therefore a great proportion will

accumulated on the surface. On the other hand, if drug crystallized prior to lipids, a drug enriched core with lipid shell will be formed. In terms of release rate, SLN with drug enriched core is more likely to have a sustained release pattern whereas drug enriched shell type have a burst release pattern(Muller, Radtke et al. 2002).

Physical stability of Solid lipid nanoparticles

SLN physical stability study focuses on change of particle size in aqueous solution and polymorphic change during storage.

Polymorphic from α to the more thermodynamically stable form β has profound impact on the stability of solid lipid nanoparticles. In addition to causing burst release of drugs, transformation also leads to aggregation and even gelation of SLN dispersion. Recent research has found that polymorphic transition leads to the increase surface to volume ratio by forming needle shaped crystals. (Helgason, Awad et al. 2009) If there is not enough surfactant to cover the extra surface, SLN dispersion would be very vulnerable to aggregation due to hydrophobic interaction. The aggregation is irreversible process. The polymorphic form transition can be triggered by different factor such temperature fluctuation, presence of impurity(Nissim Garti 2001) in bulk phase lipid based products such as chocolate. In terms of solid lipid nanoparticles, polymorphic transition in long chain lipids is slower than short chain(Bunjes, Westesen et al. 1996). More recent research has shown that polymorphic transition is a critical factor affecting the physical stability of solid lipid nanoparticles suspension.

Particle size is a crucial factor that directly related to the SLN function. For instance, for particles that circulate in blood stream, small size is required. Another example is better film forming ability than particles in micro scale for dermal application (Muller, Radtke et al. 2002) The instability of solid lipid nanoparticle can lead to growth in particle size, even phase separation. Two forces have been shown to affect the stability of SLN dispersion: Van der Waals attraction and electrostatic repulsion by the surface charges.

$$U(r) = U_A(r) + U_C(r) \quad (4)$$

$U(r)$ refers to the net potential between particles, a positive value indicates the repulsion force is in dominant where as negative value indicates attraction force is in dominant.

$U_A(r)$ represents the Van der Waals component of the potential. A is the Hamaker constant. R is the particle radius and r is the center to center separation.

$$U_A(r) = -\frac{A}{12}\left(\frac{4R^2}{r^2-4R^2} + \frac{4R^2}{r^2} + 2\ln\left[1-\frac{4R^2}{r^2}\right]\right) \quad (5)$$

$$A = \frac{3}{4}k_B T\left(\frac{\epsilon_p-\epsilon_s}{\epsilon_p+\epsilon_s}\right)^2 + \frac{3h\nu_e}{16\sqrt{2}}\frac{(n_p^2-n_s^2)^2}{(n_p^2+n_s^2)^{\frac{3}{2}}} \quad (6)$$

With the change of temperature, ion strength, components of environment change A value changes accordingly (Equation 6). k_B Boltzmann's constant, T Kelvin temperature, ϵ_p and ϵ_s are the static dielectric constant of the particle and solvent respectively. ν_e is a characteristic ultraviolet absorption frequency. n_p n_s are the refractive index for particles and solution respectively. h is Planck's constant

$$U_C(r) = \frac{(Qe)^2}{4\pi\varepsilon_s\varepsilon_0 r}\frac{\exp\left[-\kappa(r-2R)\right]}{(1+\kappa R)^2} \quad (7)$$

$U_C(r)$ is a screened Coulomb repulsion, according. Q is the surface charge of particle in units of the electronic charge e. ε_0 is the dielectric constant of vacuum. ε_s is the dielectric constant of solvent. R and r are the same as that in equation 6, κ is related to Debye radius,

which is the surface charge exhibit significant effect. It is easy to see that electrostatic repulsion increases with increase surface charge density. In order to prevent aggregation, addition charged surfactant or polymers can be added. The adsorption of these molecules will increase the energy barrier and preventing aggregation.

In addition to Van der Waals force and electron static repulsion, steric effect can also affect the stability of SLN dispersion. It main concerns the adsorption and orientation of large chain like molecules such as non-ionic surfactant, polyethylene glycol on the surface of SLN. Briefly, if the long chain extends out from the surface, it is likely to stabilize the dispersion given proper environment conditions.

Challenges of solid lipid nanoparticles

Low drug loading capacity

Accumulating evidence has shown that the loading capacity of solid lipid nanoparticles is limited by polymorphic transition.(Westesen, Bunjes et al. 1997) reported that solid lipid nanoparticles composed of single lipids such as tristearin has limited ability of loading lipophilic drug when compared to supercooled melt. Further explore in the loading capacity reveals shows that supercooled melt has the highest loading, followed by amorphous lipid matrix, then α crystals. β crystal. (Muller, Radtke et al. 2002) showed that encapsulated drugs can stay either at the imperfection of lipid crystals or in between molecules. Since β crystal has the shortest intermolecular distance, it does not have good compatibility with foreign molecules. Therefore, the highly ordered β crystals should avoid. However, it is difficult to form amorphous structure using a monoacid glyceride. As for α crystal, it is thermodynamically unstable: the polymorphic transition from α to β is

fast under ambient conditions. Increasing surfactant concentration and the use of co-surfactants has been shown in some case to be able to retard the polymorphic transition. However, many effective surfactants, such SDS, DOSS, are not allowed even in pharmaceutical industry due to toxic effect.

Burst release of encapsulated compounds

The release of encapsulated compound (drug/bioactives) is an important feature of solid lipid nanoparticles. In many cases, sustained release or triggered release are highly desired. However, research has shown that fast polymorphic transition during storage leads to burst release of encapsulated compound. The polymorphic transition can be stabilized by crystal habit modifier(Nissim Garti 2001) such as surfactant. In addition to cytotoxicity, high concentration of surfactant leads to higher solubility of encapsulated compounds in aqueous environment and thereby reduces the drug in the lipid phase resulting in low loading capacity. (Ying, Cui et al.) reviewed current research and reported an increasing attention on modifying SLN structure, however, no significant improvement has been reported so far.

Poor stability at high concentration

The typical concentration of solid nanoparticles ranges from 0.1 to 30% (Muller, Radtke et al. 2002) higher concentration leads to formation creaming during hot emulsification process.

Lipid nanostructured carriers

To overcome these limitations of SLN, spatial incompatible solid lipids and liquid lipids are brought formulation to develop the second generation of lipid nanoparticles. The

addition of different lipids gives solid lipid nanoparticles certain nanostructure and therefore being named: lipid nanostructured carriers.

Structure of lipid nanostructured carriers: reduce in crystallinity and slower polymorphic transition

One of the reasons the reason for burst release of compound in emulsion is the high mobility of drug. Prolonged releases are reported when using solid lipid nanoparticles in some cases. (Muller, Maer et al. 2000). (McClements and Li) However, burst release pattern is still major limitation in many SLN research as mentioned above. Two main reasons lead to burst release: polymorphic transition and the formation of drug-enriched shell. (Muller, Petersen et al. 2007) Therefore, early research of NLC targeted on retarding polymorphic transition to more thermodynamically stable form and reducing the overall crystallinity of lipid nanoparticles. By mixing lipids with different chain length, slower polymorphic transition has been reported in many cases. For instance, NLC composed of cetyl palmitate with different proportions of caprylic/capric triacylglycerols were fabricated by (Teeranachaideekul, Souto et al. 2007) Result showed, less ordered structure of NLC with the addition of oil content was reported. In addition, a increase in Q_{10} loadings has also be found in NLC. In another research on Compritol®888 ATO (glycerol behenate), X-ray study and DSC about structure of SLN and NLC showed NLC had much lower crystallinity (Souto, Mehnert et al. 2006). In the research by (Liu and Wu) lutein loaded NLC showed increase imperfection and sustained release pattern. Although lipid crystals still present in NLC, a great reduction in crystallinity and slower polymorphic

transition when compared SLN were found. This type of NLC is later named as type I NLC.

Improved loading capacity

To further increase drug loading capacity and avoiding burst release, it is critical to reduce crystallinity during production and storage. It is found that certain solid lipids and oil mixed together, the solid lipids will form solid but exhibits no crystalline structure. Base upon this fact second type NLC was developed. It is characterized by solid amorphous structure (Muller, Petersen et al. 2007). It should be noticed that research in fabrication of type II NLC still under developing since mechanism of inhibiting crystallization is not fully understood.

As reviewed earlier, liquid lipid usually has better compatibility of drug solid lipids. Therefore, to combine the advantage of liquid and solid lipid, the third type of NLC (type III) was developed. It was reported to have crystallized solid lipid shell with small drug loaded oil nanocompartment within the solid shell. Some research reported increase in drug loading capacity when compared to SLN.

To form the type III NLC, high concentration of oil is need to induce phase separation during the solidification process. The process is explored by different researchers, brief summary can be found in the review (Muller, Radtke et al. 2002): At high temperature, the mixed oil droplet is formed by applying external energy. When temperature drops during cooling process, lipid with high melting point will solidify, if the oil concentration is below the solubility in the crystallized lipid, then no oil compartment will be formed. When oil concentration is well above the solubility of crystallized lipid, small oil compartment will

be able to form. Forming oil compartment proved to be challenged, several attempts have been made. Results by different researchers showed that the oil compartments were localized on the surface of particles instead of inside the particles (Jores, Mehnert et al. 2004; Saupe, Gordon et al. 2006). What is worse, in some cases, drug can be easily accessed by substance from environment. The formulation of Type III NLC, therefore needs further research.

Improved long term stability at high concentration

One of the limitation of SLN is irreversible aggregation, multiple research has linked the this phenomena to fast polymorphic transition(Freitas and Muller 1999). NLC depends on formulation, has less crystallinity and exhibit slower polymeric transition. NLC should have longer shelf life than SLN under the same condition. Numerals stability studies have been carried out. (Junyaprasert, Teeranachaideekul et al. 2009) reported that NLC stored at 4℃, 25℃ and remained in the nano scale nearly one year. Normal SLN has high water contented, (70% to 90%). For NLC, improved physical stability were reported at high lipid concentration. It was later found that at high concentration, unlike SLN, NLC formed pearl like net work and released the particles when the dispersion system was diluted with water.

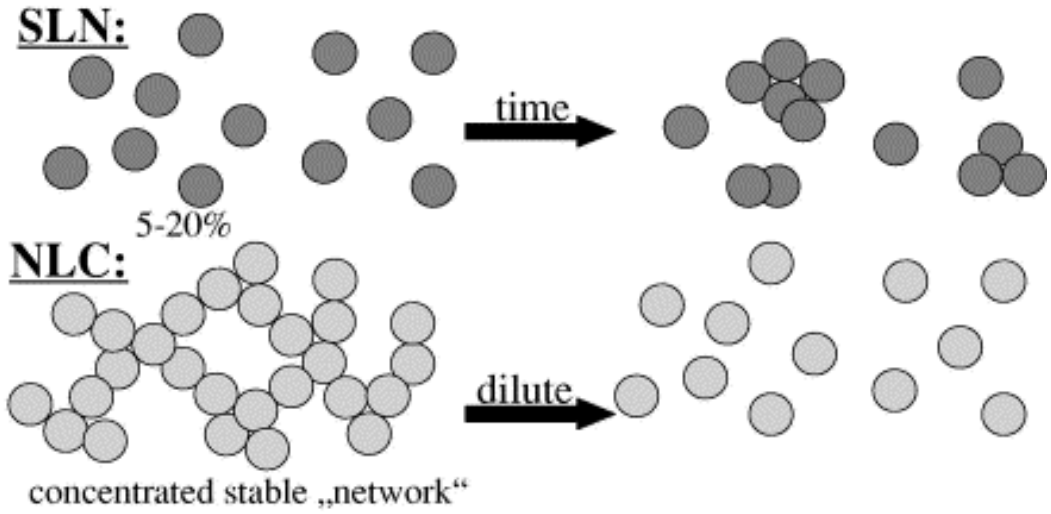

Figure 1 Schematic graph of SLN and NLC at high concentration. Adapt from (Muller, Petersen et al. 2007)

Perspective and challenges for food application

Cumulating recent scientific research has associate diet to the risk of major disease such cancers, CVDs etc(Willett 2000; Reddy and Katan 2004; Willcox, Ash et al. 2004). Reducing risk of these major diseases such as cancer from has been the driving force for both food science community and industry. Recent epidemiological studies and reviews suggest the consumption of bioacitives such vitamin E, phenolic antioxidant is inversely related to risk of fatal chronic diseases such as coronary heart diseases, some cancers and diabetes (Hertog, Feskens et al. 1993; Kushi, Folsom et al. 1996; Steinmetz and Potter 1996). Inspired by these studies, enormous effort has been spent on identifying and isolating bio-active compounds such as phytochemicals (Liu 2004) Despite the promising research results in laboratory(Ross and Kasum 2002), enriching food with these compounds have been greatly limited, because these compounds are usually highly

hydrophobic and chemically unstable(Anand, Kunnumakkara et al. 2007). Below is a table that summarized different functional ingredients that has poor water solubility, but important beneficial effects on health.

Table 1 Bioactive compounds and related health effect. Adapt from (McClements and Li)

Name	Type	Nutrition benefits
Fatty acid	$\omega - 3$fatty acids, conjugated linoleic, butyric acid	Heart disease, cancer, bone health, immune response disorders, weight gain, stroke prevention, mental health, visual acuity
Carotenoids	β-carotenoid,lycopene,lutein and zeaxanthin	Heart disease, cancer, macular degeneration, cataracts
Oil soluble antioxidant	Tocopherols, flavonoids, polyphenols	Heart disease, cancer and urinary tract diseases
Phytosterols	Stigmasterol, β-sitosterol, compesterol	Coronary diseases
Oil soluble vitamins	Vitamin A,D	Eye health, bone health cancer
Nutraceuticals	Co-enzyme Q	Hypertension, heart

	diseases, diabetes,cancer

Nanotechnology has offered promising approaches to overcome the challenges. The potential of nanotechnology was reviewed by different research group over the decades.(Weiss, Takhistov et al. 2006; Weiss, Decker et al. 2008; Sozer and Kokini 2009). The feasibility of solid lipid nanoparticles and nanostructured lipid carriers as delivery system has been explored with major focus on pharmaceutical compounds such as paclitaxel. The research results showed that SLN and NLC were able to encapsulate lipophilic drugs. In addition, SLN an NLC have been proved to be able to improve the stability and enhance the bioavailability of the liable drugs. What is more, SLN and NLC can be easily fit in large scale production as reviewed above. These advantages make them good candidate of delivery system for functional food.

Digestion of lipid based carriers is also important issue. Solid lipid nanoparticles, like emulsion, can be digested by body by lipase. It was found the chain length, physical structure and surfactant could significantly affect the digestion of lipid by lipase. The author also suggests the possibility of using this property to build lipase triggered release SLN. (Olbrich and Muller 1999). Recently,(McClements and Li) reviewed different research and summarized the results. It was summarized that for same lipid, digestion rate for liquid lipid is higher than in solid state. It was further assumed that altering the digestion time will eventually lead to sustained release.

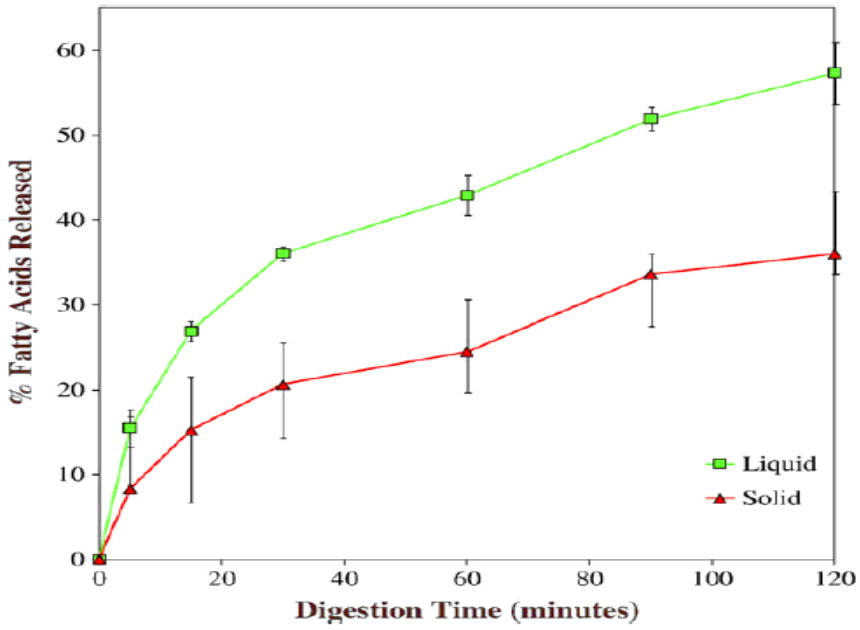

Figure 2 Different digestion time lengths for solid and liquid lipid

To apply SLN and NLC in food industry, GRAS (generally regarded as safe) materials are required. Many materials that are allowed in pharmaceutical industry are not allowed in food in large quantity. Therefore, searching for GRAS materials is the prerequisite of fabricating SLN and NLC for food applications. Lipids derived from animals, di- and monoglyceride are good choices to start. The formed SLN and NLC should have melting point above body temperature to remain solid when consumed and passes through GI tract. In addition GRAS materials, incorporating SLN and NLC into food matrix should not adversely affect the sensory effect of the product such as taste, appearance, flavor etc. Last but not the least, SLN and NLC must be stable during and after process. For instance, hot fill process will heat the beverage to inactivate harmful microorganism. In cold fill process, SLN and NLC must be compatible in the presence preservative. Since most beverages are high acid products, this means SLN and NLC must be stable under acidic environment.

Apart from the basic requirements, to be a good delivery system, loading capacity of the food grade SLN and NLC must be high enough to satisfy the nutrient need. As reviewed above, the loading capacity is closely related to the crystallinity of the lipid and polymorphic transition. A low crystalline carrier is therefore favorable to accommodate more functional ingredient. Carriers must be able to be stable and protect functional ingredient under the complex environment in GI tract(Sarmento, Martins et al. 2007). More detailed with regard to environment trait in different part of GI tract can be found in the review (McClements and Li). Ultimately, SLN and NLC should enhance the bioavailability of poorly absorb compounds.

Conclusion

SLN and NLC hold promising future for both pharmaceutical and food industry. Previous study has been focused on drug delivery, with little effort on food industry. With the increasing need for healthy safe food supply, developing lipid nanoparticles for food application is generating increasing public attention and resources. However, many challenges remain ahead: prevent particle aggregation, prevent fast polymorphic transition, increase drug loading capacity, control release kinetics, achieve on-site delivery etc. This research focuses on fabricating solid lipid nanoparticles and nanostructured lipid carrier using all food grade material and manipulating the crystallinity of lipid nanoparticles.

Hypotheses and objectives of the research projects

The ultimate goal of the research is to apply physical method to fabricate lipid nanoparticles that can be potential nutraceuticals delivery system for food application. The core hypotheses are:

1. Selected food grade materials: monostearin, methyl stearate, oleic acid and polyethylene monostearate can be used to fabricate curcumin loaded lipid nanoparticles by hot emulsification method.

2. Polymorphic transition of monostearin and methyl stearate from α to β can be retarded by adjusting the ratios of monostearin, methyl stearate, oleic acid and PEG.

There are several major objectives:

1. Fabricate curcumin loaded monostearin SLN, methyl stearate NLC, oleic acid NLC and PEG NLC with hot emulsification method.

2. Control of polymorphic transition of fabricated NLCs by altering the proportion of methyl stearate, oleic acid and poly ethylene glycol to the total mass of lipids in used.

3. Study morphology of fabricated SLN and NLC using TEM; Evaluate stability of lipid nanoparticles dispersion by DLS; Apply Raman spectroscope to explore structure of lipid nanoparticles and possible interaction between curcumin, methyl stearate, monostearin oleic acid,PEG and Tween 20.

Chapter 3 Method and Materials

Materials for SLN and NLC fabrication

Materials for SLN fabrication

Monostearin (alpha-monostearin) is the glycerol ester of stearic acid. Monostearin, according to FDA 21 CFR is obtained by esterification reaction between glycerin and stearic acid. It is order less and white powder. It is used as anti-caking agent, emulsifier in food (e.g. the head form in beer) and pharmaceutical products (e.g. control release property). It is the byproduct of fat from lipid digestion. In this research, Pure monostearin (CAS.123-94-4) is chosen. It has a melting point of 79℃. It is chosen for several reasons: 1. it is chemically stable during the rage of study (confirmed by later study)2. Monostearin has been used in the development of food (e.g. reduce the amount of high melting point or *trans* fats by forming liquid-crystalline lamellar above Krafft temperature; micron-scale bubbles stabilization) (Batte, Wright et al. 2007). 3. It is allowed to use without limitation according to FDA CFR. In some research, it is shown to have low cytotoxicity. In one of the research, it is shown that monostearin lipid nanoparticles with diameter around 200 nm has low cytotoxicity(Hu, Jiang et al. 2006)

Polysorbate 20 (also known as Tween 20) is used as surfactant in the present research. It is low toxic (up to 25mg/kg bodyweight/day) polyoxyethylene derivative of sorbitan monolaurate. Tween 20 is used in food, pharmaceutical chemical industries as surface active agent, (HLB value of 16.7). In food industry, it is used as wetting agent to improve the mouth feel, particularly in the production of ice cream. In pharmaceutical industry, it is used as surfactant to stabilize emulsion and suspension. In chemical industry, it is used as

detergent to remove stain and bacteria from surface. In this experiment, it is used in small amount to facilitate the formation of lipid particle by reducing surface tension.

Curcumin (1,7-Bis(4-hydroxy-3-methoxyphenyl)-1,6-heptadiene-3,5-dione) is a naturally occurring polyphenolic phytoconstituent, isolated from the rhizomes of *Curcuma longa Linn*, is an important health promoting compound with GRAS status. Recent research shows curcumin a powerful antioxidant: it is claimed to be able to suppress tumor growth by inducing apoptosis to cancer cell without causing side effect to normal cell. In addition, a protective effect against Alzheimer's disease is also found.(Motterlini, Foresti et al. 2000; Lim, Chu et al. 2001; Bengmark 2006; Anand, Kunnumakkara et al. 2007).Despite the great potential as antioxidant and natural anti-cancer drug, its usage is greatly limited to due to its low water solubility (Anand, Kunnumakkara et al. 2007), sensitivity to light (photon induced decomposition), heat and alkaline environment (Price and Buescher 1996; Price and Busecher 1997; Stankovic 2004).

Materials for NLC fabrication

In addition to monostearin, curcumin and Tween 20, methyl stearate, oleic acid and poly ethylene glycol are mixed with monostearin at different ratios to fabricate different nanostructured lipid carriers.

Methyl stearate is derived by reaction between stearic acid and methanol. This stearic acid ester is white orderless power, with a melting point at 49℃. Earlier research with regard to the toxicity on animal model showed methyl stearate had good bio-compatibility. FDA cleared it for the use as fat nutrient supplement for animal feed. It also obtained clearance from FDA recently for being used as direct and indirect food additive (21 CFR 172.225).

For this research project, since methyl stearate has slight structural difference with monostearin (difference is the methyl moiety and glycerol moiety) and similar specific gravity (0.836 vs. 0.8980), it is chosen to fabricate lipid nanoparticles. As reviewed in Chapter 2, the addition of methyl stearate is expected to 1. Reduces crystallinity of NLC. 2. Reduces particle size. In addition to reducing crystallinity, it is also expected the addition spetial incompatible methyl stearate is able to retard the polymorphic transition and create more imperfect crystals.

Oleic acid is a mono-unsaturated omega-9 fatty acid with 18 carbons. It is an odorless, colorless liquid fatty acid under room temperature. It is natural component of many kinds of edible oil. Its health promoting value is well documented. In addition to high nutrition value, oleic acid also serves as plasticizer to modify the surface property and improve the mechanical strength of edible film such as zein film. When added into the formulation in this research, it is expected to form nano droplet in NLC and increased the loading capacity of curcumin.

Polyethylene glycol monostearate n=40.(CAS. 9004-99-3) is an important class of nonionic surfactant. It is formed by the reaction between ethylene oxide and hydrophobic compound. Therefore, the addition of PEG is expected to reduce the energy required to fabricate lipid nanoparticles. In addition, PEG-SA has also been proved to be low toxic chemical: The material safety data sheet suggests a rat $LD_{(50)}$ oral value of 20g/kg body weight.

Table 2 Formulations for SLN and NLC

SLN	Monostearin	Methyl	Oleic acid	PEG	Curcumin

		stearate			
Monostearin	1	0	0	0	0.03
Methyl stearate NLC	Monostearin	Methyl stearate	Oleic acid	PEG	Curcumin
40% Methyl stearate NLC	0.6	0.4	0	0	0.03
60% Methyl stearate NLC	0.4	0.6	0	0	0.03
Oleic acid NLC	Monostearin	Methyl stearate	Oleic acid	PEG	Curcumin
5% Oleic acid NLC	0.38	0.57	0.05	0	0.03
10% Oleic acid NLC	0.36	0.54	0.1	0	0.03
20% Oleic acid NLC	0.32	0.48	0.2	0	0.03
PEG NLC	Monostearin	Methyl stearate	Oleic acid	PEG	Curcumin
5% PEG NLC	0.33	0.57	0.05	0.05	0.03
10% PEG NLC	0.38	0.47	0.05	0.1	0.03

Methods

Fabrication of monostearin solid lipid nanoparticles and nanostructured lipid carries

SLN and NLC are prepared by modified hot melt-emulsification method (Hu, Jiang et al. 2006).Detailed fabrication process is as follow: a total of 1g lipid mixture is melt at 85℃. For nanostructured lipid carriers, different lipids are mixed together before melting. The temperature is maintained by water bath above the melting temperature of monostearin at 85℃. Sonication (level 4) is applied to ensure the complete melting of lipid and mixture of curcumin and lipid. 50ml 2w/v% Tween 20 aqueous solution is prepared. 20 ml is heated up to 85℃ mixed with melt lipid. The mixture is sonicated for 5 minutes with 5 seconds on 3 seconds off to obtain melted micro-emulsion. After sonication, the emulsion is poured into a 100 ml flask with 30ml 2% Tween solution at 1℃ -2℃. Weak Sonic (level 2) is

applied at 5s on and 3s off for 10 minutes to preventing undesirable aggregation. The formed nanoparticles suspension is storage 4℃ in the fridge.

Characterization of lipid nanoparticles

X-ray diffraction (XRD)

X-ray diffraction utilizes the different elastic scattering pattern of X-ray atoms to study the atomic structure of materials. It is one of the most common methods to study the crystal structure of metal crystals. With the development of lattice refinement technique, it is also possible to yield information about given material. In addition, the size of crystals can also be reflected in diffractogram in which the diffraction peak becomes broader. Quantitative analysis of crystal size can be given by Scherrer equation. On the other hand, lipid molecules are able to arrange themselves in different pattern, therefore exhibit different crystallographic structures. The existence of multiple crystallographic structures is known as polymorphism. For lipid nanoparticles, these structures and the transition from one structure to another is able to affect the loading capacity and release pattern of encapsulated compound. X-ray therefore, is an excellent technique to reveal lipid molecule arrangement.

In the present study, the polymorphic form of the lipid is studied by X-ray diffraction. Bruker/Siemens Hi Star multi-wire area detector and rotating anode x-ray generator are used. Freeze dried samples are used in this part of study. Capillary is used to hold the samples. The wavelength is 1.5418 Å. Scan range of 10 degrees is applied. WXRD data is processed using Fullprof software. The obtained data is compared with that in database and previous research report to confirm the polymorphic structure.

Differential scanning calorimeter (DSC)

Differential scanning calorimeter is thermal analytical technique. There are different kinds of DSC commercially available. In the present study, power compensate DSC is chosen for its high sensitivity. The melting point of lipid nanoparticles is an important parameter. DSC analysis can also provide information about polymorphism of lipids: each polymorphic form (α, β, β') has its unique melting point. Polymorphic analysis by DSC, like x-ray diffraction, is well established by previous research, especially on lipid.

In the present study, differential scanning calorimeter (DSC7, Perkin-Elmer, USA) is used to obtain thermal properties of lipid nanoparticles and bulk phase materials. Empty standard aluminum pans are purchased from Perkin Elmer and used as reference. Temperature scan is programmed as following: samples and reference is held at 5℃ for 1 min and then heated to 80℃ at 12℃/min. After reaching 80℃ they are held at 80℃ for 1 min. After heating, the samples are cooled to 5 ℃ at 12 ℃/min and held for 1 min at 5℃. The Pyris (Perkin-Elmer, USA) software is used to analyze the data obtained during the scan. Bulk phase materials, curcumin loaded lipid nanoparticles and lipid nanoparticles without curcumin are studied. Processed thermograms are obtained to study the thermal behaviors of different particles with different components. The onset temperature is measured since it is not significantly affected by cooling or heating gradient. In addition, the enthalpy is also calculated by integrating the area under the peak with the aid of the software. The enthalpy of well crystallized and that of lipid nanoparticles aggregate is compared to provide crystallinity information.

Dynamic light scattering (DLS)

Dynamic light scattering is useful method to measure the average sizes, sizes distributions of lipid nanoparticles. Unlike electron microscopy, it does not require sample preparation. It measures hydrodynamic radii. In most cases, sizes and shapes are obtained by relating transitional and/or rotational diffusion coefficients to theoretical relation (R.Pecora 2000). Photon correlation spectroscopy (PCS) is used to characterize lipid particles. PCS is able to record the intensity of light scattering from sample particles and analyze Brownian motion of dispersed particles. To be more detail, the intensity of light is the result of interference on the surface of the detector which depends on the shape and position of dispersion particles. When Brownian movement of these particles takes place, the intensity fluctuates accordingly. An auto-correlator is used to do rapid real-time calculation of the scattered intensity time correlation function. Then calculate the diameter of the dispersed samples. Recently, the use of avalanche diodes as detectors has reduced the intense of laser and improved the accuracy of measurement by reducing the danger of over-heating.

Average hydrodynamic radii of lipid nanoparticles are determined by photo correlation spectroscopy using 90 PLUS Particle Size Analyzer (Brookhaven Instrument Corporation) at a fixed angle of 90^{o} at 25℃. The wavelength of the laser is 658 nm. All samples and controls are kept at 4℃ for a week and then sonicated for 5 seconds and kept under 25℃ for 30 minutes. Each sample is taken from the middle layer of the mother solution and diluted ten times before taken to measurement. The elapsed time is set to be 6 minutes to achieve better fitting results. Due to limited amount of sample, the viscosity is approximated as

pure water at the same temperature. The average diameters are calculated by the program based on Stokes-Einstein equation.

Transmission electron microscopy (TEM)

Transmission electron microscope enables the examination of structures which is smaller than the smallest resolvable object under normal light microscope. It has been used to observe the structure of cell, semiconductors etc. Multiple researchers have used TEM to exam nano colloidal system such as micelles, emusions etc. In this research, JEOL 1230 transmission electron microscope at Rutgers University is used to study the morphology of curcumin loaded particles. Curcumin loaded lipid nanoparticles are dispersed directly into copper grid and stained by 1wt% phosphotungstic acid (PTA) solution. After dried under room temperature, Samples were taken for TEM measurement.

Raman spectroscopy

Raman effect is attributed to inelastic scattering due to change in molecular vibration, rotation and electronic energy. The changes in frequency will be detected by the detector and plotted against the intensity. Peak shift reflects interaction between molecules.

Raman spectroscopy is a very sensitivity method to explore conformation of lipid molecules. Many researchers have utilized Raman spectra to explain structural changes in lipid. Although it is a sensitive technique, the scattering intensity is usually weak compared to background. As a result, Raman signal is very weak. To increase the signal without complicating the experiment, nanoparticles dispension is dipped on different substrate: Glass tube, glass slide and aluminum.

The Kaiser Optical Systems Raman RXN1 Analyzer with 180^{o} reflected, charge-coupled device (CCD) detector and 785 nm stabilized external cavity diode laser is applied to obtain Raman spectra. The spectrograph is fiber-optically coupled to a probe head allowing for the attachment of both contact and non-contact objectives and probes. KnowItAll 8.0(Bio-Rad Laboratories, Inc.) is used to analyze original spectra, namely, peak picking/subtraction. The intensity of peak, with proper reference peak, is able to provide quantitative information of the sample. In addition to finger print chemical compounds. Comparison between spectra can also reveal the structure of lipid nanoparticles can also be explored by Raman spectra.

Protective effect of lipid carrier in high pH environment

0.1 g of curcumin loaded SLN is weighed and dissolved in 100 ml 0.01mol/L NaOH solution. Then the solution is diluted 10 times. 0.003 g of curcumin is added into 100 ml 0.01mol/L NaOH solution. SLN dispersion and curcumin solution is stored in dark room for 5 hours. SLN is obtained by centrifugation and washed with distill water once. Raman spectra of the alkaline treated SLN and curcumin solution are taken.

Chapter 4 Characterization of solid lipid nanoparticles and nanostructured lipid carriers

Introduction to curcumin loaded solid lipid nanoparticles

Current market has detected intense need for antioxidant enriched beverage. However the use of polyphenolic antioxidant is limited due to low solubility and unstable chemical nature. Lipid nanoparticles provide potential solution: lipid nanoparticles have been shown to be able to increase the solubility in water and chemical stability of liable lipophilic compounds. However, little research work has been done on SLN for food application.

As reviewed in chapter 1, Solid lipid nanoparticles can be fabricated by ultrasonication without organic solvent. In this process, lipid and compound to be encapsulated are mixed together and heated up 10℃ above the melting point of monostearin. Aqueous solution of surfactant typically 2%-5% is mixed with lipid melt at the same temperature. Shear force from sonication will facilitate the formation of particles. The droplet size is governed by energy dissipation, temperature and other factors. The hot emulsion is then cooled down to form solid particles. During this process, heterogeneous nucleation will take place from outer shell. Depending on the cooling rate, lipid can form crystals of different structure, which will directly affect the encapsulation capacity. During storage, polymorphic transition can occur and lead to particle aggregation and burst release of encapsulated compound. Therefore it is highly desired to fabricate solid lipid nanoparticles in α or amorphous form.

In this project, food grade materials are used to fabricate curcumin loaded solid lipid nanoparticles. Monoglycerides are the most commonly used additives in the food industry.

The main applications for monoglycerides are emulsion- and foam based foods, low-fat products, and convenience and instant foods. (Corma, Iborra et al. 1998; Sagalowicz, Leser et al. 2006; McSweeney, Healy et al. 2008; Shen, Powell et al. 2008). Curcumin, a power polyphenolic antioxidant is chosen in this project. The research focus on fabrication of solid lipid nanoparticles and exploring the structure of curcumin loaded SLN.

Characterization of solid lipid nanoparticles

Dynamic light scattering study

The size distribution of SLN is shown below. The monostearin SLN shows three separate regions: Both SLN control and the one load with curcumin exhibited size distribution in three regions. 10-100nm, 100-500nm and 1000-2000nm. The encapsulation of curcumin does not change the size distribution. However, the intensity of fraction of larger size increases.

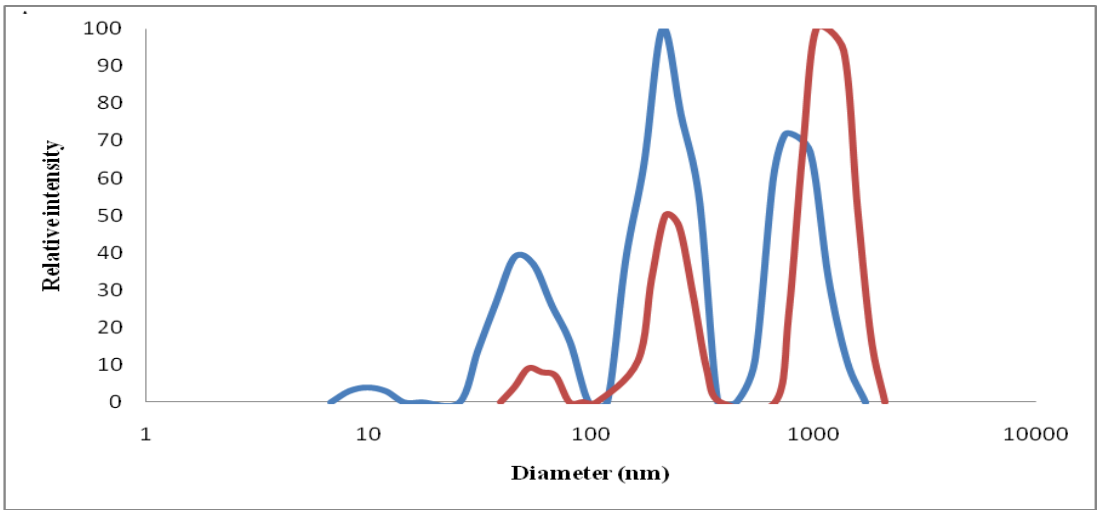

Figure 3 Size distribution of control SLN and curcumin loaded SLN. Blue solid line refers to control SLN; Red solid line refers to curcumin loaded SLN

TEM study of monostearin SLN

In TEM study, lipid nanoparticles are found to be in the range of 10-500nm. No particle larger than 800nm is found. Therefore the intensity peak above 100nm in DLS can be attributed to particles aggregation. The particles showed in Figure 4 is a typical curcumin loaded SLN under TEM. It has a diameter of 200nm In addition to size, TEM photo of curcumin loaded SLN also provide structural information of SLN (Figure 4): The dark region in the center of the particle in curcumin loaded lipid nanoparticles indicates the existence of curcumin. Black dots across the particles may be attributed to lipid crystals. One thing note worthy, when the electron beam energy reaches 85KV or higher, "dark dots" are observed to melt and form larger "dots" with irregular shape, suggesting the polymorphic transition from α form to β form. The low crystalline nature and core shell structure of lipid nanoparticles will be discussed in greater detail combine the data of other analytical data.

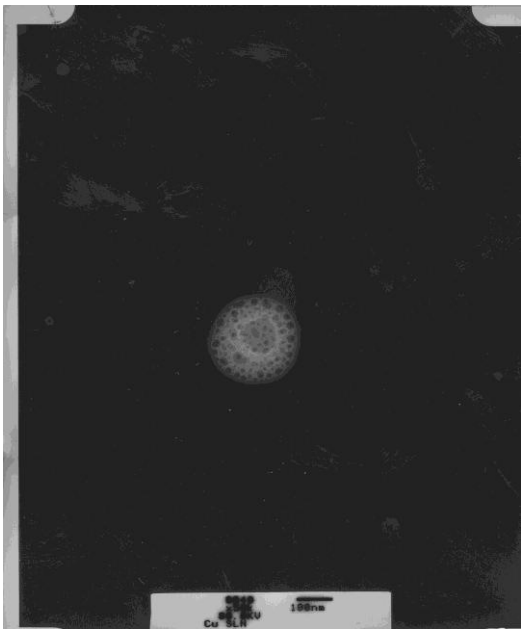

Figure 4 TEM photos of curcumin loaded solid nanoparticles

Raman spectroscopy study

To study the lipid nanoparticles, the spectra of bulk phase materials: monostearin, curcumin and Tween 20 are collected. The spectra of lipid nanoparticles are also collected by surface enhanced method (discussed in detail later). Specific peaks for each material, as shown the table below, are assigned by comparing the spectra with each other.

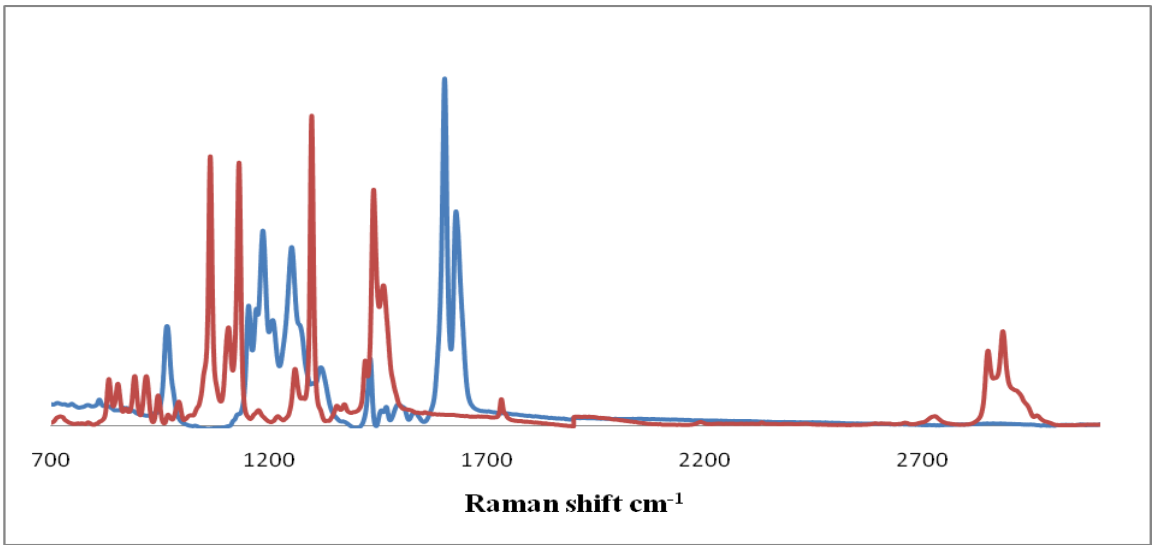

Figure 5 Spectra of bulk phase materials. Blue solid line refers to monostearin; Red solid line refers to curcumin

Table 3 Raman assignment to molecular vibration (Mendelsohn and Moore 1998)

Peaks (cm^{-1})	Assignment	Indication
2882	CH_2 asymmetric stretching	

2847	CH_2 symmetric stretching	The ratio of I_{asy}/I_{sym} is used to give quantitative measurement of the mobility of alkyl chains.
1731	C=O stretching	Saturated ester (Monostearin)
1627	C=C stretching, C=O stretching	Curcumin specific
1601	C=O stretching, C=C stretching (benzene ring)	Curcumin specific
1495	Aromatic ring stretching and in-plane bending	Curcumin specific
1462	CH_2 deforming	Monostearin
1439	CH_3 asymmetry deforming	Monostearin
1295	Skeleton vibration	Monostearin
1250	Aromatic CCH in plane bending; enolic part COH bending	Curcumin specific
1184	C-C in-plane bending; CH_3 in-plane bending(connected to keto part) (C-O-C)	Phenol
889	CH_3	Rocking

Confirm the encapsulation of curcumin in monostearin SLN

All four curcumin specific peaks of 1184 cm^{-1}, 1250 cm^{-1}, 1627 cm^{-1},1601 cm^{-1} appeared in the SLN spectra , indicating the presence of curcumin.

Exploring the structure of monostearin SLN

To elucidate the structure of nanoparticles, two models are made. The similarity and difference in their Raman spectra are observed. Spectra of curcumin/monostearin mixture, and the same mixture with a thin monostearin layer on top are collect. The differences between the two spectra, if there is any, must be attributed to the different structure. The comparison between two spectra shows major difference is in 1400 cm^{-1}-1500 cm^{-1} region: two strong peaks at 1439 $cm^{-1}$and 1462 cm^{-1} are found for mixture with monostearin top layer whereas single strong peak at 1495 cm^{-1} followed by three small broad peaks for curcumin/monostearin mixture.

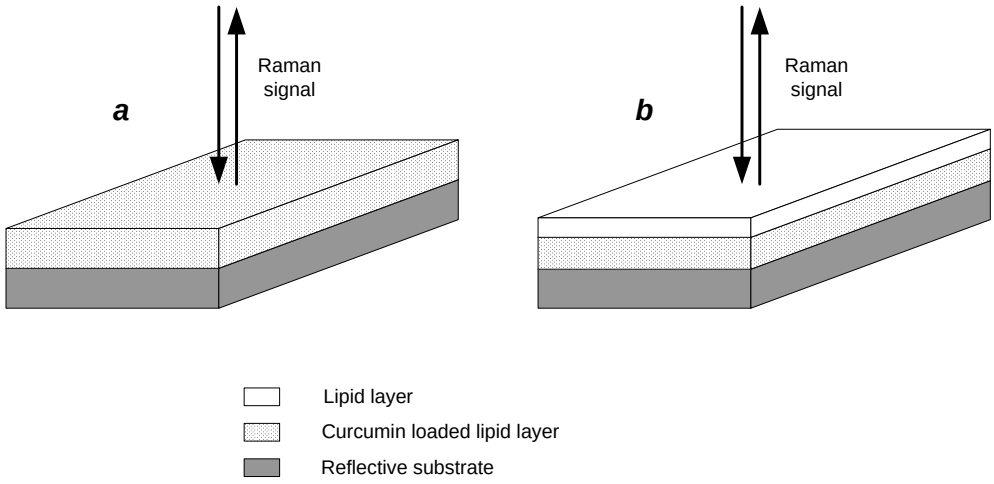

Figure 6 Macro-models used to investigate effect of the lipid outer layer on the subsurface Raman signal

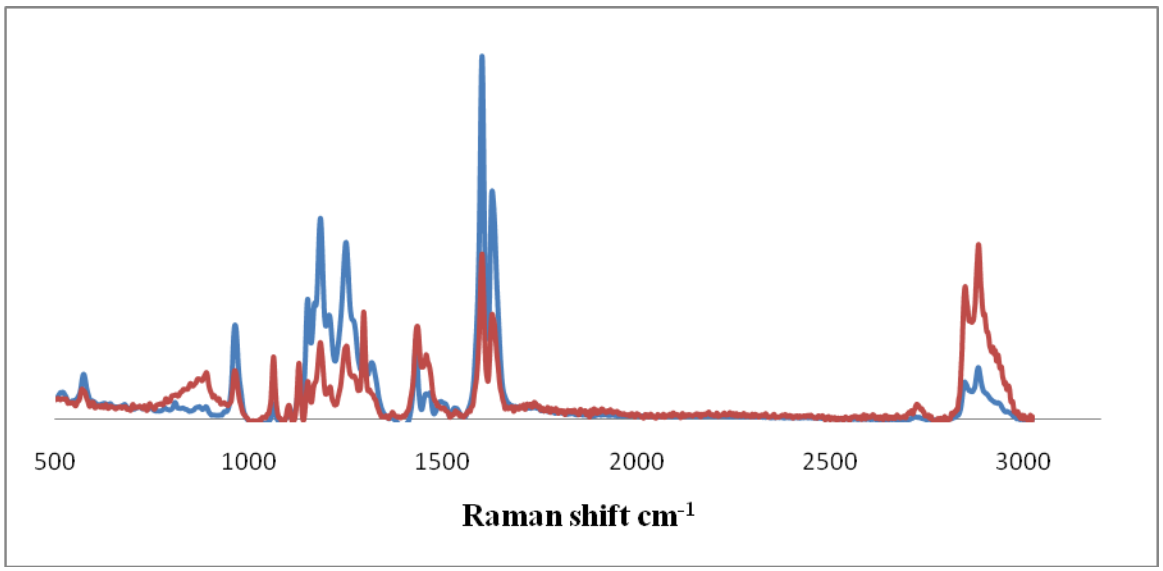

Figure 7 Spectra of curcumin/monostearin mixture and curcumin loaded SLN. Blue line refers to curcumin/monostearin mixture; Red line refers to curcumin loaded SLN

Next, we compare the spectra of curcumin loaded monostearin particles to that of two models(Figure 7,Figure 8).Major difference can be found in the region of 1400 cm^{-1}-1500 cm^{-1} is found between SLN and that from curcumin monostearin mixture(model a). In Figure 8, similar peaks appearance can be found between curcumin loaded SLN and model b. Therefore it is reasonable to propose that the structure of the nanoparticles can be monostearin shell with curcumin/monostearin core. Slight difference between curcumin loaded SLN and Figure 8 model a. This can be attributed thickness of the monostearin top layer and incorporation Tween 20. In addition, the incorporation of Tween 20 on the surface of the particles also leads to the increase curcumin signal (e.g. the increase intensity 1627 cm^{-1}). A proportion of curcumin stays at the surfactant layer. A small shift from 1250 cm^{-1} to 1247 cm^{-1}in curcumin specific indicates that the curcumin in the surfactant layer is

able to interact with Tween 20. According Table 3, it is possible that the hydroxyl group on curcumin forms hydrogen bond with Tween 20 molecules.

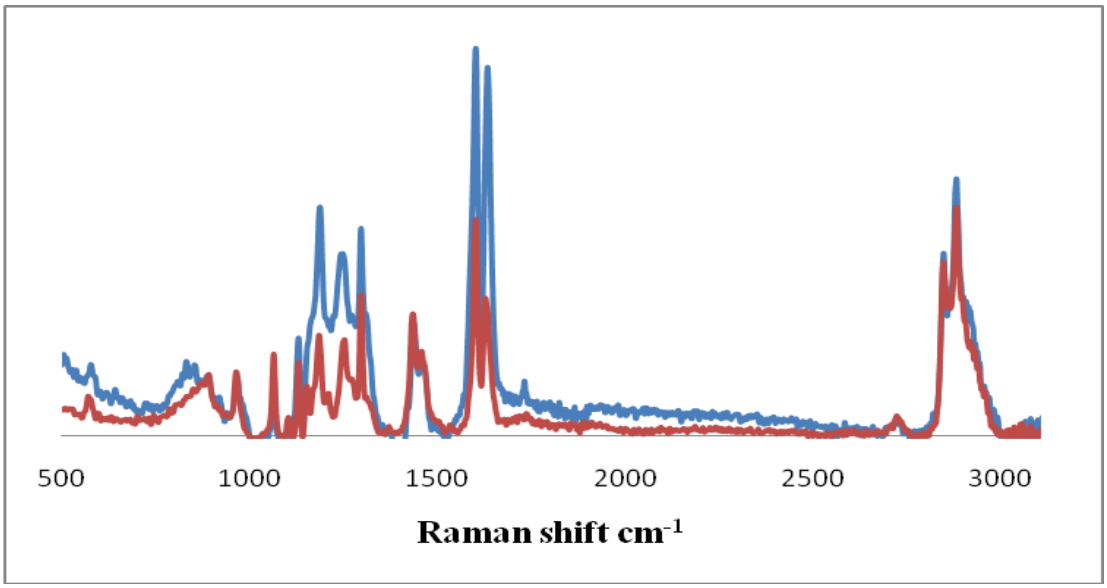

Figure 8 Comparison between curcumin loaded SLN and sandwich structure model. Blue solid line refers to curcumin loaded SLN; Red solid refers to sandwich structure

The protective effect of curcumin in alkaline condition

Curcumin is an oil-soluble pigment, practically insoluble in water and soluble in alkali. Preparations of water-soluble curcumin by incorporation into various surfactant micellar systems (e.g. sodium dodecyl sulfate, cetylpyridinium bromide, gelatine, polysaccharides, polyethylenglycol, cyclodextrins) have been reported (Humphrey, 1980, Tonnesen, 2002). In solution the curcumin exhibits keto-enol tautomerism and, depending on the solvent, up to 95% is in the enol form. The kinetics of hydrolytic degradative reactions of curcumin over the pH range 1- 11 is studied using HPLC technique (Tonnesen and Karlsen, 1985). At pH <1, aqueous solutions of diferuloylmethane have a red color which indicates the

protonated form (H4A+). In the pH range 1-7, the majority of diferuloylmethane species are in the neutral form (H3A). Water solubility is very low in this pH range and solutions are yellow. At pH>7.5, the color changes to red. The principal coloring components of curcumin are relatively stable at acidic pH, but they rapidly decompose at pH above neutral. In a study of alkaline degradation of compound (Tonnesen and Karlsen 1985), products of decomposition at pH 7-10 were determined by HPLC. The initial degradation products are formed after 5 minutes at pH 8.5. Ferulic acid and feruloylmethane are formed initially. Feruloylmethane rapidly forms colored (mostly yellow to brownish-yellow) condensation products. Degradation products formed by hydrolysis of feruolylmethane are vanillin and acetone and their amount increase with incubation time.

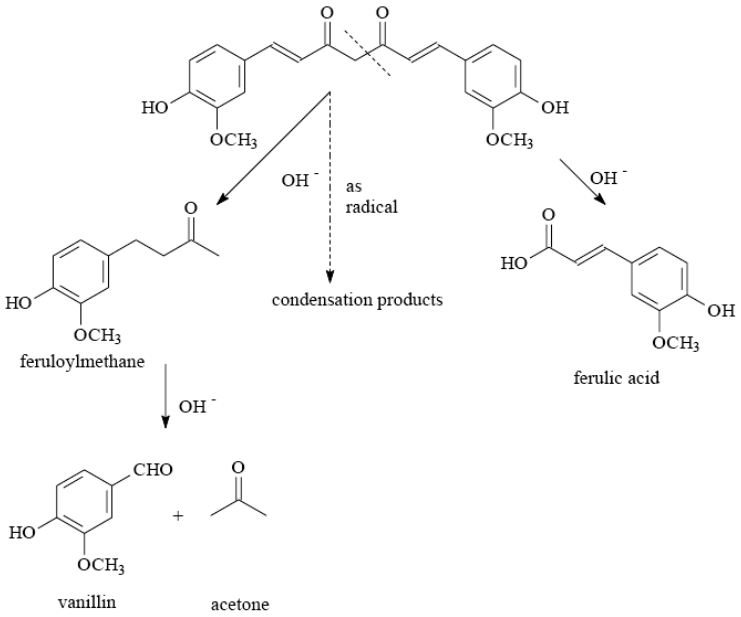

Figure 9 Degradation of curcumin

The stability of curcumin is greatly improved after its encapsulation in solid lipid nanoparticles. After 5 hours in NaOH solution with pH=12, (Figure 10) Curucmin specific

peaks at 1600 cm^{-1}-1700 cm^{-1} and 1184 cm^{-1} (noted by black lines) are found SLN in the spectra (although it is very weak) whereas no sign of curcumin could be found in control group.

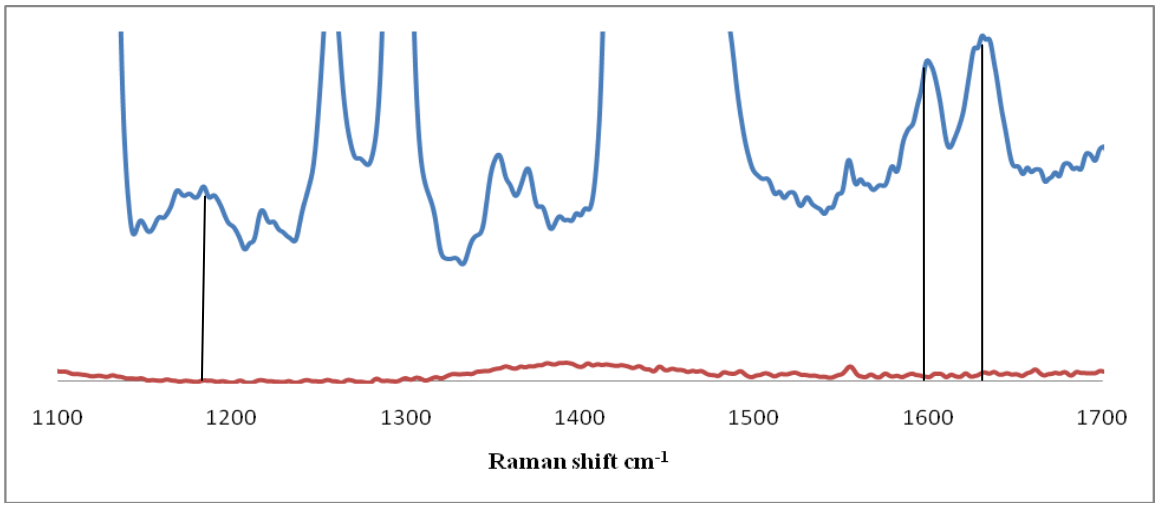

Figure 10 Spectra of curcumin loaded SLN and bulk phase curcumin dispersed in 0.01 mol/L NaOH solution for 5hours. Blue solid line refers to curcumin loaded SLN; Red solid line refers to bulk phase curcumin

Differential scanning calorimetry study

Differential scanning colorimeter measures the difference in energy input to maintain the same temperature between sample and control. It is highly sensitive equipment to measure thermal events even with small amount of samples. Previously it has been used to study the polymorphic form and crystallinity of SLN (Lutton and Jackson 1948; Siekmann and Westesen 1994; Unruh, Bunjes et al. 1999; Mehnert and Muller 2001; Dunn 2008; Helgason, Awad et al. 2008; Vereecken, Meeussen et al. 2009). The crystallinity is defined as the ratio between the heat of transition of SLN to that of bulk phase transition, more

detailed information is provided in later section. In this experiment, DSC is used to provide the polymorphism and thermal properties of the SLN.

Presence of multiple polymorphic form and depression of melting point

A visual exam of the thermogram of nanoparticles shows that endothermic peak for control SLN is about 10℃ wider than that of curcumin loaded SLN. (Figure 11) In addition, the peaks for control SLN and curcumin loaded SLN are both asymmetric. The asymmetry can be is more attributed to the overlapping of endothermic peaks. multiple polymorphic forms coexist in the sample can be the explanation of multiple endothermic peaks: According to the previous research (Lutton and Jackson 1948), different polymorphic forms had different thermal properties, the difference of some polymorphic form is small (melting point, heat of fusion etc). Given the above situation, it is reasonable to expect when multiple polymorphic forms present in the same sample, endothermic peaks could be expected overlap each other. In fact, the XRD data confirms the existence of multiple polymorphic forms in control SLN. Similarly, the narrower peak broadness of curcumin loaded SLN compared to control SLN suggests that majority of the crystals is in same polymorphic form.

The difference in melting point can be attributed to the size distribution. Smaller particles have lower melting point than larger particles of the same component due to Kelvin effect. This will be shown in the following section.

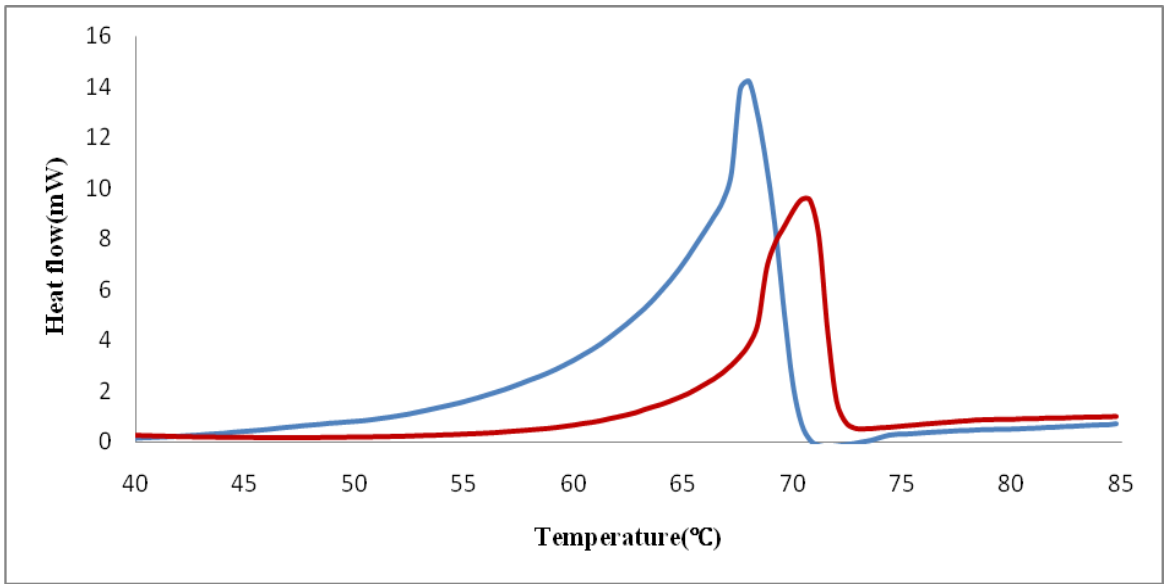

Figure 11 Thermograms of control SLN and curcumin loaded SLN (endothermic up), Blue solid line refers to control SLN; Red solid line refers to curcumin loaded SLN

Freeze dried SLN has lower onset temperature and maximum temperature than bulk phase material. This could be partially attributed to Kelvin effect (Bunjes, Koch et al. 2000): The smaller the particle size the lower the melting point.

Crystallinity of monostearin SLN

To measure the degree of crystallinity by DSC that involves determination of the baseline from the first onset of melting to the last trace of crystallinity and determines the enthalpy of fusion from the area under this endothermic. (zur Muhlen, Schwarz et al. 1998; Attama and Muller-Goymann 2008) The degree of crystallinity is then defined as following:

$$x_c = \frac{\Delta H_f(T_m)}{\Delta H_f^0(T_m^0)} \qquad (8)$$

where x_c is the weight fraction extent of crystallinity, $\Delta H_f(T_m)$ is the enthalpy of fusion measured at the melting point, T_m, and $\Delta H_f^0(T_m^0)$ is the enthalpy of fusion of the totally crystalline polymer measured at the equilibrium melting point, $T_m{}^0$. The result shows that SLN has lower crystallinity when compared to bulk phase material (Table 4). This could be attributed to the incorporation of surfactant in the lipid layer.

Table 4 DSC results

Material	Onset temperature	Melting point, ℃	Enthalpy change, J/g	Crystallinity
Monostearin (bulk phase)	74.59	75.69	117.6873	100%
Monostearin particles	64.68	67.99	61.1799	54.7%
Monostearin particles with curcumin	67.37	70.38	85.57	76.62%

X-ray diffraction study

Effect of cooling rate on monostearin crystallization

XRD diffraction is well established method used to study the lattice structure of the lipid crystals (Alexander 1974; P.Klug and Alexander 1974; Zavalij 2008). Bragg's law is assumed to predict the space between different crystal planes. According to previous study,

different polymorphic form is assigned and used to study lipid in food product such as chocolate. (Lutton and Jackson 1948; Mandzuka and Knez 2008). More recently, it has been used to study the polymorphism of lipid crystals in SLN. In this experiment, it is used to provide crystallinity and structural information about the SLN in addition to DSC study. The nomenclature of polymorphic forms is as follow (Lutton and Jackson 1948; Esposito, Fantin et al. 2008):

Table 5 XRD finger print of different types of crystals

Crystal type	Strong spacing line	Medium strong spacing line
α	4.15Å	
β'	4.15Å	3.65Å
β	4.55 Å, 3.9Å	

Research result of this experiment shows that majority of monostearin is in β (strong peak at 3.9 and 4.5 Å) form before melting. After rapid cooling by ice bath, the XRD shows re-crystallized monostearin has a single strong peak at 4.15Å (Figure 12). According to Lutton, the re-crystallized monostearin is in α form(Lutton and Jackson 1948)

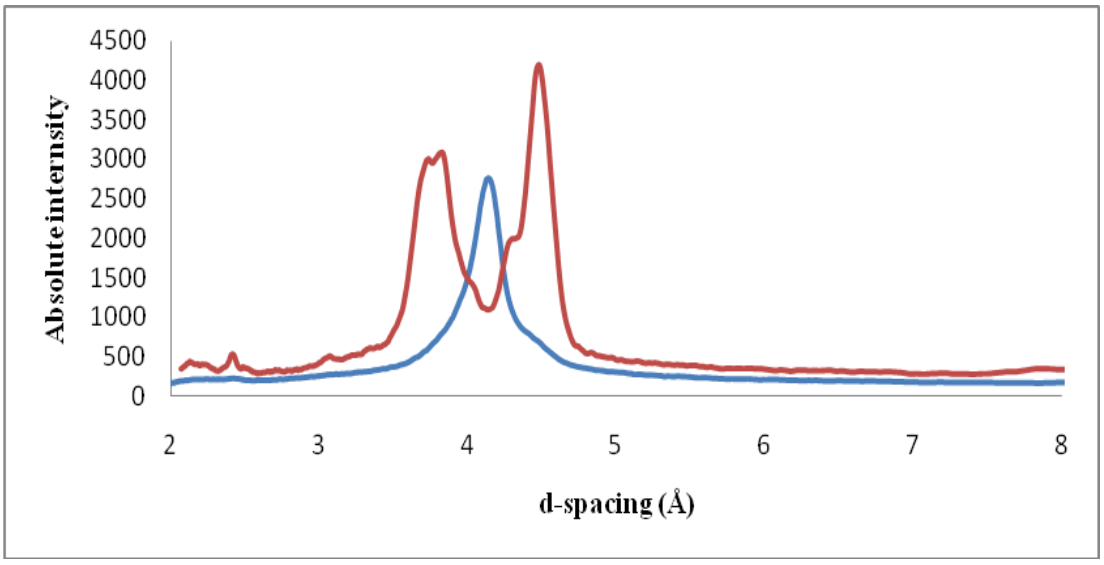

Figure 12 Diffractograms of re-cyrstallized bulk phase monostearin and bulk phase monostearin before re-crystallization, Blue solid line refers to re-crystallized bulk phase monostearin; Red solid line refers to bulk phase monostearin before re-crystallization

Polymorphic change of monostearin SLN during solidification

When hot emulsification process is applied, lipid crystals in nanoparticles form multiple polymorphic forms. Since there are multiple peaks appeared in XRD data. A strong peak at 4.5 indicates beta form. (Lutton and Jackson 1948).In addition to the dominate beta form crystal in freeze dried sample, a significant decrease in absolute intensity suggested low crystallinity. In other word, it suggests that a greater proportion of the particles are at amorphous states(Zavalij 2008). Besides absolute intensity, the peak for nanoparticles is broader than that of bulk phase monostearin. According to Scherrer equation(Alexander 1974), this is because of the small sized particles.

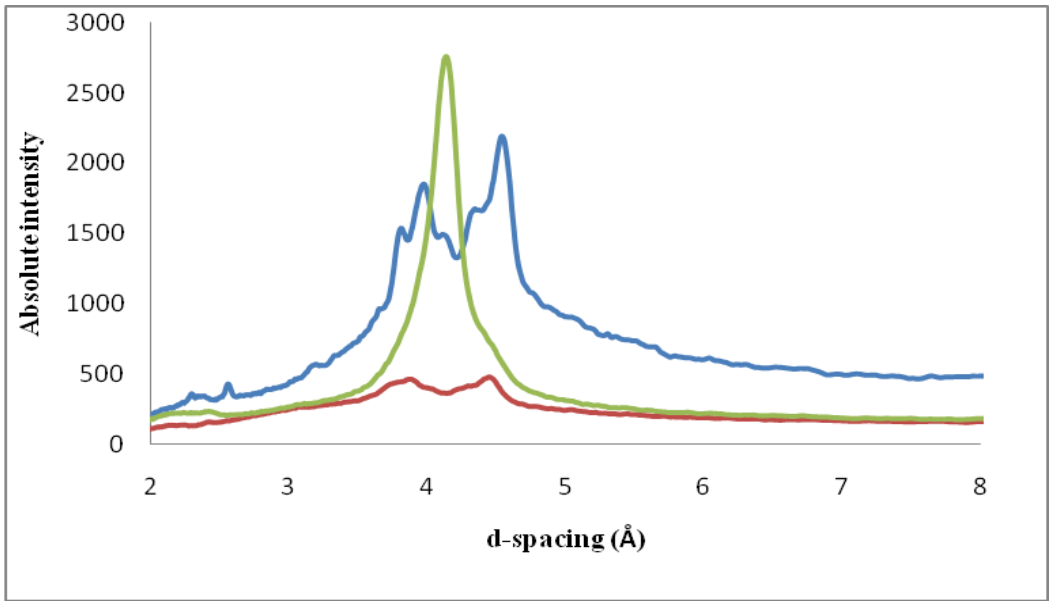

Figure 13 Diffractograms of control SLN, curcumin loaded SLN and re-crystallized bulk phase monostearin. Blue solid line indicates control SLN; Red solid line refers to curcumin loaded SLN; Green solid line refers to recrystallized bulk phase monostearin

It can be seen under the temperature gradient in this experiment, bulk phase monostearin will have hexagonal lattice structure(Hikosaka 2001). However, when the same temperature gradient is applied to fabricating SLN (Figure 13), a mixture of β and β' polymorphic forms are found. The presence of multiple polymorphic forms suggests that even after freeze drying, the conformation of lipid molecules could change in terms of tilt angle and packing patterns. The smaller of SLN the more unstable they will be thermodynamically. There are two ways to reduce the Gibbs energy: 1. Forming larger particles; 2. Change in molecule arrangement to more stable form. Therefore, it is possible that hot emulsification and cooling process, sintering effect or Ostwald ripening could have taken place. During storage, the major concern will be polymorphic transition. It is

possible that increasing the amount of surfactant will help since the addition of surfactant could kinetically (Nissim Garti 2001) retards polymorphic transformation.

Low crystallinity of curcumin

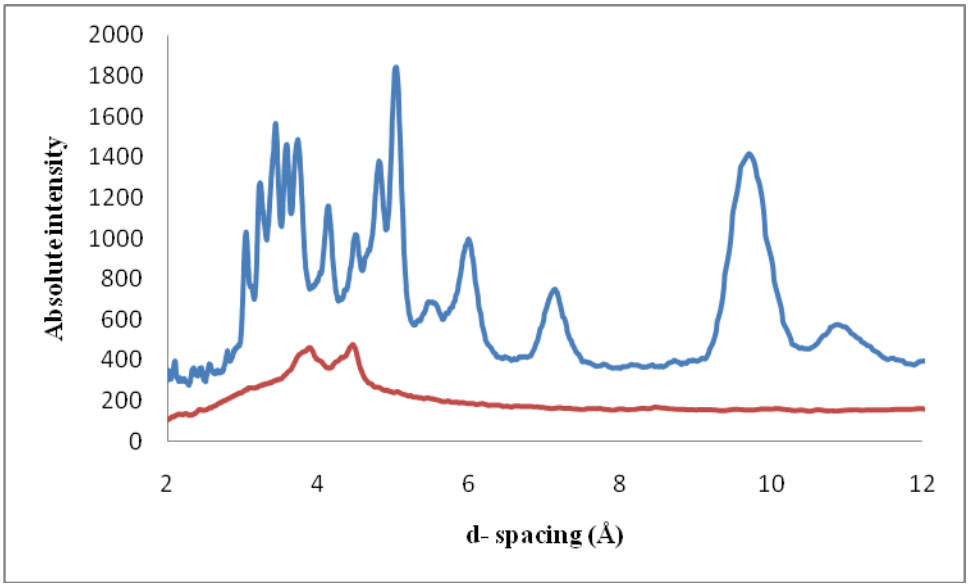

Figure 14 Diffractograms of bulk phase curcumin and curcumin loaded SLN. Blue solid line refers to bulk phase curcumin; Red solid line refers to curcumin loaded SLN

In the present study, only lipids crystals can be identified. Although curcumin has certain crystals in bulk phase, little crystals are formed in SLN. It is possible that majority of curcumin is in amorphous form.

Discussion

Surface enhancement of Raman signal

Due to the small size of lipid nanoparticles and the presence of high water content, Raman signal from SLN has high noise to signal ratio. Therefore it is critical to enhance signals of Raman spectra. Surface enhance on a flat surface is quite minor since the local field which

given by Fresnel equation is only twice of the incident field. The enhancement is much stronger for metallic surface when the momentum of the incident light matches the electromagnetic resonance of metal surface(Richard K. Chang and Thomas E.Furtak 1982). In this research, different substrates are used. Raw data are collected and compared with each other. The signal of lipid nanoparticles from 5 ml 2% lipid nanoparticles dispersion on glass plate is obtained. To increase the concentration of lipid nanoparticles centrifugation at 10000rpm for 30 minutes is applied. Precipitate is disposed on glass plate. Finally, 5 ml 2% lipid nanoparticles dispersion is disposed and dried on aluminum plate to utilize possible surface plasmon effect.

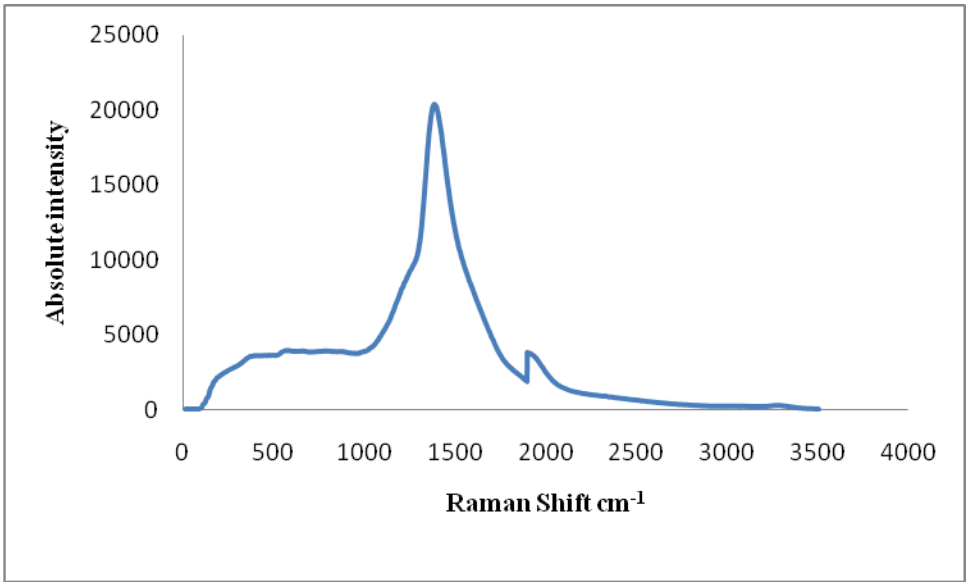

Figure 15 Raman spectra of SLN dispersion on glass substrate

When dispersion droplets are dried on glass slide, aggregation can be seen with visual exam. However, Raman spectra only show a strong peak at 1367 cm^{-1}. No other peak is shown. Therefore, concentration of lipid nanoparticles in dispersion must be increased.

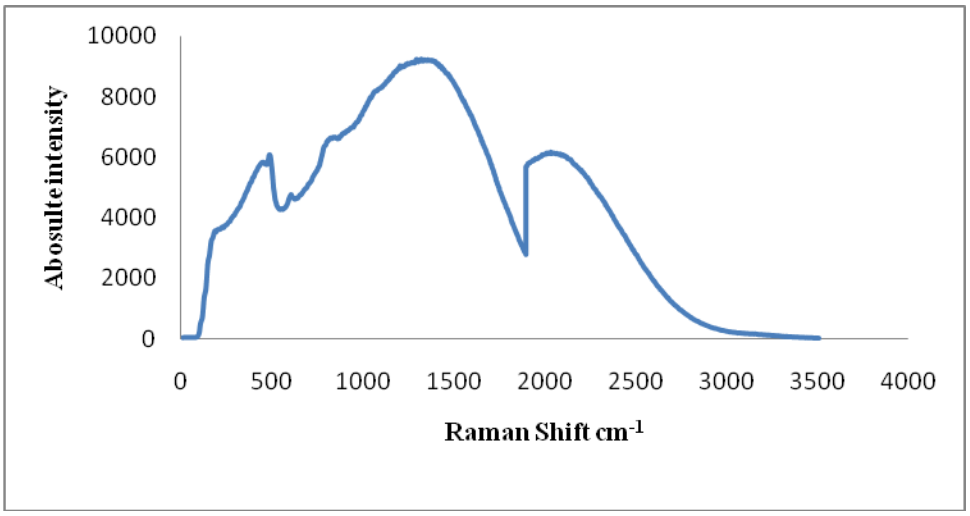

Figure 16 Raman spectra of SLN precipitate on glass substrate

After centrifugation at 10000rpm for 30 minutes, precipitate is mounted on glass slide. Multiple small peaks could be observed at different Raman shift. However, it is clear that the raw data has huge noise to signal ratio since peaks are not distinguishable by observation.

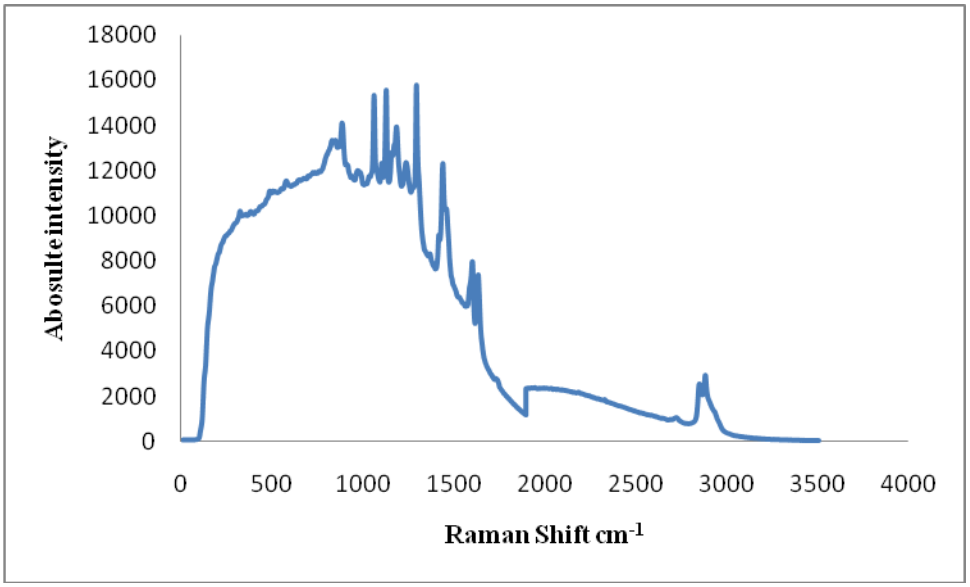

Figure 17 Raman spectra of SLN dispersion on aluminum substrate

5ml of 2% SLN dispersion is mounted on the surface of aluminum plate. Previously, this concentration has been proved to be undetectable when mounted on glass. When the SLN dispersion is dried, Raman spectrum is obtained under the same condition. A simple observation will find that the peaks are well defined. Therefore, Aluminum is chosen to be the substrate in this study.

Prediction of polymorphic by Raman spectroscopy

XRD and DSC are well established methods to study polymorphic forms of lipid crystals. In addition to these traditional methods, a few research reports have focused on using Raman spectroscope to identify polymorphic form due its high sensitivity to conformational changes.

In this study, combined with XRD and DSC data, feasibility of applying Raman spectroscope to identify different polymorphic forms of SLN complex is discussed.

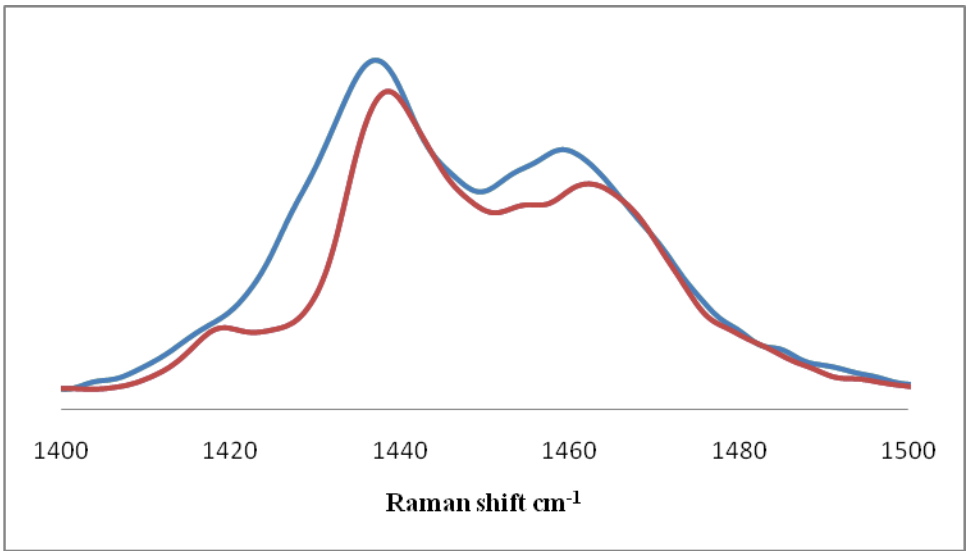

Figure 18 CH_2 scissoring vibration of α form (re-crystallized monostearin) and β (bulk phase monostearin)Blue solid line refers to (α form) re-crystallized monostearin; Red solid line refers to β form (bulk phase monostearin)

As shown in Figure 18, in Raman spectra re-crystallized bulk phase monostearin, no shoulder peak around 1410 cm^{-1} - 1420 cm^{-1} can be found in re-crystallized sample. This region is highly sensitive to different polymorphic forms of lipids (Da Silva, Bresson et al. 2009). In addition, research about lipid conformation also shows that the small shoulder peak at 1420 cm^{-1} disappears as temperature increases. Therefore, it is reasonable to believe that the disappearance of 1420 cm^{-1} peak in this experiment indicates the presence of α form.

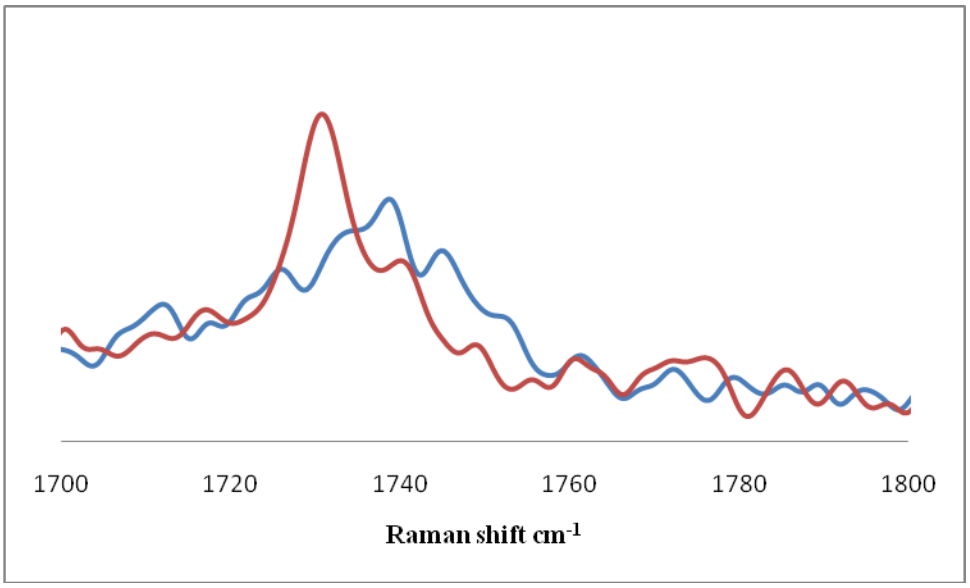

Figure 19 C=O stretching of α form (re-crystallized monostearin) and β form (bulk phase monostearin). Blue solid line refers to alpha form (re-crystallized monostearin); Red solid line refers to beta form (bulk phase monostearin)

Peak at 1730 cm^{-1} shifts to 1740 cm^{-1} in re-crystallized monostearin sample (see Figure 19). Previous research in tristearin and other triglycerides shows similar shifts (Bresson, El Marssi et al. 2006; Da Silva, Bresson et al. 2009). Da Silva et al. attributed to the shift of C=O to higher energy state of α form in their research results. It is possible the same explanation can be applied re-crystallized monostearin.

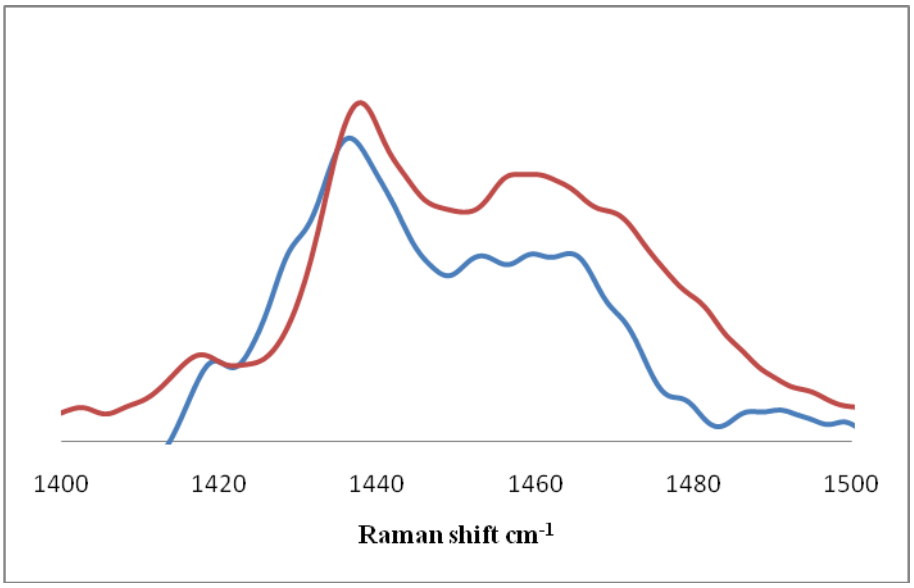

Figure 20 CH_2 scissoring vibration of curcumin loaded SLN and control SLN. Blue solid line refers to curcumin loaded SLN, Red solid line refers to control SLN

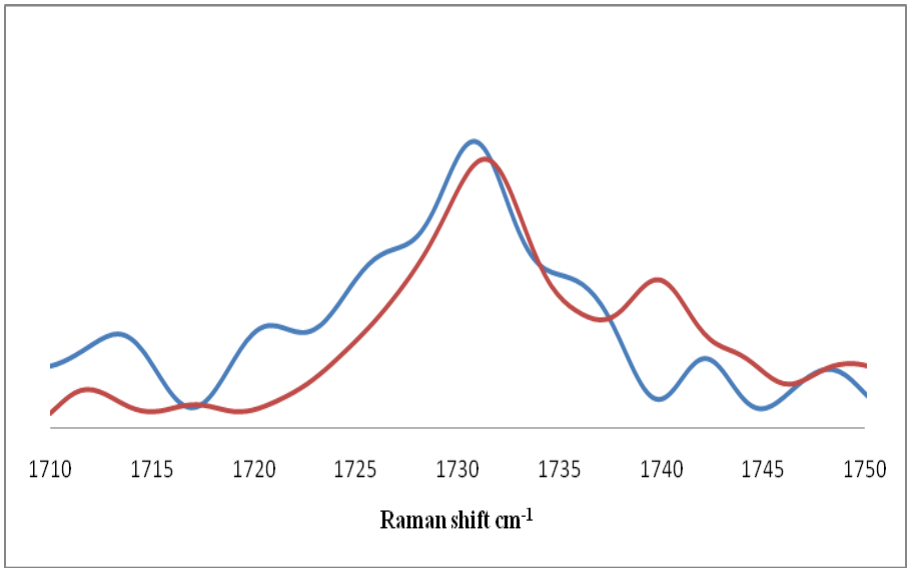

Figure 21 C=O stretching of curcumin loaded SLN and control SLN. Blue solid line refers to curcumin loaded SLN; Red solid line refers to control SLN

Raman spectra of CH_2 scissoring region shows that both curcumin loaded and control SLN have confirmed the existence of β form. In addition, spectrum of control SLN at C=O stretching region shows two peaks (Figure 21). Since monostearin only has one ester carbonyl group per molecule. The presence of double peaks (one at 1730 cm^{-1}, the other at 1740 cm^{-1}) in monostearin control SLN can only be explained by the presence of multiple polymorphic forms as XRD data and DSC have shown previously. In short, in this experiment, the change in Raman spectra is well correlated to polymorphic form transition.

Curcumin encapsulation and structural organization of fabricated SLN

Comparison between Raman spectra of bulk phase models and that of nanoparticles (Figure 8) suggests that curcumin loaded SLN have multilayer structure: a thin monostearin layer and curcumin/monostearin core. Specific Raman peak of curcumin in lipids/curcumin mixture is compared to that of bulk phase curcumin. No shift of curcumin specific peak is found, indicating that no chemical and detectable interaction between lipids matrix and curcumin occurs. Raman spectra of mixture of Tween 20 and curcumin shows peak shift from 1250cm^{-1} to 1238cm^{-1}, indicating presence of interaction between curcumin and Tween 20. This small shift is used as an indicator of the presence of curcumin on the surfactant layer.

Another experiment supporting the assumption of core shell structure is the curcumin stability study. 0.1 gram of freeze-dried sample is dispersed in 0.01mol/L NaOH solution (pH=12) for 5 hours and then washed with distill water once. Although extremely weak in intensity, curcumin specific peak could still be observed at 1700 cm^{-1} to 1800 cm^{-1} (Figure 10). Further experiment (not shown) with bulk phase curcumin/lipid mixture shows that

NaOH solution first causes swollen of the layer and penetrates the lipid layer causing degradation of curcumin. A closer visual comparison between spectra of NaOH treated SLN and curcumin/lipid mixture showed a extreme similar peaks at the region 1200 cm^{-1}-1300 cm^{-1} and 1400 cm^{-1}-1500 cm^{-1}, This indicates the presence of curcumin in the lipid core.

XRD study (Figure 13) reveals curcumin loaded SLN has dominant polymorphic form β whereas control SLN has multiple polymorphic forms. The presence of single rather than multiple polymorphic forms in curcumin loaded SLN can be attributed to fast polymorphic transition from α to more stable form. In another word, the presence of curcumin leads to faster polymorphic transition. In fact, since excessive curcumin could act as impurity in the crystallization process. It is possible that curcumin acts as nucleation sight and leads to faster nucleation which favors the formation of more stable polymorphic form on the surface when temperature drops. During solidification process, a proportion of curcumin is also pushed towards the core area as Raman study shows curcumin also presents in the core. XRD study shows a reduced absolute intensity in curcumin loaded SLN when compared to bulk phase material and control SLN. DSC study shows heat of fusion for curcumin loaded SLN is much higher than control SLN. These facts support the following process: When curcumin is pushed towards the core, it retards lipid molecule packed in a firmly manner. Since the greater pressure inside the particle, the solubility of curcumin in lipid could be higher than under normal condition. As it solidification process continues, some curcumin become partially crystallized and contributes higher heat of fusion.

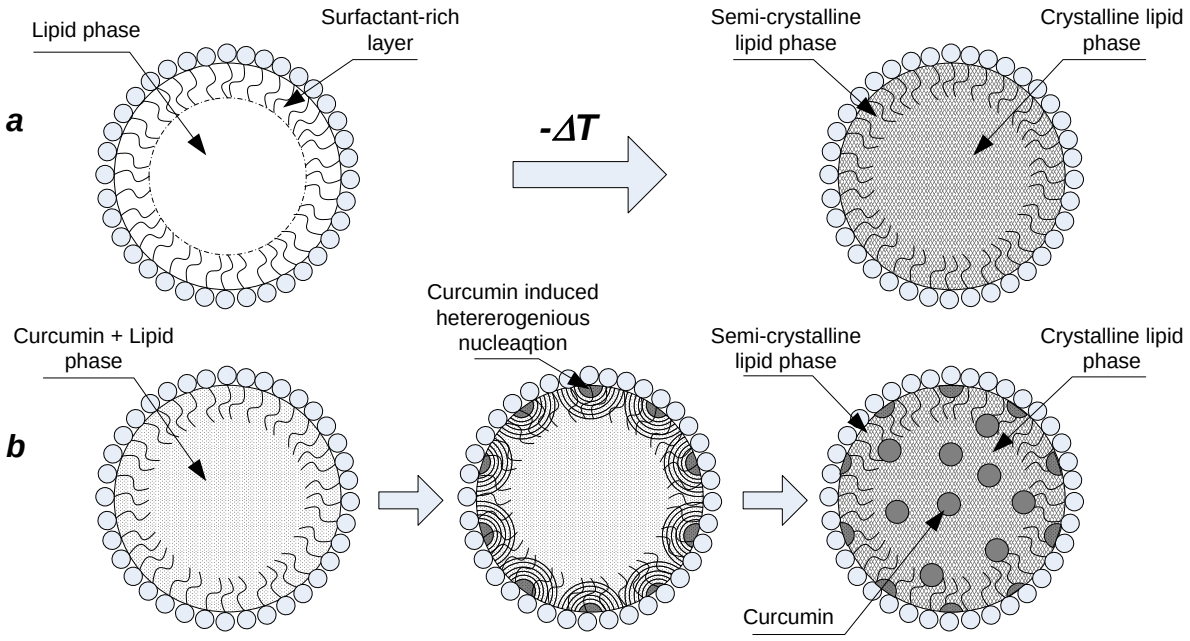

Figure 22. Proposed mechanism of SLN formation and encapsulation of curcumin

The formed particles are not stable and quickly formed aggregates due to insufficient nonionic surfactant on the surface. This contributes to the wide size distribution in DLS. In fact, when the beam power of TEM reached 85KV, it is observed that small spherical particles are melt down. Larger irregular particles form when the beam is moved away. Therefore, it is highly possible that during the cooling process, small solid particles are formed, and then joined together due to polymorphic transition.

Conclusion

Monostearin solid lipid nanoparticles are successfully fabricated via hot emulsification. Curcumin is encapsulated in SLN. Chemical stability of curcumin under alkaline condition (pH=12) is significantly improved after encapsulation. X-ray and DSC study shows that monostearin lipid nanoparticles have reduced crystallinity than well crystallized bulk

phase materials. During storage, curcumin leads to faster polymorphic transition and causes aggregation.

Introduction to curcumin loaded nanostructured lipid carriers

Nanostructured lipid carriers (NLC) are the second generation developed after solid lipid nanoparticles. In many cases, high crystallinity of solid lipid nanoparticles limits the drug loading capacity. In addition, fast polymorphic transition has been detected. Research has linked lipid polymorphic transition to more thermodynamically stable form with the aggregation of solid lipid nanoparticles and burst release of encapsulated compound.

Nanostructured lipid carriers are developed to overcome these limitations. NLC are composed of several different lipids instead of single kind of lipid. Applying multiple lipids leads to the presence of more imperfect crystals during crystallization. Consequently, higher loading capacity than SLN is expected. In addition, stability study of NLC has shown slower polymorphic form transition.

In this research project, different materials, including monstearin methyl stearate, oleic acid and polyethylene glycol are used to fabricate curcumin loaded NLC. Obtained particles are characterized by with the same method used in SLN characterization. The effects of methyl stearate, oleic acid and PEG on polymorphic transition of NLCs are major focus of this section.

Characterization of nanostructured lipid carriers

Dynamic light scattering study

Dynamic light scattering (DLS) shows that methyl stearate is able to reduce average size by 200nm (60% methyl stearate). The addition of oleic acid does not affect the average

particle size. PEG does not affect particle size in of lipid nanoparticles without curcumin either.

In the presence of curcumin，60% of methyl stearate reduces the average particle size by 500 nm. The addition of even 5% of oleic acid into the formulation will reverse the size reducing effect of methyl stearate. 10% of oleic acid shows average size reduction effect (from 787nm to around 430nm). Continue increasing oleic acid 20% shows a dramatic increase in average particle size. The addition of another co-surfactant PEG-SA in the presence of 5% oleic acid is able to reduce average particle size. In fact, 5% PEG-SA is able to keep the average size around 400 nm. Continue increasing PEG level does not affect average particle size

Table 6 Hydrodynamic diameters of different NLC

	GMS	40%MS	60%MS	5%OA	10%OA	20%OA	5%PEG	10% PEG
Curcumin loaded particles(nm)	772.2	859	203.2	787.8	437.5	800	471.4	463
Control particles(nm)	399.3	418	191.4	158.6	193.1	157	160.1	184.1

In addition to average particle size, Intensity distributions are also collected to reveal more detailed information on the effect each component on size distribution of NLC dispersion.

The size effect of methyl stearate is shown below (Figure 23). The blue line is intensity distribution of lipid nanoparticle composed solely of monostearin. Replacing 40% monostearin with methyl stearate in the formulation leads to reduction in the intensity of peak at 1000nm. This indicates less aggregation occurs during storage in the case of methyl stearate NLC. Continue increasing the usage of methyl stearate to 60% results in bimodal distribution with all detectable lipid nanoparticles below 400nm.

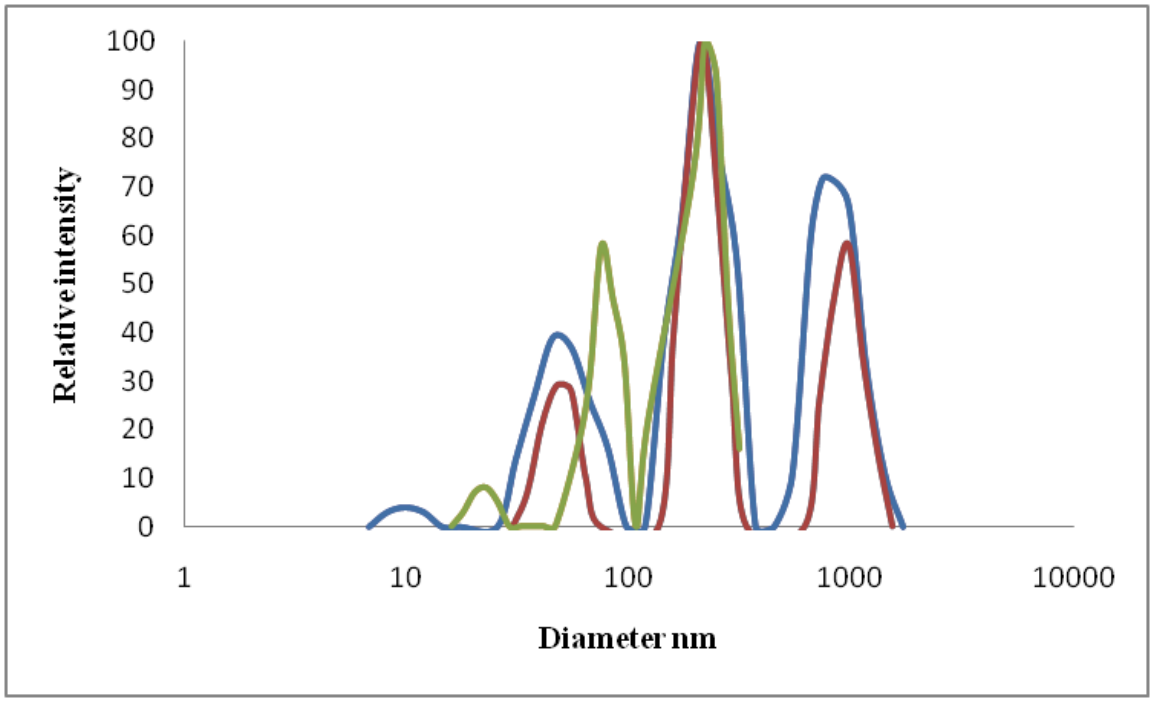

Figure 23 Effect of methyl stearate on size distribution in aqueous environment. Blue solid line refers to monostearin SLN; Red solid line refers to NLC composed of 40% methyl stearate and 60% monostearin; Green solid line refers to NLC composed of 60% methyl stearate and 40% monostearin

With 5% oleic acid added into the formulation which originally composed of 60% methyl stearate and 40% monostearin, a broad peak ranges from 60nm to 400nm appears. A little joint peak with peak appears at 33nm. 10% Oleic acid results in biomodal distribution with peaks value at 69nm and 215nm. Continue increasing oleic acid usage to 20% leads to 1.

Smaller particle size; 2. Narrowing of size distribution. The peak at 164nm in 20% Oleic acid has a peak width of 100nm while the peak at 215nm (in 10% oleic acid NLC group) has 250nm peak width.

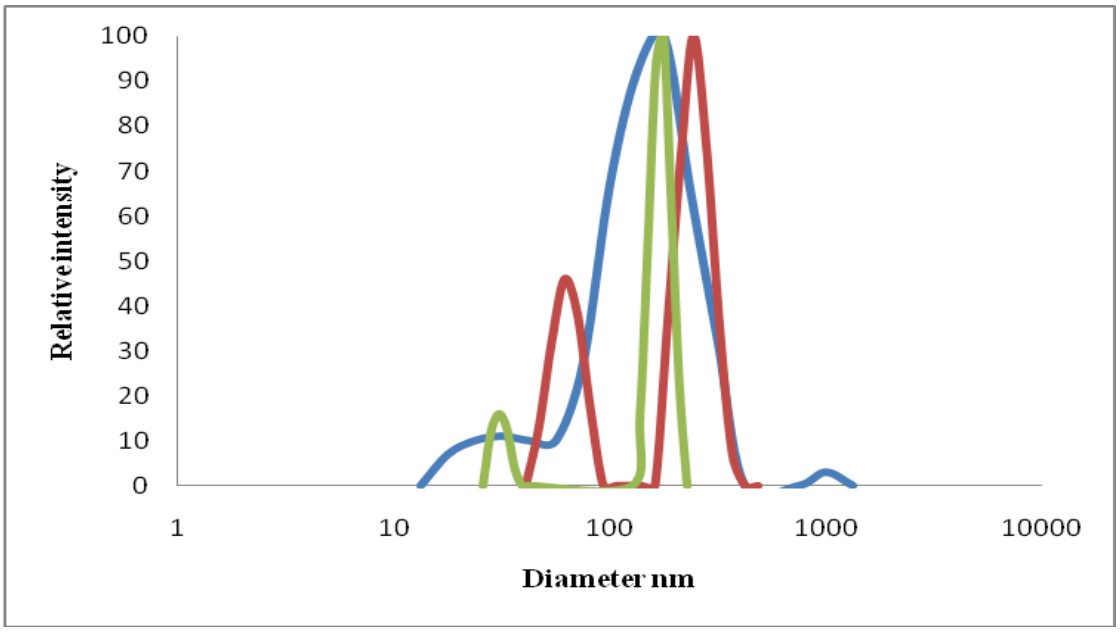

Figure 24 Effect of oleic acid on size distribution. Blue solid line refers to NLC composed of 5% oleic acid; Red solid line refers to NLC composed of 10% oleic acid; Green solid line refers to NLC composed of 20% oleic acid

Based on 5% oleic acid NLC, PEG-SA is added as replacement for methyl stearate. 5% of poly ethylene glycol does not change the size distribution. Continue increasing PEG level to 10% leads to bimodal distribution of NLC. Two peaks appear at 68nm and 256.7nm respectively. In addition, size distribution narrows by 52% with the increase of PEG from 5% to 10%.

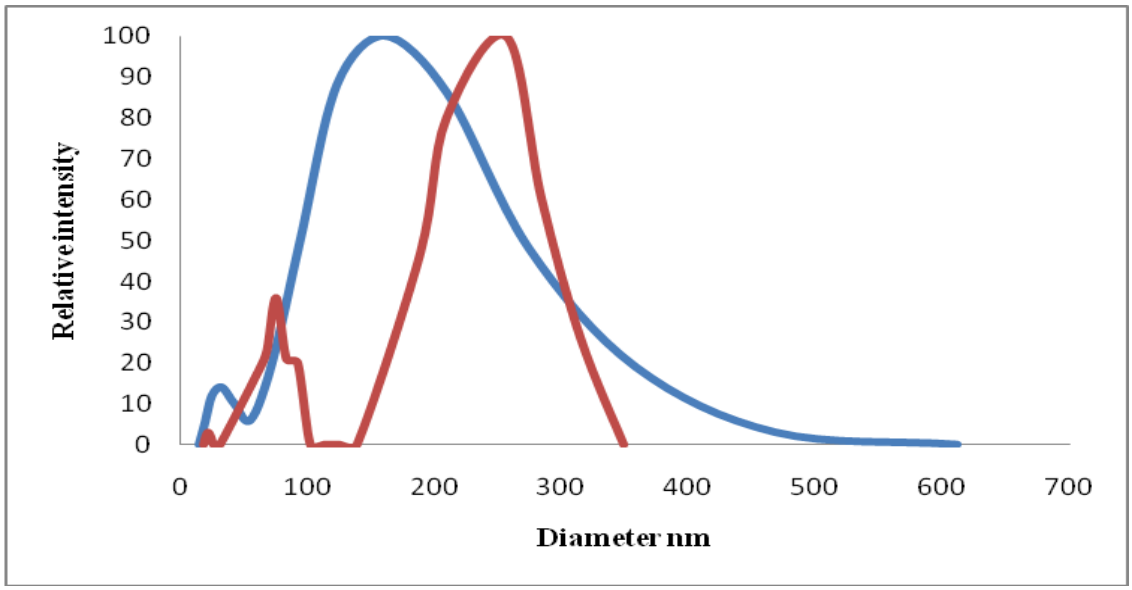

Figure 25 Effect of poly ethylene glycol (PEG) on size distribution. Blue solid line refers to NLC composed of 5% PEG; Red solid line refers to NLC composed of 10% PEG

In the present study, curcumin effect on methyl stearate NLC is explored. Blue solid line refers to NLC without curcumin while red lines refer to curcumin loaded particles. (Figure 26 A,B,C) shows that the addition of curcumin resulted in decreasing in intensity of "small particles" fraction while increasing in intensity of "larger particles" fraction. When the ratio of methyl stearate to the total mass of lipid mixture reached a certain level, (in this experiment, when methyl stearate reached 60% of the total mass of lipid mixture) average particles size is significantly reduced (Table 6). Comparison between Figure 26 A, B and C reveals that methyl stearate decreasing intensity of peak at 1 micrometer. Especially, the size distribution of 60% methyl stearate is significantly narrowed: all below 1000 nm. The similar pattern between 60% methyl stearate NLC and curcumin loaded 60% methyl stearate NLC shows methyl stearate does not interact with curcumin molecule.

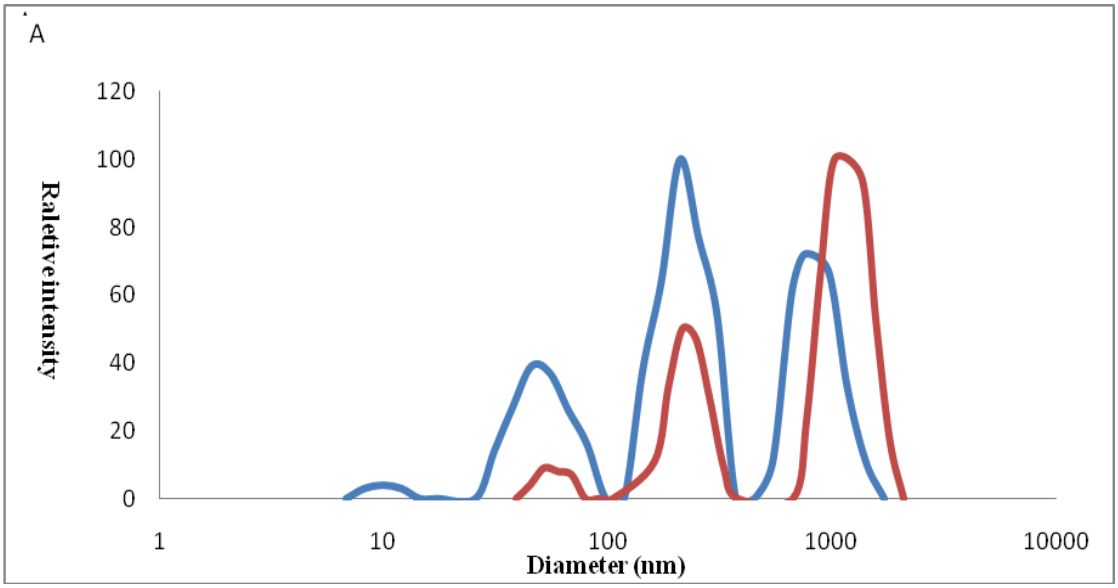
A
120
100
80
60
40
20
0
Raletiveintensity
1
10
100
1000
10000
Diameter (nm)

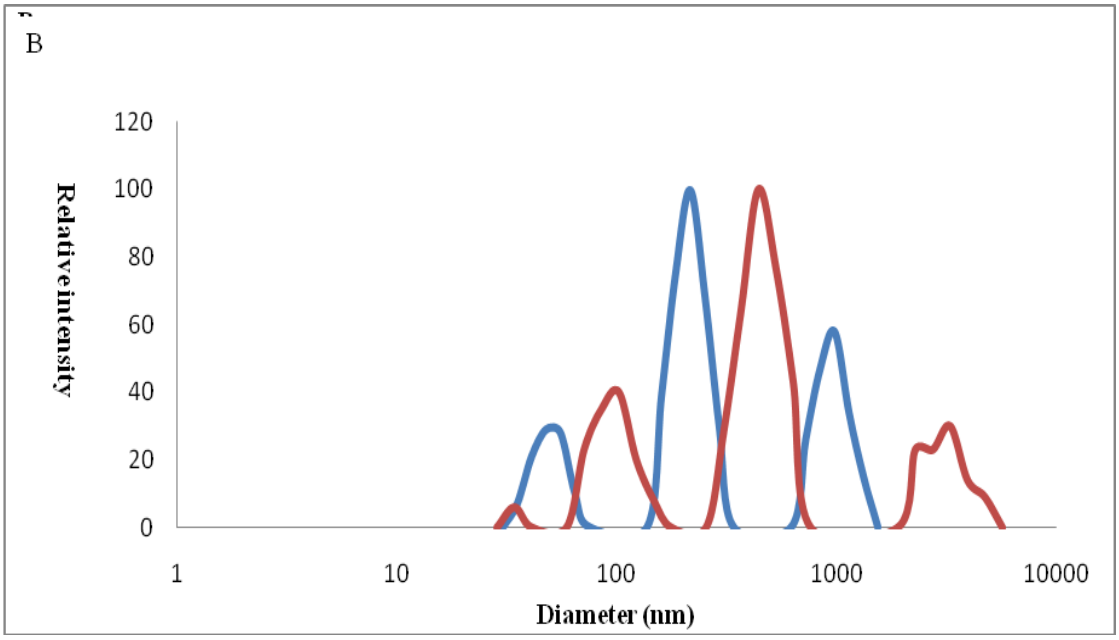
B
120
100
80
60
40
20
0
Relativeintensity
1
10
100
1000
10000
Diameter (nm)

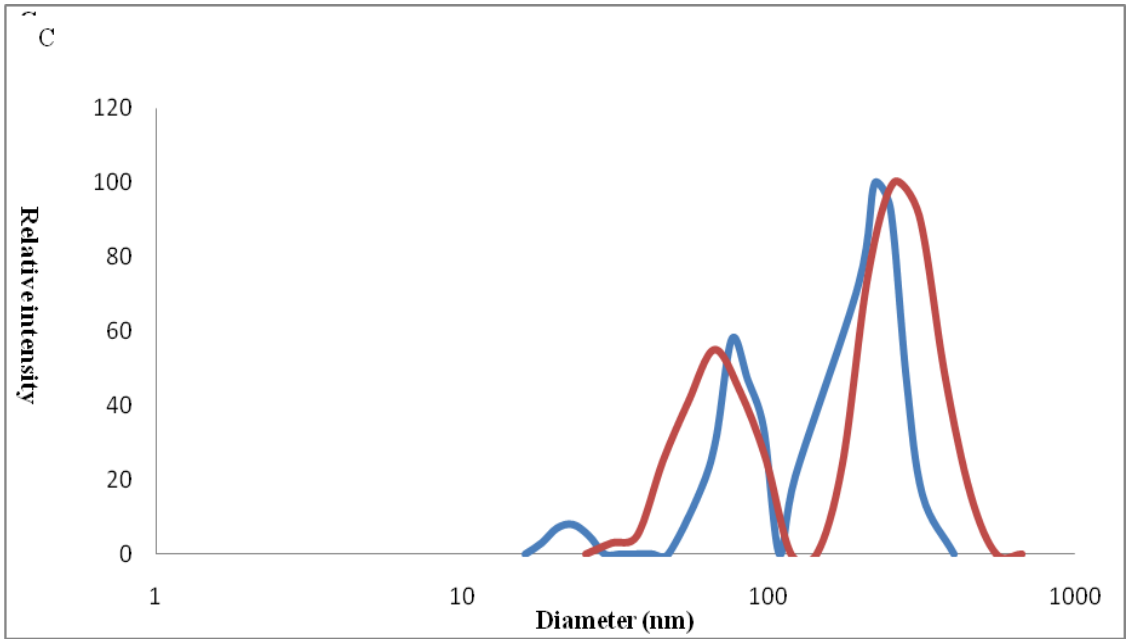

Figure 26 Size distributions of curcumin loaded NLC with differnt proportion of methyl stearate. Fig 26 A:Blue solid line refers to size distribution of monostearin particles without curcumin, while red solid line refers to that of monostearin particles loaded with curcumin; Fig 26 B: Size distribution of particles with 40%(w/w)methyl stearate. Blue solid line refers to particles without curcumin, while red solid line refers to particles loaded with curcumin. Fig 26 C: Size distribution of lipid nanoparticles with 60% methyl stearate. Blue solid line refers to particles without curcumin, while red solid line refers to particles with curcumin

In curcumin loaded oleic acid NLC, encapsulation of curcumin leads to the increase of average particle size (Figure 27A,B,C). Intensity distribution shows two major changes of curcumin loaded sample when compared to control group. First, new peak at 1000nm appears, peak in this region broadens as the usage of oleic acid (from 5% to 20%) increases. Second, the addition of curcumin also induces the formation of small particles at 100 nm. The relative intensity of peak in this region also increases as the usage of oleic acid. At 20% oleic acid, it joined the peak at 100-1000nm region and become

indistinguishable. This indicates that curcumin and oleic acid could be on the surface of NLC and interact with each other. This leads to 1. Modification the surface morphology of NLC; 2.Formation of small particles;

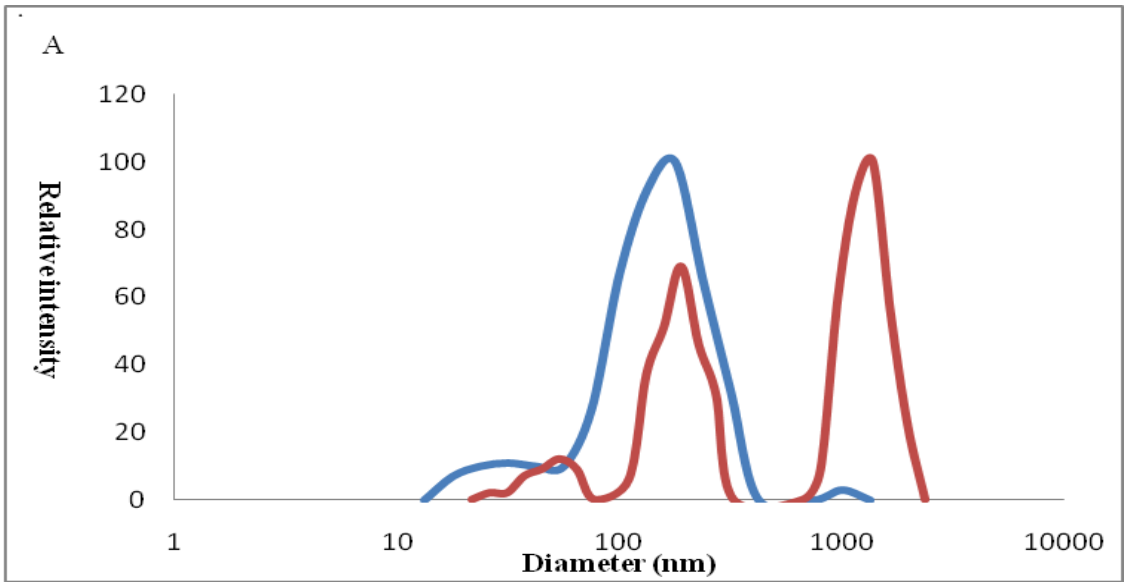

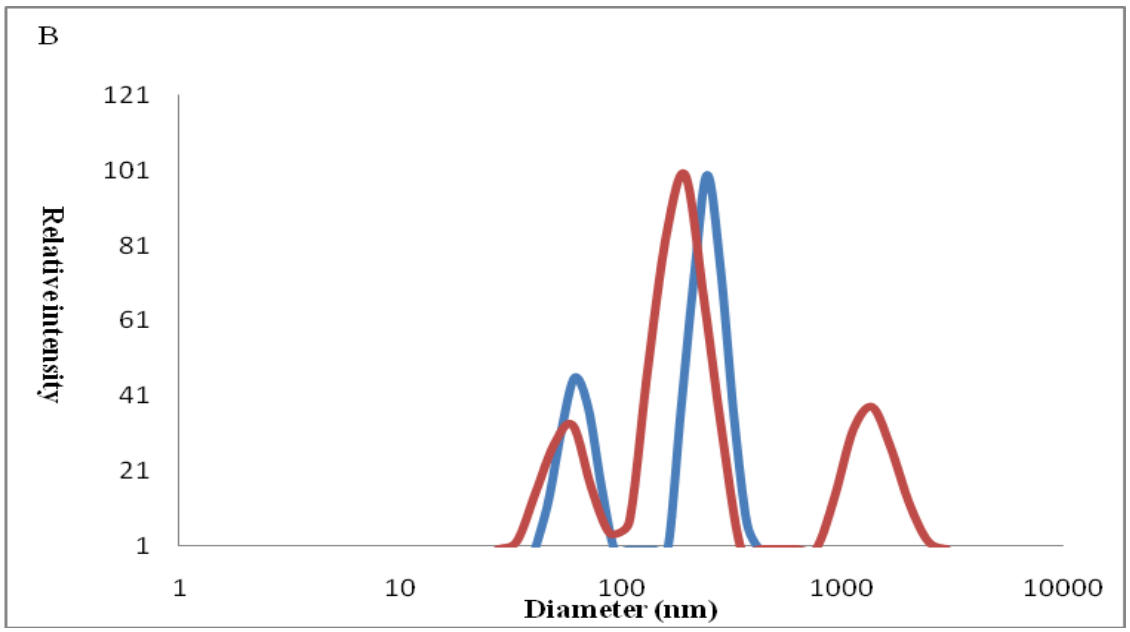

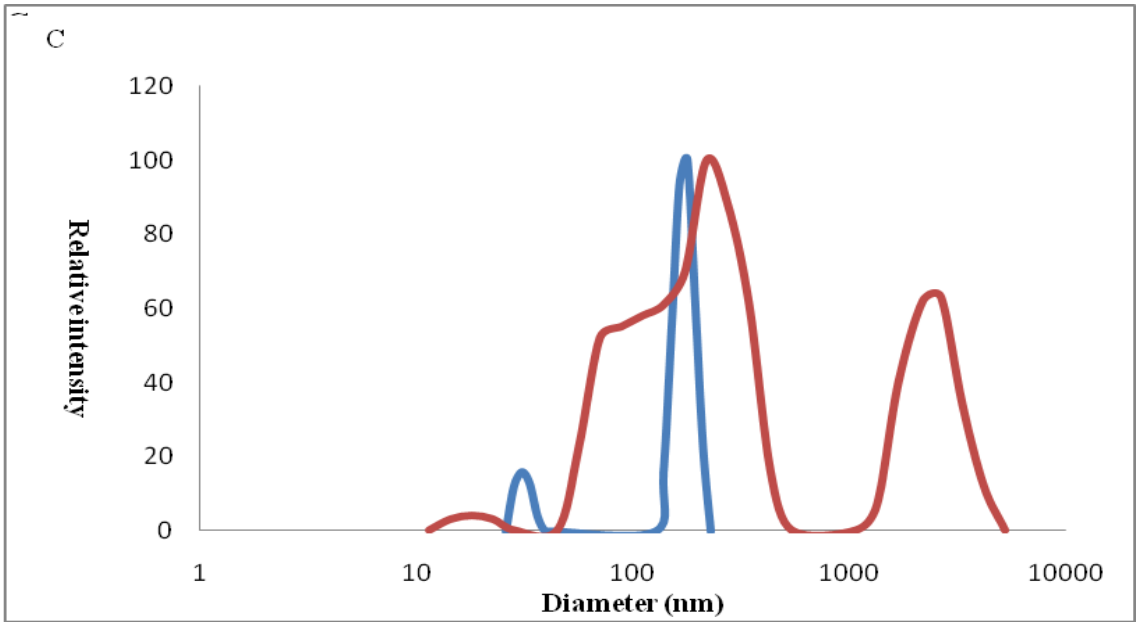

Figure 27 Size distribution of curcumin loaded NLC with different proportion of oleic acid. The ratio of monostearin to methyl stearate is maintained the same while different amount of oleic acid is added. Red solid lines represent curcumin loaded particles while blue line refers to corresponding control particles. The percentage is the w/w of oleic acid to total mass of lipid mixture Fig 27 A: 5% oleic acid. Fig 27 B: 10% oleic acid, Fig 27 C: 20% oleic acid

When curcumin is loaded in PEG NLC, new peak at 1000 appears when compared to control NLC(Figure 28A,B). Compare with curcumin loaded sample in Figure 28 A and Figure 27 B reveals that curcumin only induces peaks at 1000nm. Majority of the particles still have a size around 400nm. In addition, comparison between the size intensity distribution of curcumin 5% oleic acid and curcumin 5% PEG sample reveals that the addition of PEG either reduce the formation larger particle or prevent aggregation, since the relative intensity at 1000nm decreases after introducing PEG in the formula.

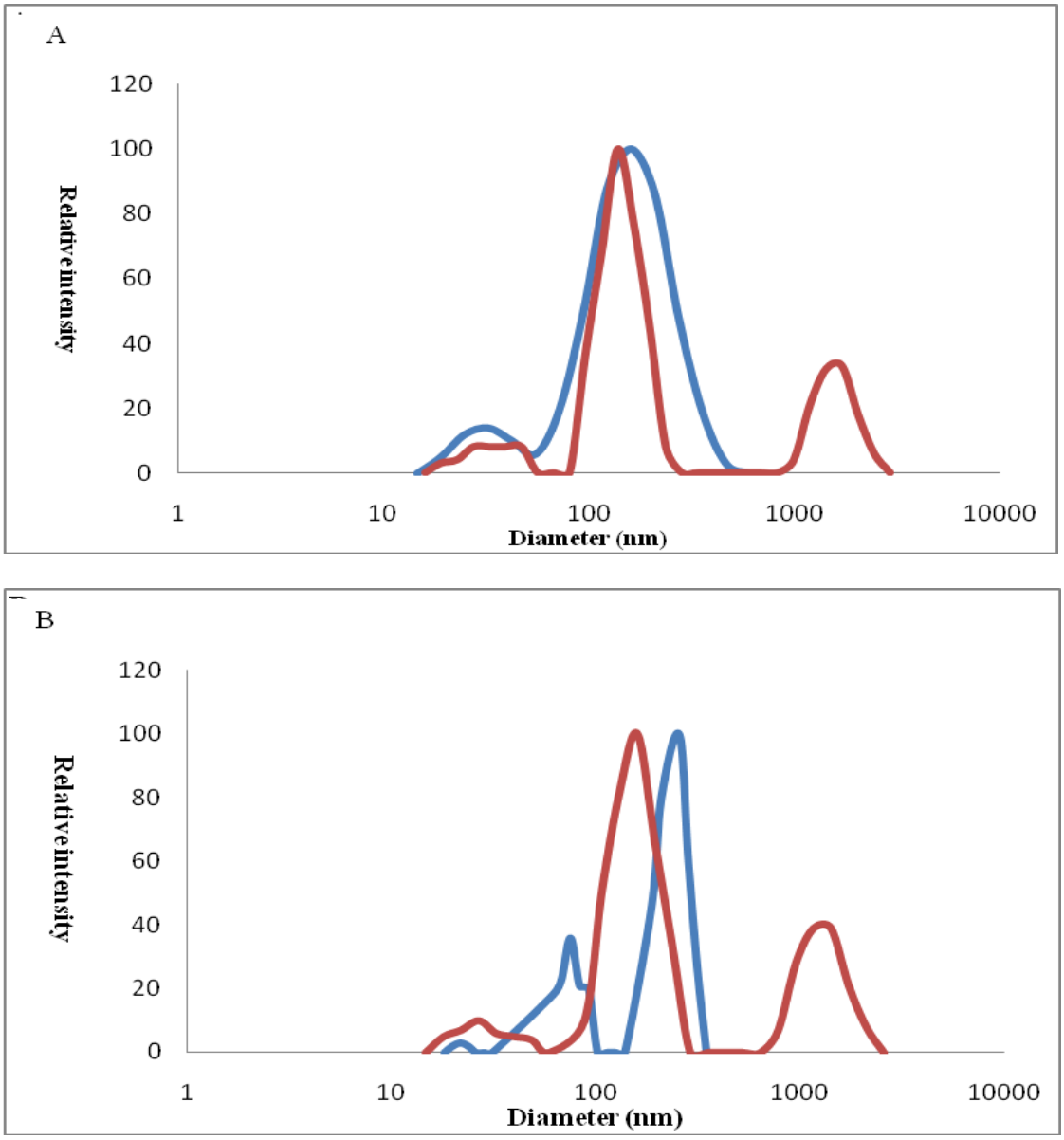

Figure 28 Size distribution of curcumin loaded NLC with different proportion of PEG . Maintaining 5% oleic acid and replace the same weight of methyl stearate with PEG. The percentage is the w/w of PEG to total mass of lipid mixture. Fig 28 A: 5% PEG, Fig 28 B:10% PEG

The addition of methyl stearate, oleic acid and PEG 400 in the formula is able to narrow down size distribution in lipid nanoparticles without curcumin. (Peaks became sharper and shifted to smaller diameter). However, different pattern in curcumin loaded particle could

be observed. This indicates the interaction of curcumin between different components affects the surface property during nucleation and crystallization process.

TEM study of NLC

TEM study shows that the addition of methyl stearate leads to formation of spherical particles around 50nm. However, aggregation could be seen from the photo (Figure 29). In addition, joint particles also appeared in the picture. This could be attributed to the small diameter of lipid nanoaparticles. It may also indicate that not enough surfactant covers the surface of each particle.

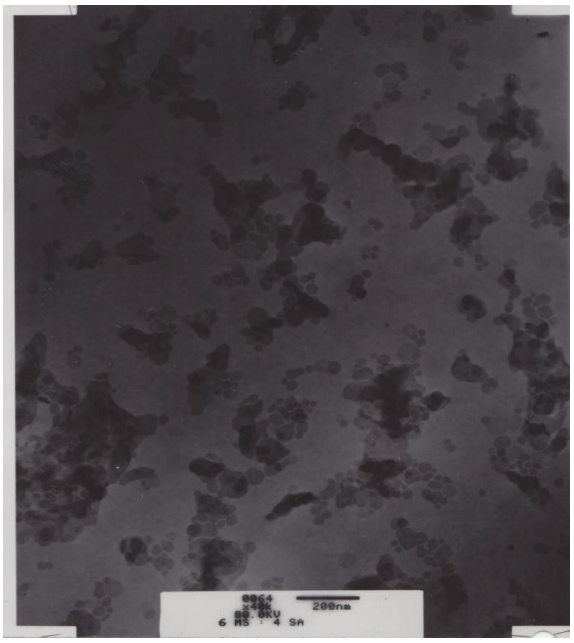

Figure 29 TEM photo of curcumin loaded NLC composed of 60% methyl stearate

The addition of oleic acid modifies the surface of the lipid nanoparticles (Figure 30). First of all, small spherical particles around 20 nm appear in the photo. Second, these spherical

particles form pearl network. This happened to fit the description by Muller (Muller, Petersen et al. 2007), in which NLC form pearl net work.

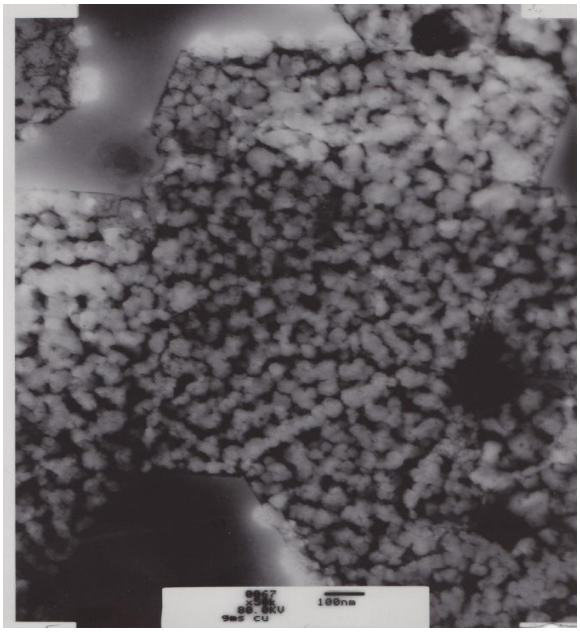

Figure 30 TEM photo of curcumin loaded NLC composed of 20% oleic acid

Co-surfactant PEG theoretically should stabilize particles in aqueous dispersion. However TEM photo shows otherwise. Large aggregation with diameter of more than 500nm appeared (Figure 31).

Figure 31 TEM photo of curcumin loaded NLC composed of 10% PEG

Raman spectroscopy study

This part of the study is carried out to: 1.confirm the encapsulation of curcumin in NLC; 2.study conformation changes induced by the addition of different component; 3.explore the possible interaction between different components.

Encapsulation of curcumin in lipid nanoparticle

Similar to Chapter 1, spectra of monostearin, methyl stearate, oleic acid, PEG-SA, curcumin and Tween 20 are taken (Figure 33). Specific peaks that can act as finger print for specific component are identified with the aid of software. The peaks and their implications are listed below (

Table 7).

The presence of curcumin, in this case, can be confirmed if curcumin specific peaks appear in the spectrum. Figure 32 is a typical Raman spectrum of curcumin NLC. No major shift is found in the spectra, indicating no chemical reactions took place during assembly process.

The of peaks at 1184 cm^{-1},1250 cm^{-1},1607 cm^{-1} 1 1627 cm^{-1} in curucmin loaded NLC confirm the encapsulation of curcumin . When compared to bulk phase curcumin, the well defined peaks for curcumin become broader; Peaks such as peaks at 1151 cm^{-1} 1206 cm^{-1} disappears after encapsulation due to overlapping with peak from other components.

In most NLC, small shift indicates 1254 cm^{-1} to 1238 cm^{-1} is found, since this peak indicates the hydroxyl group on curcumin, shift to lower Raman shift indicates the formation of hydrogen bond or other type of weak forces. When compared to unassembled samples (bulk phase mixture without Tween 20), no shift is observed. This suggests lipid components does not interact with curcumin. On the other hand, similar shift to lower Raman shift is detected when curcumin is mixed with Tween 20. This suggests that curcumin is able to form hydrogen bond with Tween 20.

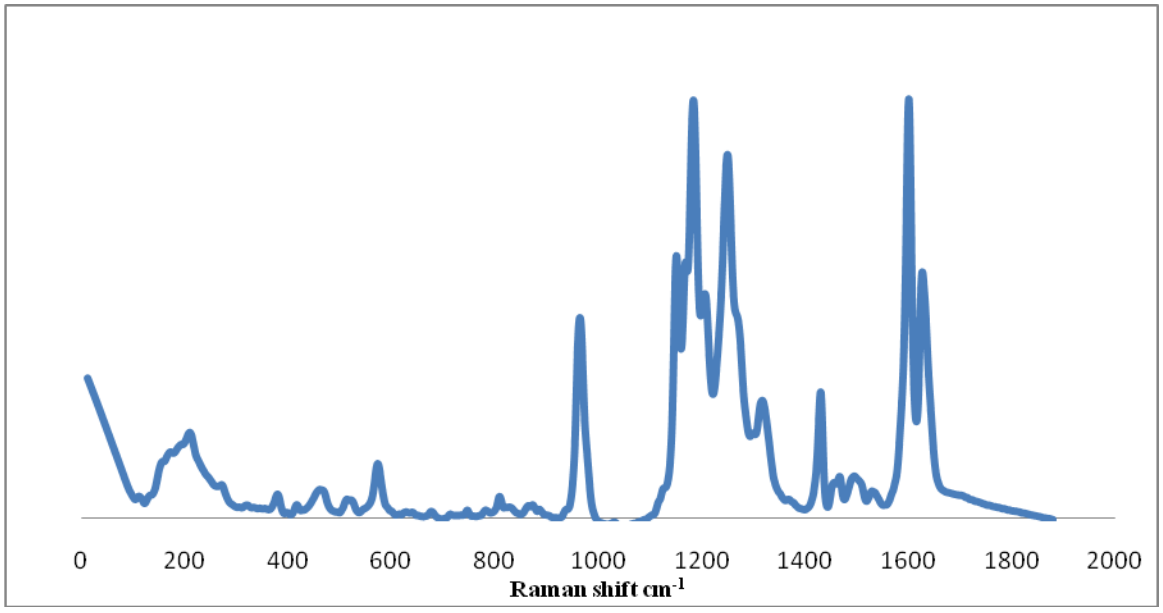

Figure 32 Typical spectra of curcumin in NLC. Curcumin specific peaks at 1184 cm^{-1},1250 cm^{-1},1601 cm^{-1} and 1627 cm^{-1}

The spectra of major lipids are shown below:

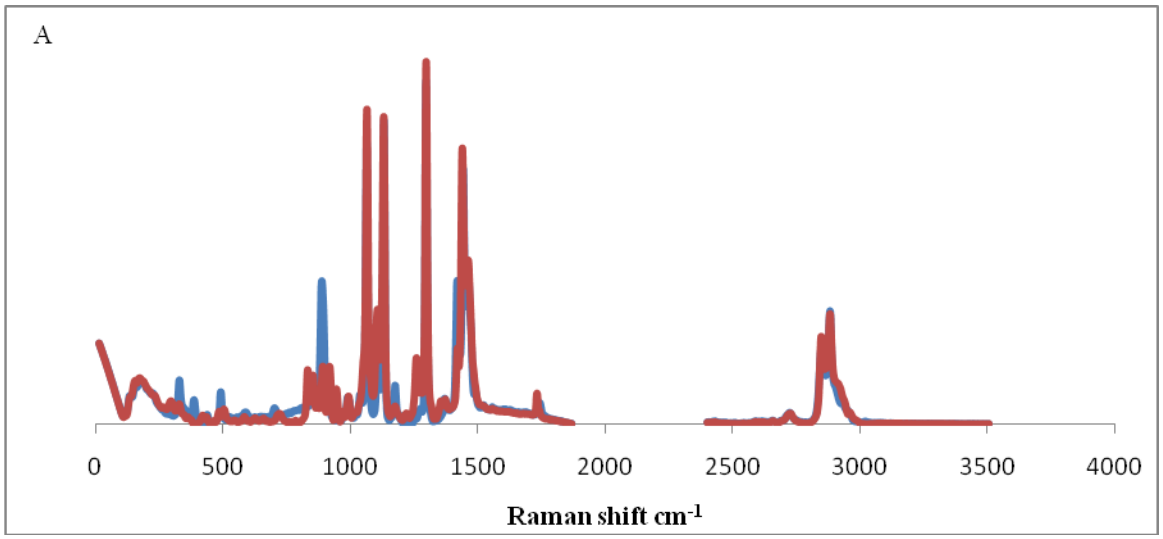
A
0
500
1000
1500
2000
2500
3000
3500
4000
Raman shift cm-1

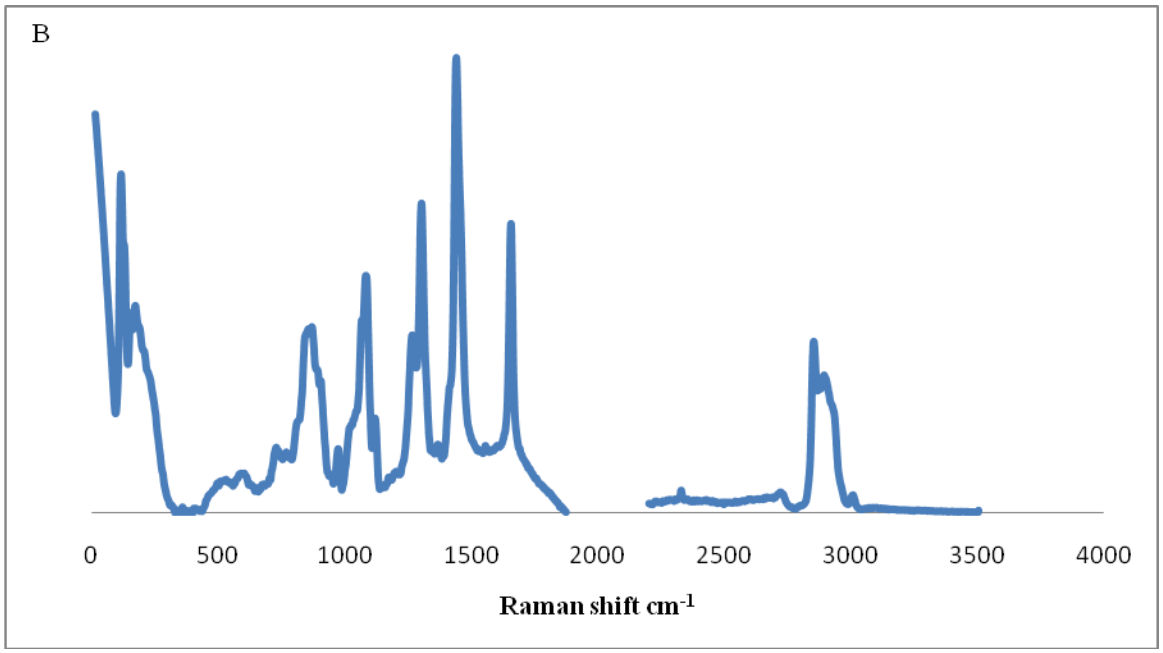
B
0
500
1000
1500
2000
2500
3000
3500
4000
Raman shift cm-1

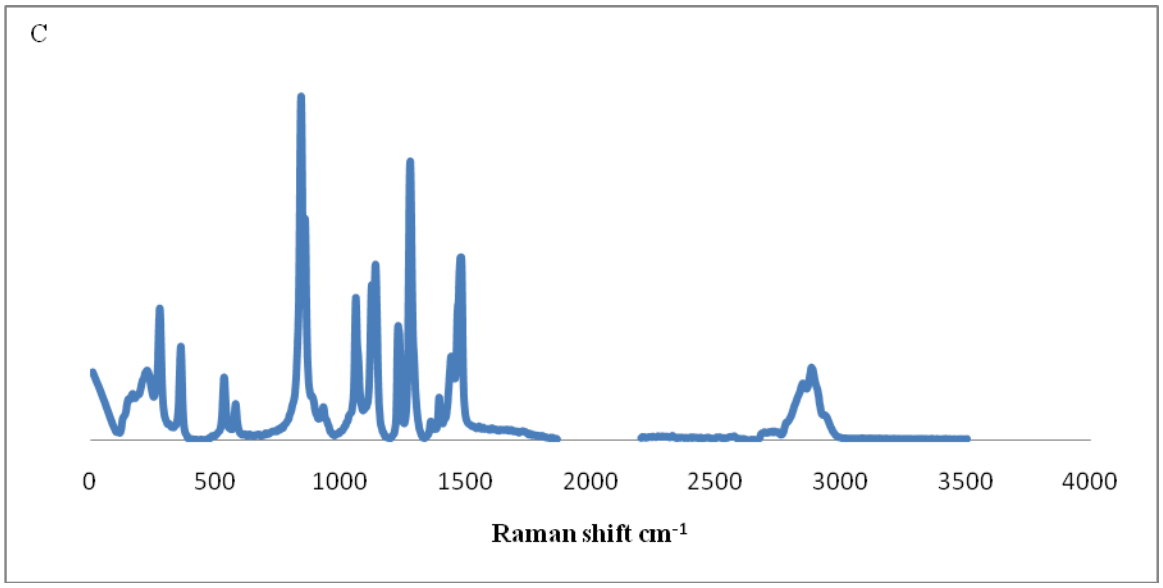

Figure 33 Spectra of bulk phase materials. Bulk phase lipids (A): monostearin and methyl stearate.The blue solid line refers to methyl stearate; the red solid line refers to monostearin (B) Bulk phase oleic acid (C) Bulk phase PEG-SA

Table 7 Raman assignment to molecular vibration

Peaks (cm^{-1})	assignment	indication
2882	CH_2 asymmetric stretching	
2847	CH_2 symmetric stretching	The ration of Iasy/Isym is used to give quantitative measurement of the mobility of alkyl chains.
1731,1741	C=O stretching	Lipid
1627	C=C stretching, C=O stretching	Curcumin
1601	C=O stretching, C=C stretching (benzene ring)	Curcumin
1495	Aromatic ring stretching and in-plane bending	Curcumin
1467	CH_3 in-plane bending	

1462	CH_2 deforming	Lipid
1439	CH_3 asymmetry deforming	Lipid
1430	CH_3 in-plane bending	
1295	Skeleton vibration	Lipid
1250	Aromatic CCH in plane bending; enolic part COH bending	Curcumin
1184	C-C in-plane bending; CH3 in-plane bending(connected to keto part) (C-O-C)	Curcumin
1151	Phenyl C-C-H in-plane-bending C-O-C in plane bending	Curcumin
1129	C-C stretching	
1062	Asymmetric C-C skeletal vibration	
889	C-O-C	Alkyl chain

Chain mobility: 3000 cm^{-1} to 2800 cm^{-1}

The range 3000 cm^{-1}-2800 cm^{-1} in this research is attributed to the CH_2 stretching vibration. A number of groups who have studied this region(Larsson and Rand 1973) agreed with each other on the point that CH_2 stretching is sensitive to the different packing pattern of lipids. It is reported that the presence of peaks near 2860 cm^{-1} is evidence to the existence of triclinic lattice, while vibration, at lower Raman shift to 2850 cm^{-1}, indicates the presence of hexagonal lattice. (Huang, Mason et al. 1983) studied this region and concluded in their work that study in this region were able to yield information of both intra-chain conformation and inter-chain interactions. The relative intensity ratio between

symmetric to asymmetric peaks serves as a measure of the mobility of lipid chain(Orendorff, Ducey et al. 2002). More recently, the use of intensity ratio of these two vibrations is reinforced by the study of(Bresson, El Marssi et al. 2006). Similar approach is applied to the study of characterization of the three major polymorphic forms and liquid states of tristearin by (Da Silva, Bresson et al. 2009).

In this research the comparison of the relative intensity ratios between the asymmetric stretching vibration (2880 cm^{-1}) and symmetric stretching (2840 cm^{-1}) of NLC, curcumin loaded NLC and unassembled sample are listed below

Table 8 I(2880 cm^{-1})/I(2340 cm^{-1}) The ratio is an indicator of chain mobility. Higher value indicates the lower chain mobility

	GMS	40%MS	60%MS	5%OA	10%OA	20%OA	5%PEG	10%PEG
Curcumin loaded NLC	1.17897	1.27966	1.17490	1.03990	1.03003	1.02332	1.1591	1.051724
Control NLC	1.23809	1.22429	1.24795	1.10029	1.19782	0.98643	1.09945	1.26009
Unassembled sample	1.26066	1.21020	1.24870	1.24912	1.15957	1.13686	1.22764	1.15957

The higher the ratio, the less the alkyl chain mobility, and the more strict the packing pattern. Comparing unassembled sample and particles with curcumin, one could find unassembled samples usually have higher value than real colloidal system. Since the only difference between curcumin loaded NLC and unassembled sample is the presence of surfactant, therefore, its difference can be partially attributed to incorporation of Tween 20 onto the surface.

The presence of methyl stearate does not change the ratio indicating that methyl stearate does not affect the chain mobility. The addition of oleic acid, increases the chain mobility, it is possible due to the fact that oleic acid is liquid oil and occupies the imperfection NLC and inhibits the formation of well crystallized lipid crystals. In addition, it also suggests that oleic acid could be near the surface of the NLC.

Molecule arrangement: 1500 cm^{-1} to 1300 cm^{-1}

This region composed of CH wagging and bending modes (scissoring, degenerate, deformation), which is sensitive to packing pattern of the carbon chain. Researchers have used this region to explain the lipid molecules arrangement during crystallization. ((Bunow and Levin 1980; Da Silva, Bresson et al. 2009). Lots of Research, such as the one done by Eric showed that different peaks shape can be used as indication of different polymorphic form of lipid crystal. Other researchers associate crystal sub cell structure (hexagonal etc) (Mendelsohn and Moore 1998) to peaks at 1400-1500 cm^{-1}. For example, 1440 cm^{-1} is due to the CH_2 scissoring vibration. This peak shape contains information about chain packing(Gaber, Yager et al. 1978). In addition to the presence of peaks at different Raman shift in this region, the broadening of these peaks is also an indicator of increasing disorder in molecular arrangement.

In the present study, three peaks at 1418 cm^{-1}, 1437 cm^{-1} and 1458 cm^{-1} are studied to review the molecule arrangement of different NLC. In general, three peaks in NLC spectra are broader but weaker than their bulk phase mixture. This is due to the addition of surfactant and weak scattering effect due to small size.

In NLC composed of methyl stearate (Figure 35), peak at 1437 cm^{-1} shifts to 1440 cm^{-1} with the increasing proportion of methyl stearate. The spectra of bulk phase methyl stearate and monostearin show that methyl stearate has a peak at 1440 cm^{-1} and monostearin has a peak at 1437 cm^{-1}(Figure 34). Therefore, the shift can be attributed to the increasing proportion of methyl stearate. In addition, the width of the three consecutive peaks does not change indicating that methyl stearate may not affect lipid molecules arrangement. (Bresson, Marssi et al. 2005) (Figure 34,Figure 35)

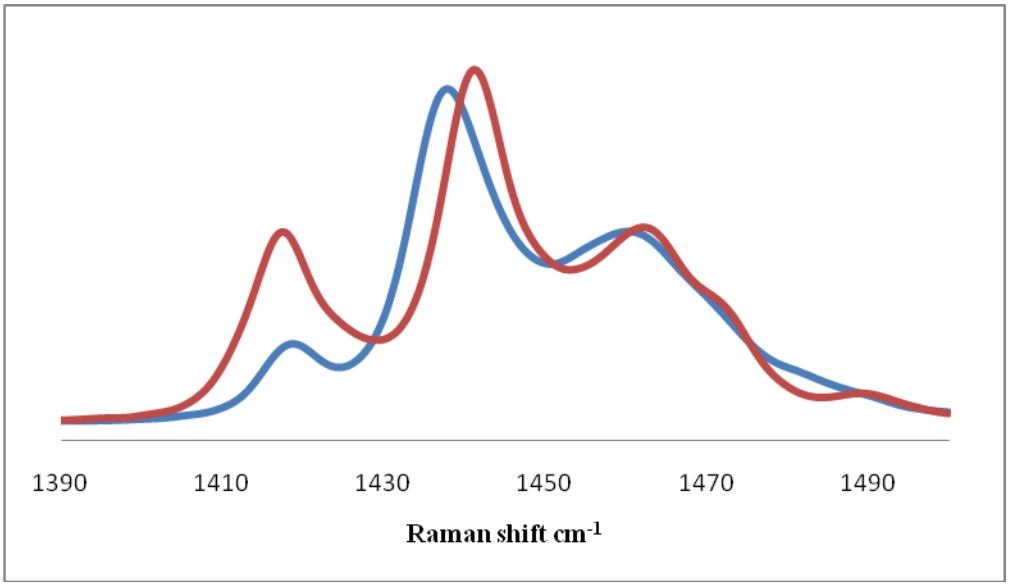

Figure 34 Scissoring vibration of monostearin and methyl stearate, Blue solid line is bulk phase monostearin; Red solid line is bulk phase methyl stearate

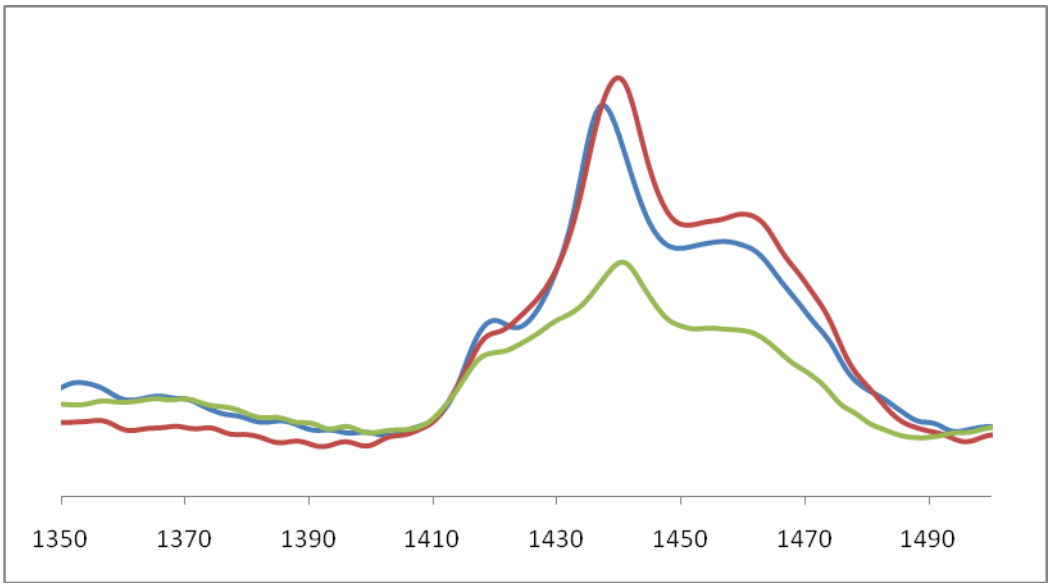

Figure 35 Shift of peak at 1440cm^{-1} 1440 cm^{-1} with increasing proportion of methyl stearate. In addition, one should notice that the relative height of this peak decreased with increasing amount when use 1420 cm^{-1} as reference. Green solid line refers monostearin particles without curcumin; Red solid line refers to NLC composed of 40% methyl stearate; Blue solid line refers to NLC composed of 60% methyl stearate

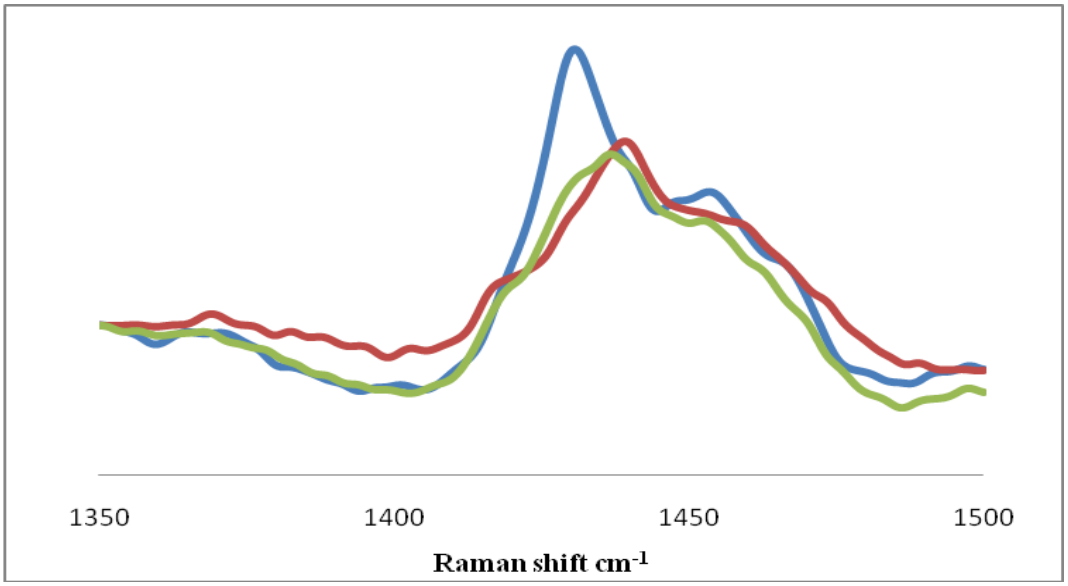

Figure 36 Change of peak shape in NLC with oleic acid. New peaks at 1430 cm^{-1} with a shoulder at higher Raman shift appear. Compared with the spectra of bulk phase oleic acid, this indicates increasing disorder in molecular arrangements. Green solid line refers to NLC with 5% oleic acid; Red solid line refers to NLC with 10% oleic acid; Blue line refers to NLC with 20% oleic acid

Oleic acid, unlike methyl stearate, affects the arrangement of lipid molecules and the distribution of curcumin. The increasing proportion of oleic acid (up to 20%) in the formula leads to disappearance of peak at 1418 cm^{-1}, and the presence of shoulder peak at 1462 cm^{-1} According to the study by Da Silva, Bresson and Rousseau, the peak pattern in matches the description of α and β'. oleic acid induces disorder in molecular arrangement that is favored for curcumin encapsulation. In addition to create less perfect lipid crystals, oleic acid also affected the distribution of curcumin. In lipid nanoparticles composed of 20% oleic acid. A new peak appeared at 1438 cm^{-1} (Figure 36). This peak belongs to curcumin. The presence of this peak in spectra of oleic acid NLC but not in other formula indicates that oleic acid is able to trap curcumin.

PEG does not induce further change of polymorphic forms of lipid crystals: The spectra of PEG NLC remain the same with the increasing usage of PEG. Compared to the results of Da Silva, the major polymorphic form in the NLC should be beta prime.

In the present study, the C=O strectching vibration peaks at 1730 cm^{-1}-1740 cm^{-1} of methyl stearate and monostearin change with different monostearin and mthyl stearate ratio. As shown below (Figure 37 A), C=O stretching for monostearin is represented by peak at 1731 cm^{-1}, and that for methyl stearate is represented by peak at 1740 cm^{-1}. The spectrum of physical mixture shows joint peak of both indicating the two lipids does not interact with each other. When methyl stearate is covered with a layer of monostearin, only a weak peak at no peaks appears 1731 cm^{-1} and 1740 cm^{-1}, whereas only a sharp peak at 1740 cm^{-1} appears when methyl stearate covers monostearin. For methyl stearate NLC, monostearin C=O peak is much more obvious than that methyl stearate even though the intensity of monotearin C=O stretching decreases as methyl stearate usage increases (Figure 37 B,C). The presence of these two peaks suggesting that during crystallization, a majority of methyl stearate is covered with monostearin. The coverage of monostearin decreases as methyl stearate increases.

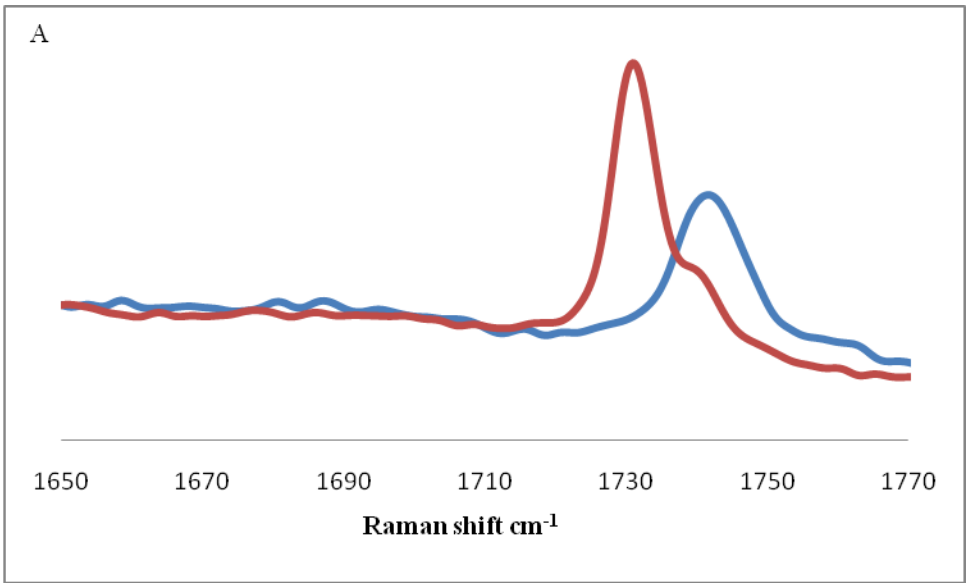
A
1650
1670
1690
1710
1730
1750
1770
Raman shift cm-1

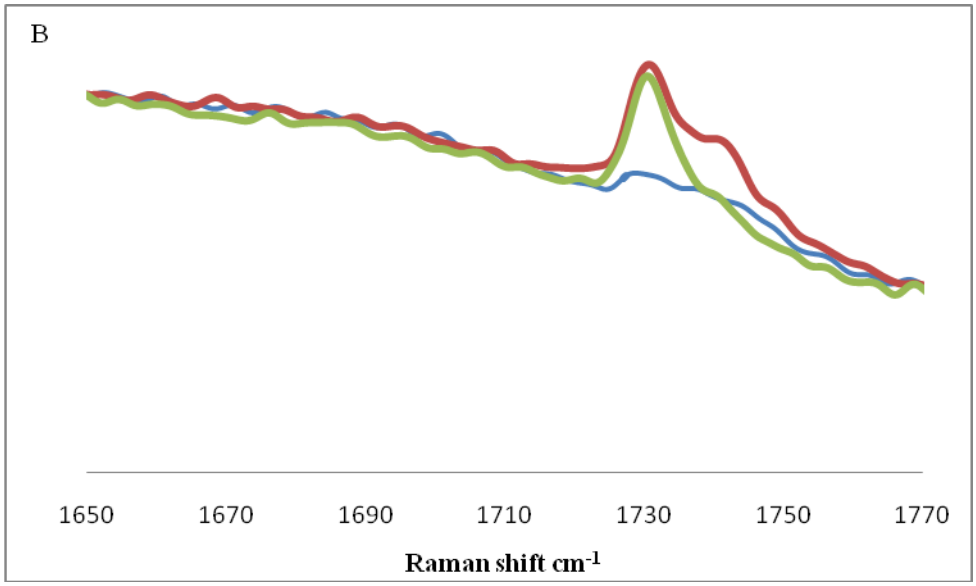
B
1650
1670
1690
1710
1730
1750
1770
Raman shift cm-1

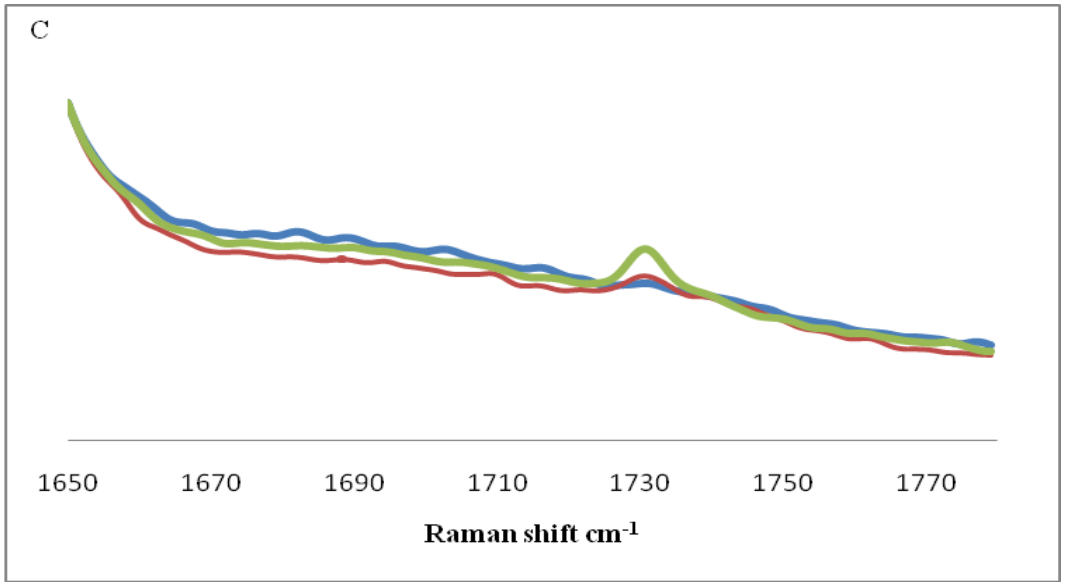

Figure 37 Change in Carbonyl stretching peak. The bulk phase material of monostearin and methyl stearate gave rise to peaks at 1731 cm^{-1} and 1740 cm^{-1} respectively. Both in curcumin loaded NLC and control NLC, the peak for monostearin disappears while no peaks for methyl stearate appear. Figure.37 A: Blue line refers to bulk phase methyl stearate; Red line refers to bulk phase monostearin. Figure.37 B. Green solid line refers to monostearin particles without curcumin; Red solid line refers to NLC with 40% methyl stearate; Blue solid line refers to NLC with 60% methyl stearate.Figure.37 C: Green solid line refers to monostearin particles with curcumin; Red solid line refers to NLC with 40% methyl stearate; Blue solid line refers to NLC with 60% methyl stearate

Alkyl chain conformation: 1300 cm^{-1}-1000 cm^{-1}

Researches within this region focus on several peaks to yield information about alkyl chain conformation. Peak at 1063 cm^{-1} is widely used to present the *all –trans* in alkyl chain while the presence of peaks While broad band at 1080 cm^{-1} -1100 cm^{-1}, is an indicator of gauche forms. Peak at 1295 cm^{-1} can be assign skeletal vibration of $(CH_2)_n$ in-phase twist, it is used as indicator of order of molecule arrangements. In the research by Ho and

Pemberton by when temperature goes up, the peak at 1295cm^{-1} became weak, indicating higher disorder packing pattern.

In the present study, well defined peaks appears at the 1063 cm^{-1}, 1105 cm^{-1} and 1130 cm^{-1} in methyl stearate and PEG added NLC indicating a firm alkyl chain structure.. When loaded with curcumin, the absolute intensity of these peaks decreases slightly, indicating slight higher disorder in alkyl chain region of lipids.

The addition of oleic acid leads to higher degree of disorder. The addition of 5% oleic acid decreases and broadens the peak at 1062 cm^{-1} and 1130 cm^{-1}. The broadening of peaks is more obvious when the proportion of oleic acid is increase to 20%. The increase in chain mobility(Da Silva, Bresson et al. 2009) can leave more space for the encapsulation of foreign molecule.

In addition to increasing chain mobility, oleic acid also competes with Tween20 to interact with curcumin. Curcumin specific peak originally at 1250 cm^{-1} shifts to 1237 cm^{-1} in the presence of Tween20 due to the existence of hydrogen bonding. This peak shifts back to 1247 cm^{-1} in 20% oleic acid NLC. (Figure 38) This shift suggests that oleic acid stays in the imperfection of lipid crystals and separates curcumin from surfactant layer.

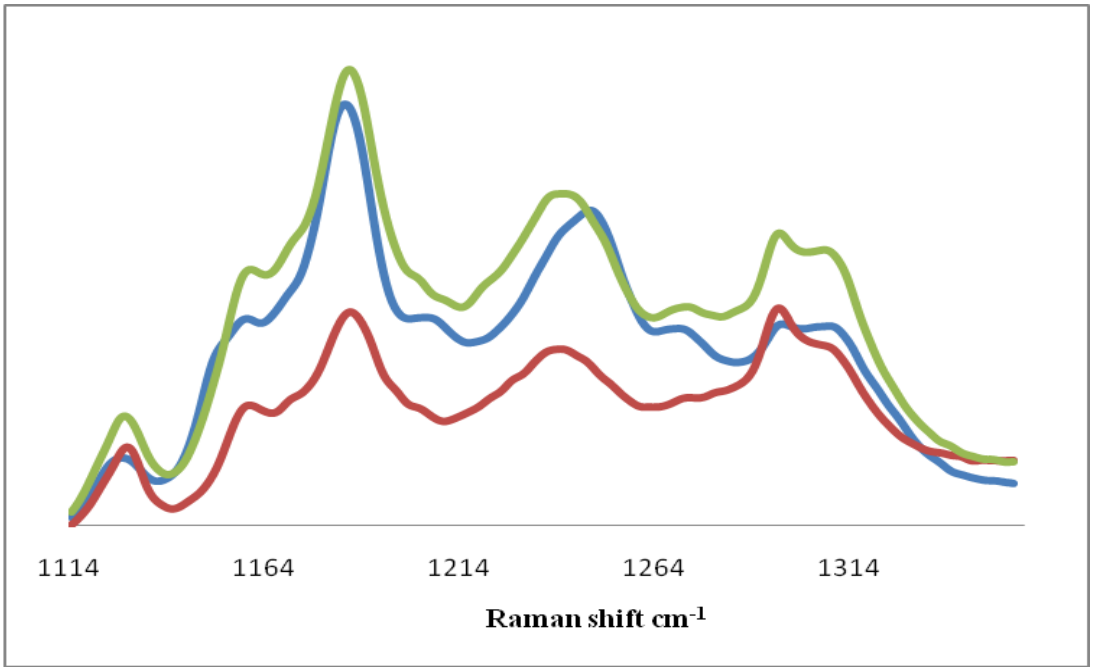

Figure 38 Change of overall spectra with increasing amount of oleic acid. 20% oleic acid (red line) significantly reduces the intensity of 1063 cm^{-1}, 1127 cm^{-1} and 1297cm^{-1}. Green solid line refers to NLC with 5% oleic acid; Red solid line refers to NLC with 10% oleic acid; Blue solid line refers to NLC with 20% oleic acid

Differential scanning calorimetry study

Differential scanning calorimetry measures the difference in energy flow needed to maintain same temperature between sample and reference. The signal measured is voltage initially, then converted to heat flux. Since there is always a difference in heat capacity between sample and reference, the baseline will not be horizontal. This could be calibrated by software by multiplying calibration factor.

With regards to the peaks, only gives rise to first order phase transition while other's like glass transition only gives rise to the change in baseline. In the present study, the presence

of multiple peaks for lipid is due to polymorphism of lipid. There are 3 major polymorphic forms for lipids: α, β and β'. They can be formed by the same kind of lipid due to the different cooling rate, presence of impurity etc. Melting points of same lipid with in different polymorphic forms are different because different molecular arrangement. In the present study, DSC is used to study polymorphic forms of lipid in NLC by recording phase transition temperatures (melting points). Research about lipid polymorphism is of great interest because it is directly related to the ability of lipid crystal to accommodate "foreign" molecule such as curcumin. The structural effects of methyl stearate, oleic acid, PEG and curcumin are explored by analyzing thermograms obtained by DSC. Bulk phase materials are studied to obtained basic thermal properties of materials, then the physical mixture of bulk phase materials according to the formulations of different NLC are analyzed.Finally, control NLC and curcumin loaded NLC are studied. The onset temperatures, melting points, enthalpy changes during phase transition are recorded to elucidate structural effect of each component on NLC.

In this research, average cooling rate is 12℃/min. There are two reasons for choosing this cooling gradient. First, fast cooling rate will force melt lipid crystallize and form alpha crystals. Second, fast cooling rate will lead to smaller particles.

The melting points of lipid nanoparticles when compared to physical mixture with same components are generally lower. One explanation for the reduced melting point is the Kelvin effect(Unruh, Bunjes et al. 1999; Bunjes, Koch et al. 2000), the Kelvin-Thomson equation stated that the change in melting temperature is proportional to the inverse of diameter of particles, the smaller the particle, the larger change in melting point(Han, Li et al. 2008), Due to the small diameter of nanoparticles, the melting point will be dramatically

lowered according to this theory. Besides Kelvin effect, the different melting points can also be attributed to polymorphism of lipid crystals. (Lutton and Jackson 1948; Vereecken, Meeussen et al. 2009). It should be emphasized that in this research, methyl stearate, oleic acid, PEG, monostearin and curcumin have different structure and surface activity. The presence of these components will change the crystallization process when compared to the crystallization process of single pure lipid. Some of these changes are reflected by the endothermic peaks (because of first-order phase transition). Others may by second phase transition that is not revealed in DSC thermograms.

Effect of curcumin

Curcumin is able to form crystals based upon the well defined peaks in X-ray diffraction study (Figure 14). However, in the temperature of study, (from 0℃ to 85℃), It exhibits no thermal event. Encapsulation of curcumin into lipid matrix alters the crystallization process and facilitates the formation of β and β’ crystals.

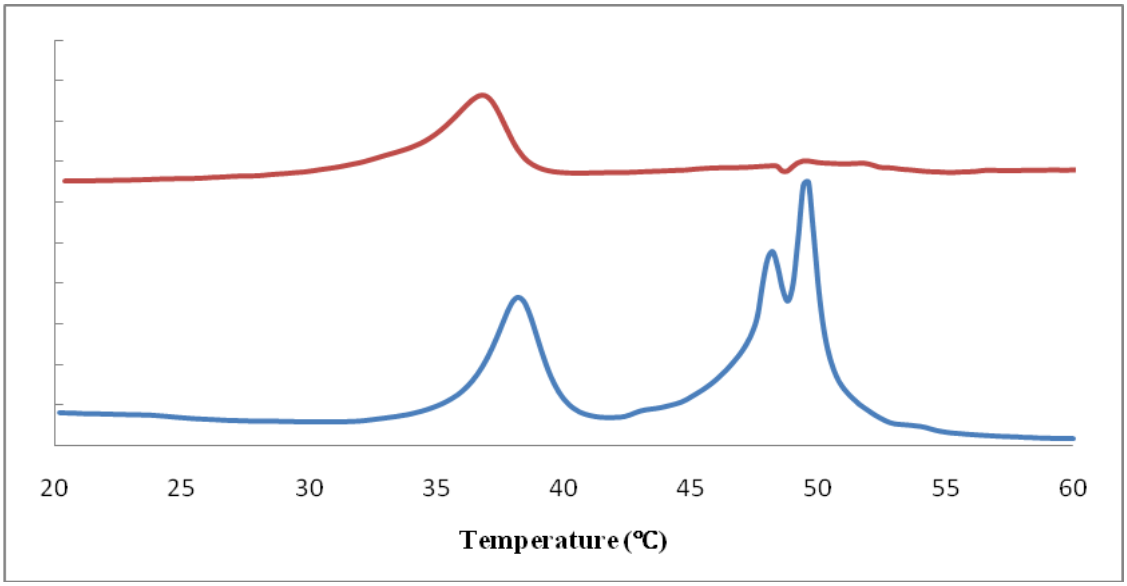

Figure 39 Thermograms of curcumin loaded NLC and control NLC. Red solid line refers to control NLC; Blue solid line refers to curcumin loaded NLC

The above (Figure 39) is one of the typical thermograms of curcumin loaded NLC and control NLC. In control NLC, only a broad band could be observed in the region of 45℃ to 60℃. This broad band appears in all methyl stearate NLCs. Since Raman spectroscope does not detect any chemical change, the presence of this broad band indicates that methyl stearate inhibits the crystallization of monostearin. In another word, majority of monostearin is in amorphous status (discussed in later section). When curcumin is loaded into methyl stearate NLCs, peaks at higher temperature (45℃-50℃) began to appear. Joined peaks of different shape could be observed (Figure 40). The following facts: 1. No chemical reaction take place (Raman spectroscopy has confirmed this) 2.Curcumin does not have thermal event in this region. The presence of joined peaks can only be attributed to the formation of lipid crystals. Nissim Garti suggested that when liquid monoglyceride is cooled down at a certain rate(Nissim Garti 2001), α and transformed into sub-α crystal

structure it was cooled further. Then forms β' as time passing by and finally the most stable form β.(Lutton and Jackson 1948) agreed that for 1-monostearin, the melting point for sub-α is around 49℃, α is at 77℃, β' was at 79℃ and β is at 82℃. Therefore, the endothermic peaks appear around 49℃ in (Figure 40) can be attributed to the formation of sub-α crystals. On the contrary, Methyl stearate endothermic peak at 37℃ does not change with the addition of curcumin. Similar change can be observed in curcumin loaded PEG NLC. For oleic acid NLC, curcumin does not induce crystallization of monostearin when oleic acid is in the range of 5%-10%.

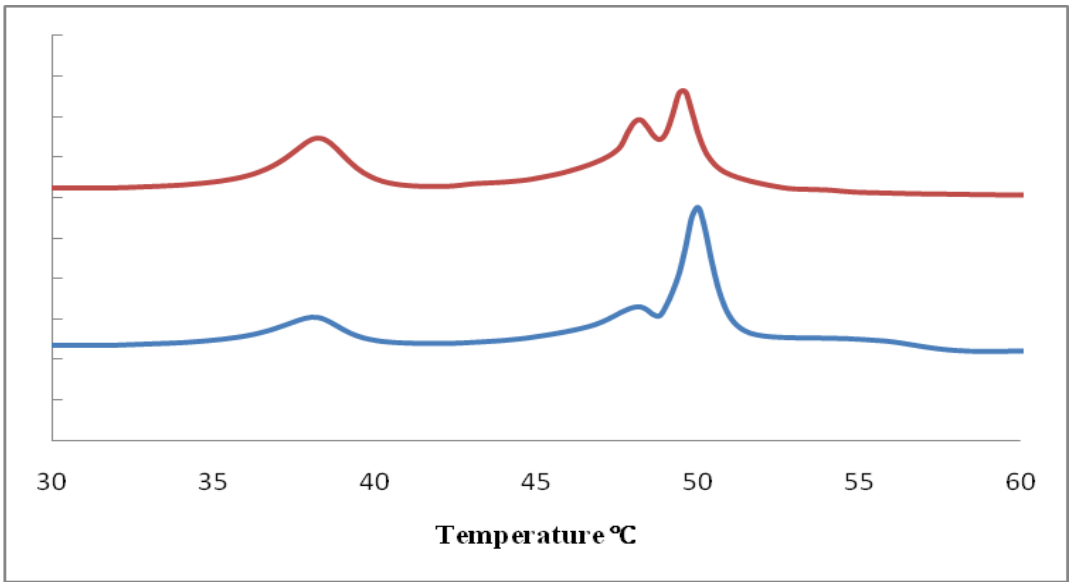

Figure 40 Thermograms of curcumin loaded NLC with different proportion of methyl stearate. Increasing percentage of methyl stearate induces new endothermic peaks at lower temperature and alters the shape of peaks at higher temperature. Blue solid line refers to NLC with 40% methylstearate; Red line refers to NLC with 60% methyl stearate.

Effect of methyl stearate

Addition of methyl stearate is able to suppress crystallization of monostearin and retard polymorphic transformation. In pure monostearin SLN, only one endothermic peak at 71℃ appears. This is due to the presence of β crystals. With addition of methyl stearate, only endothermic peak appears at 37℃, whose presence is due to methyl stearate crystals. A close exam of 50℃ to 60℃ region reveals that a broad band. This is due to partial crystallization of monostearin. In the case of curcumin loaded NLCs, methyl stearate is able to retard polymorphic transformation from α to β. With the increasing proportion of methyl stearate, broad band at 50℃-60℃ completely disappears. This indicates that increasing methyl stearate is able to inhibit the formation of β monostearin crystals. In addition, the peak height of endothermic peak at 47℃ increases with increasing proportion of methyl stearate, suggesting increasing number of sub-α crystals. Area under the endothermic peak at 37℃ also increases as methyl stearate increases. Indicating increasing number of methyl stearate crystals (Figure 40). The endothermic peak at 37℃ also suggests that methyl stearate crystallization is not affect by monostearin, curcumin and Tween 20.

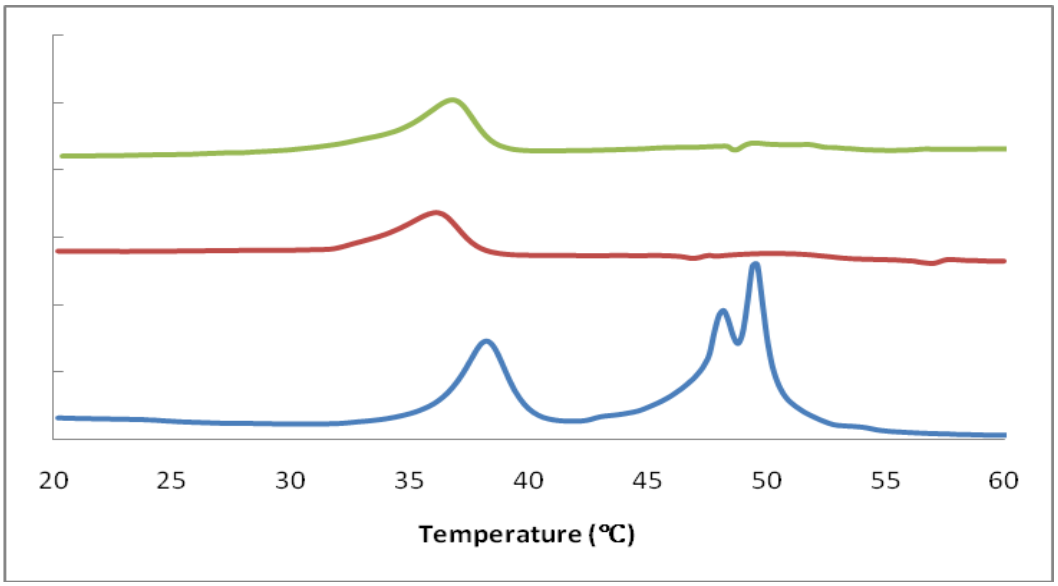

Figure 41 Thermograms of curcumin loaded NLC with different proportion of oleic acid. Note the change in peaks at 45-50℃. Green solid line refers to NLC with 20% oleic acid; Red solid line refers to NLC with 10% oleic acid; Blue solid line refers to NLC without oleic acid

Effect of oleic acid

Oleic acid is able to inhibit the crystallization of monostearin. Thermogram of curcumin 5% of oleic acid in oleic acid NLC shows only one endothermic peak at 37℃ (Figure 41). The disappearance of endothermic peaks at 50℃-70℃ region suggests oleic acid inhibits the formation of sub-α monostearin crystals. Continue increasing oleic acid to 10% oleic acid shows similar result. This could be attributed to several reasons: 1.oleic acid uses in this experiment contain a *cis* double bond (disrupt the Van der Wall force between trans-trans alkyl chain). 2. Oleic acid could partially dissociate in aqueous phase and therefore interacts with polar group of curcumin and blocks curcumin from monostearin. However, 20% of oleic acid leads to strong broad endothermic "band" in the range of 45℃-50℃. This peak can be attributed to type II aggregation due to high oil content.

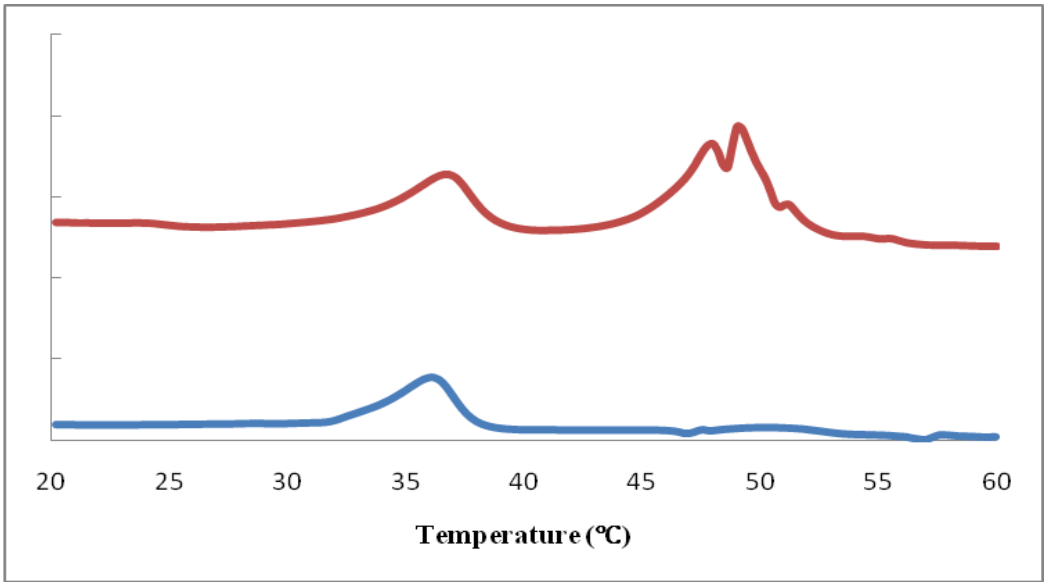

Figure 42 Thermograms of curcumin loaded NLC with different proportion of PEG. PEG and oleic acid are both used as co-solvent. Excessive amount of PEG, lead to crystallization and formation of tight packing pattern. Red solid refers to NLC with 10%PEG; Blue solid line refers to NLC without PEG

Effect of poly ethylene glycol stearate

Polyethylene Glycol Monostearate is added as co-solvent and surfactant. However, it leads to crystallization of monostearin at 55℃-60℃ (Figure 42). In this experiment, the PEG is added and replaces the same weight of methyl stearate. In other word, the proportion of methyl stearate is reduced. In this case, the change can be attributed to the increasing proportion of "monostearin". The long carbon chain of PEG may also cause second type aggregation of small crystals during the crystallization. And this may be account for the broadening of the joined peak. (also see Figure 28).

X-ray diffraction study

X-ray diffraction is an accurate technique to study crystallographic structure of crystal structure. Studying of polymorphic form of lipid by X-ray has been established as a standard method. In the present study, re-crystallized (at cooling rate of 12℃/min) bulk phase material are studied to justify the use of cooling rate of 12℃/min. Diffractogram of and curcumin loaded NLC are taken to studied.

Effect of average cooling rate

It has been reported that fast cooling rate favors the formation of α crystals whereas slow cooling rate results in the formation of β crystals. In this research, α crystals are desired because it leaves more space to accommodate foreign molecules such as curcumin. The cooling rate in most research is chosen as 5-15 minutes per minutes. In the present study, 12℃/min is chosen. To confirm this cooling rate favors the formation of α crystals, bulk phase materials are recrystallized under 12℃/min and diffractograms are taken to study the crystallographic structure.

When bulk phase monostearin is re-crystallized at 12℃/min, only a single strong peak at 4.15 Å appears in diffractogram (Figure 12). According to previous research, characteristic peaks for three major polymorphic forms are summaried in (Table 5). According to this description, monostearin will be in α form under this cooling temperature. When Bulk phase methyl stearate is re-crystallized at 12℃/minutes, it has three peaks at 3.7 Å, 4.0 Å and 4.3Å. According to ICDD, these three peaks indicate the methyl stearate in β form.

Generally, diffractograms of NLC show no curcumin specific peaks, indicating no crystallized curcumin presence in NLCs. Another thing note worthy is the curvature of the baseline. When compared to the flat baseline of well crystallized bulk phase materials, the

baselines of lipid nanoparticles have huge curvature. This also suggests presence of amorphous structure of NLC.

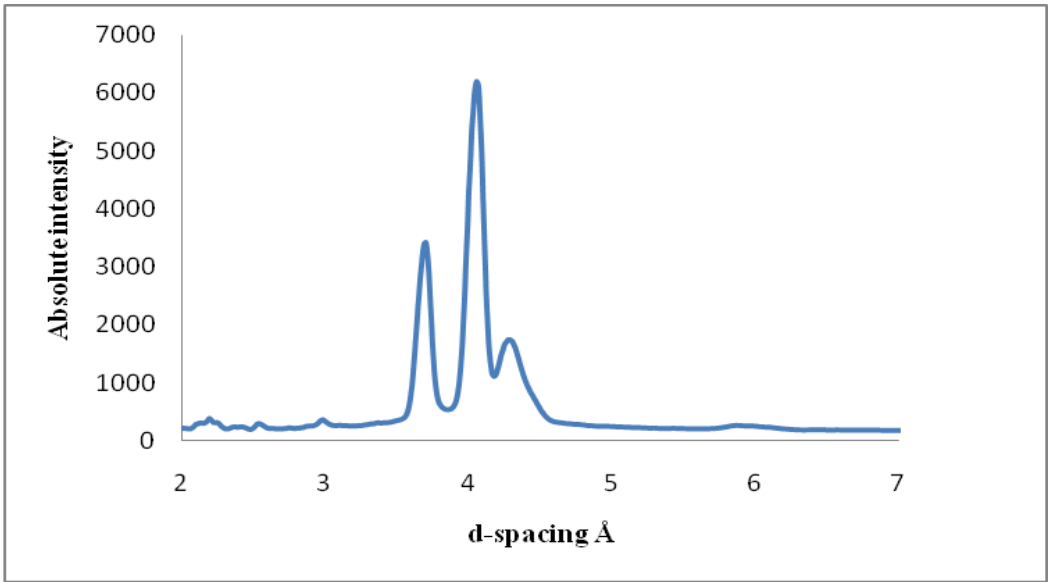

Figure 43 Diffractogram of re-crystallized methyl stearate

Effect of methyl stearate

When mixed with monostearin, peaks remained the same (0.2Å error).Only methyl stearate characteristic peaks appear. No monostearin specific peak is revealed, indicating monostearin arranges in highly disordered manner, while a proportion of methyl stearate formed β crystals. However, the presence of weak peak at 4.45Å suggests the existence of crystallized monostearin (Figure 44). It is reasonable to believe that methyl stearate interferes monostearin crystallization and retard polymorphic transition during storage.

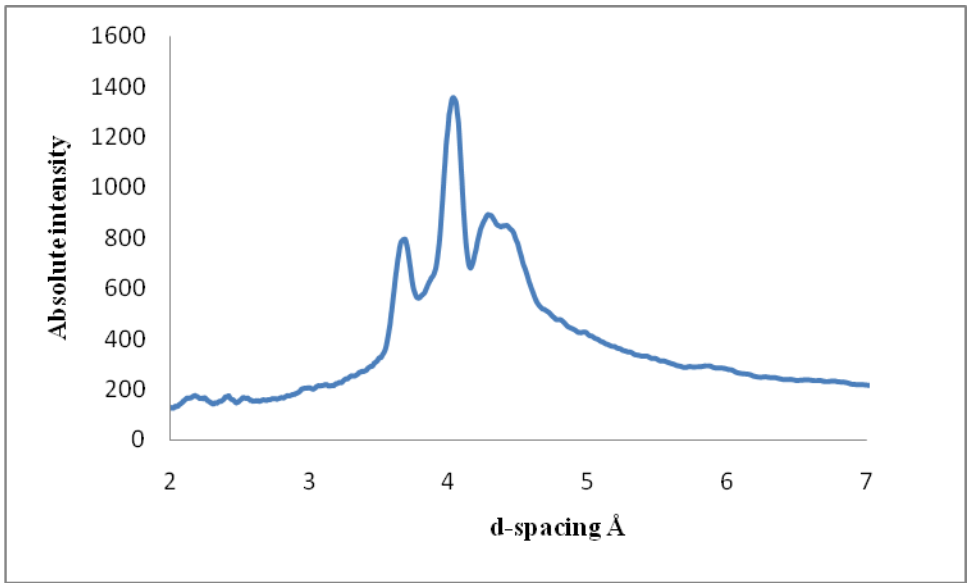

Figure 44 Diffractogram of curcumin loaded NLC composed of 60% methyl stearate

Effect of oleic acid

The addition of oleic acid induces change in diffractogram (Figure 45) when compared to that of methyl stearate NLC (Figure 43). Peak at 4.5Å becomes more obvious in the presence of oleic acid. This may indicate that increasing number of imperfect crystals. It is also possible that a proportion of monostearin is crystallized in β form.

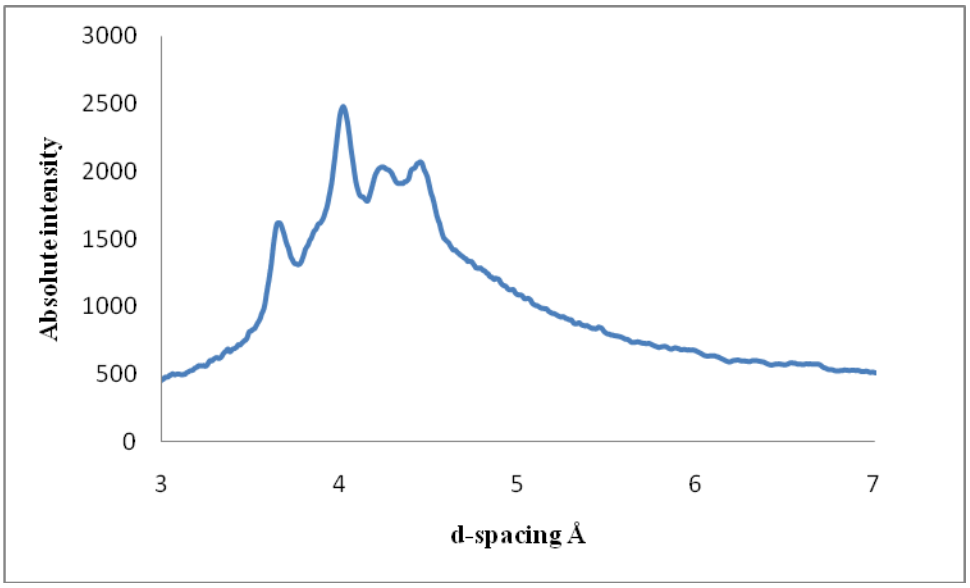

Figure 45 Diffractogram of curcumin loaded NLC composed of 20% oleic acid

Effect of poly ethylene glycol stearate

Re-crystallized PEG has single strong peak at 4.0 Å and two weak peaks at 3.7Å and 4.2Å. These peaks do not over laps with the specific peak of methyl stearate. In diffractogram of PEG NLC, only methyl stearate peaks can be identified. This indicates that PEG does not affect crystallization of monostearin and methyl stearate when used in NLC. It also suggests that PEG is unable to function as crystal habit modifier that inhibits crystallization of methyl stearate.

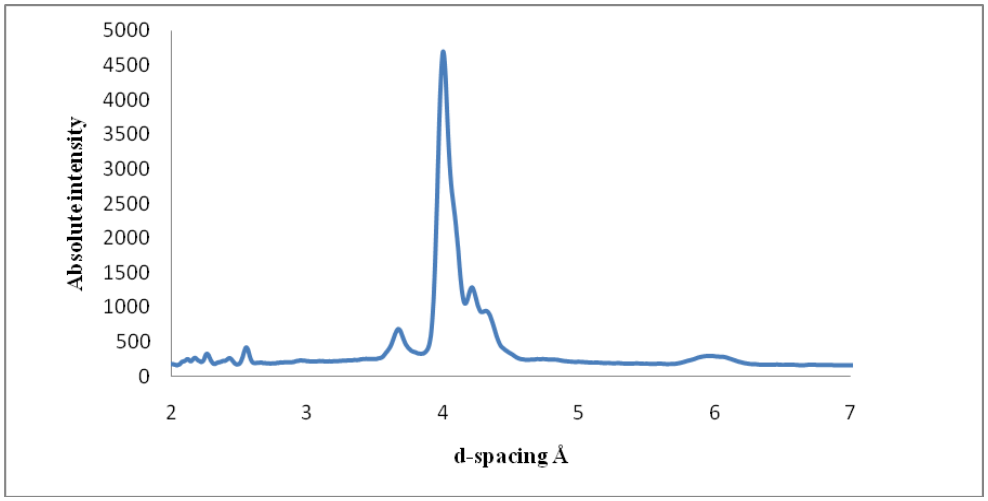

Figure 46 Diffractogram of re-crystallized PEG

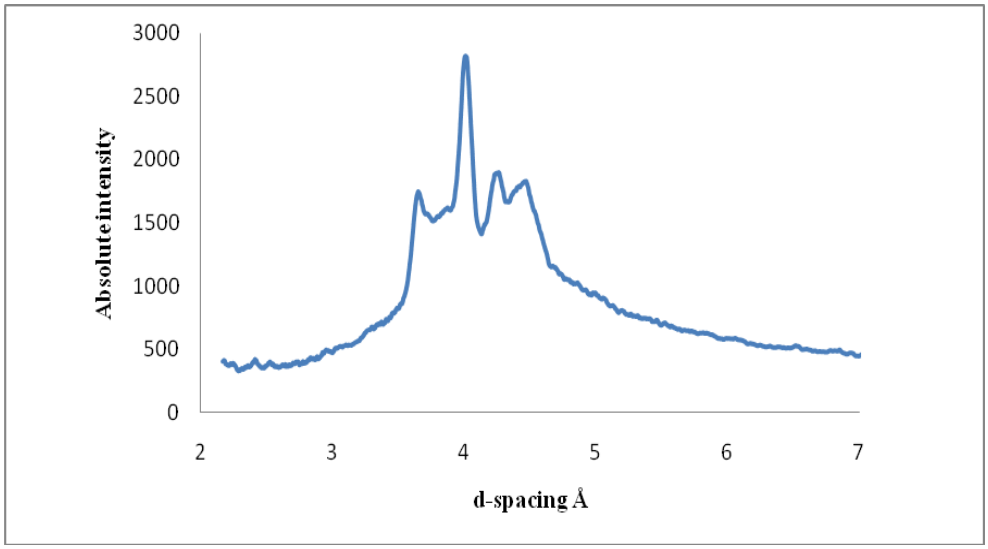

Figure 47 Diffractogram of curcumin loaded NLC composed of 10% PEG

Discussion

The purpose of adding different lipids, according to Muller, is to prevent the formation of perfect lipid crystals during crystallization and storage for improved stability. Based upon the above results, the effect of each component of crystallinity and polymorphic transition is discussed.

Effect methyl stearate on crystallization of monostearin (bulk phase)

Methyl stearate is chosen for it is structure is different from monostearin. In addition, it is non-toxic material that has been used in food industry. Before adding to formulation for NLC, bulk phase mixture experiment is carried out. Differential scanning calorimetry is used to study the effect of methyl stearate on crystallization behavior of lipids mixture. The ratios of methyl stearate and monostearin includes: 1:0, 1:4, 2:3,3:2, 4:1 and 0:1.

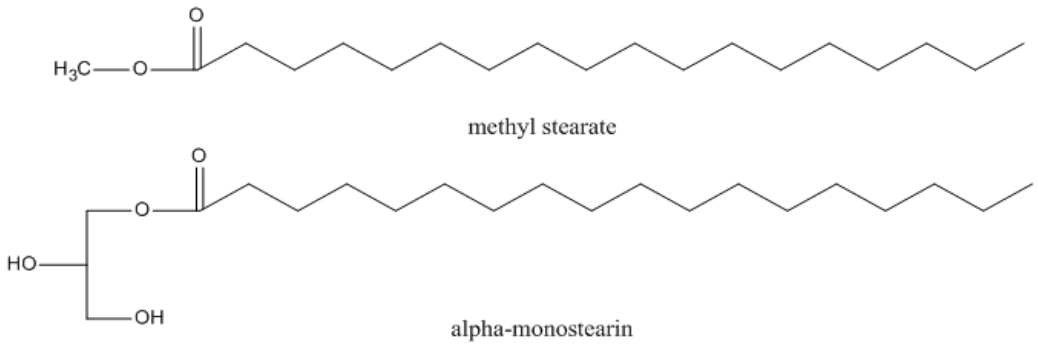

Figure 48 Chemical formulas of methyl stearate and monostearin

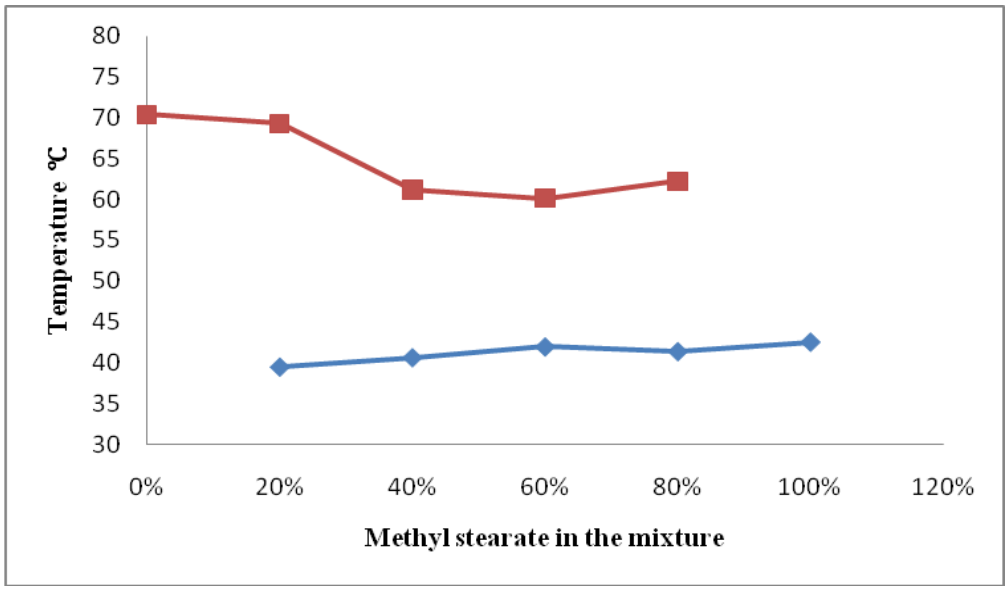

Figure 49 Effect of methyl stearate on the melting behavior of monostearin. Blue solid line refers to melting point of methyl stearate; Red solid line refers to the melting point of monostearin

DSC scans show two endothermic peaks: 39℃ and 50-70℃. Since no literature reported that monostearin crystal possesses a melting point below 45℃, endothermic peak can be attributed to methyl stearate crystals. However, mixture composed of pure methyl stearate shows a melting point of 47℃. It is possible that presence of monostearin disrupts inter-molecular interactions of methyl stearate molecules to some extent. Endothermic peaks at different temperature between 50℃-70℃ appear when ratio between the two components changes. In 1:4 and 4:1 ratio, monostearin endothermic peak appears at 71℃, when the ratio is between 3:2 to 2:3, monostearin endothermic shifts to 50℃ (Figure 49). The shift to lower temperature indicates that methyl stearate is able to suppress polymorphic transition of monostearin or favoring the formation of sub-α monostearin crystal during crystallization. To further confirm the suppressing ability of methyl stearate, the cooling curves of physical mixture are also recorded and studied.

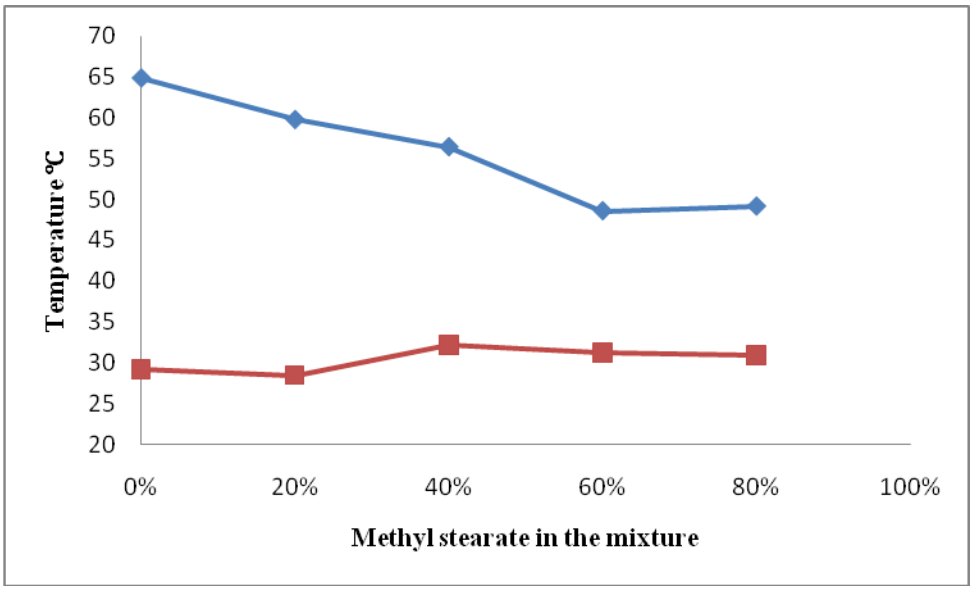

Figure 50 Effect of methyl stearate on the crystallization behavior of monostearin. Blue solid line refers to the melting point of monostearin; Red solid line refers to the melting point of methyl stearate.

The difference in phase transition temperatures (Figure 50) when compared to heating curves (Figure 49) is due to the fast cooling rate. It can be seen that the phase transition temperature (melting/freezing point) of monostearin is reduced by 15℃ as content of methyl stearate increases. Therefore, it is reasonable to believe that methyl stearate is a crystal habit modifier, which inhibits the crystallization of monostearin.

Effect of curcumin

Curcumin is used as model compound to be encapsulated. Even in small amount, (3% to the total mass of lipid) curcumin is capable of introducing polymorphic transition of NLC and change of surface morphology of lipid nanoparticles.

In the present study, the encapsulation of curcumin induces crystallization of monostearin. In methyl stearate NLC, the addition of curcumin leads to endothermic peaks at 40℃-50℃. These peaks are attributed to presence of α monostearin crystal. It is possible that in during the solidification process, a small amount of curcumin near the surface of the oil droplet, acts as catalytic impurity and facilitates the formation of small monostearin crystals. Finally, it will lead to surface heterogeneous nucleation when temperature drops. Since the oil droplet will crystallize from outer shell, a proportion of curcumin will be pushed out as monostearin and methyl crystallize. At the same time, some curcumin will be pushed towards the center, resulting in a “drug enriched core” as Muller proposed in his review. Curcumin stays in amorphous since no curcumin crystal specific peak can be found by X-ray study and DSC. The melting point of methyl stearate does not decrease by the presence curcumin, it is possible that curcumin is not incorporate in the lattice of methyl stearate, or have any effect on the general arrangement of methyl stearate molecules.

In oleic acid NLCs, absolute intensity of curcumin increases as oleic acid. Since intensity of Raman peak is positively correlated to its concentration, it is reasonable to believe that curcumin concentration is higher in oleic acid NLCs. However, in 20% oleic acid NLC, high concentration of curcumin reverses the crystallization inhibitor effect of oleic acid and causes monostearin crystals. In addition, the shift from 1238 cm^{-1} to 1248 cm^{-1} indicates interaction curcumin and Tween 20 is blocked by oleic acid. Therefore, it possible that curcumin stays with oleic acid in oleic acid NLCs. TEM photo suggests that curcumin stays with oleic acid on the surface and leads to small particles join together and form gel like structure.

Effect of methyl stearate

Research results suggest that methyl stearare is 1. Pushed inside the NLC during crystallization; 2. Able to change molecules arrangement of monostearin crystals to less restrict packing pattern such as sub-α and amorphous (Previous research shows that the melting point of sub α monostearin is around 49℃ (not a fixed temperature)

40% to 60% of methyl stearat reduces the amount of monostearin crystals. DSC data of Control NLC shows that no endothermic peak appear in 50℃ to 70℃; In curcumin loaded NLC contains 40% methyl stearate, only sub-α monostearin. For freeze dried methyl stearate NLC, X-ray study only shows methyl stearate specific peaks. It is true that monostearin and methyl stearate specific peaks could overlap to some extent. However, the lack of appearance of monosterain specific peak and huge curvature (compared to bulk phase materials) indicates the existence of amorphous monostearin. In the cooling curve of different mixture, exothermal peak for monosterain shifts to lower temperature from 65℃

to 50℃ when the ratio of methyl stearate and monostearin, this also suggests that the presence of methyl stearate suppress crystallization of monostearin. According to Nissim Garti(Nissim Garti 2001), impurity is able change the crystallization habits, and favors the formation of specific crystal structure in their experiment with stearic acid. In this case, methyl stearate may be the crystallization inhibitor for monostearin.

When hot emulsion is cooled down below melting point of lipid, solidification of oil droplets will occur. Monostearin will begin to solidify from shell to core. In the beginning, monostearin will crystallized in α formed, due to the hydrophobic nature of methyl stearate, it tend to be locked inside the solid shell. Therefore, when monostearin crystallized inside particles, high concentration of impurity will stabilize metastable phase of monostearin for a long time. At the same time, a proportion of methyl stearate, due to high concentration inside the lipid nanoparticles, could form β crystal as shown in XRD study. In addition, spiral growth theory suggests that the presence of impurity like methyl stearate could also create imperfection by occupying the growth site of crystals. it will cause imperfection crystals which can help accommodate curcumin (Muller, Radtke et al. 2002) Nissim pointed out that in some cases, structural resemble molecules could be encapsulate in crystals during crystallization and form amorphous structure. On the other hand, the disappearance of clear peak at 1731cm^{-1} in Raman spectra can be attributed to intermolecular interaction that suppresses C=O stretching. Therefore it is possible that during the crystallization process, intermolecular hydrogen bonding could be formed (Figure 51). The presence of methyl stearate, interrupts the hydrogen bonding and since the methyl group is not a good hydrogen donor, the total force that hold the crystal together will be weakened, and poisons the growth of the particles.

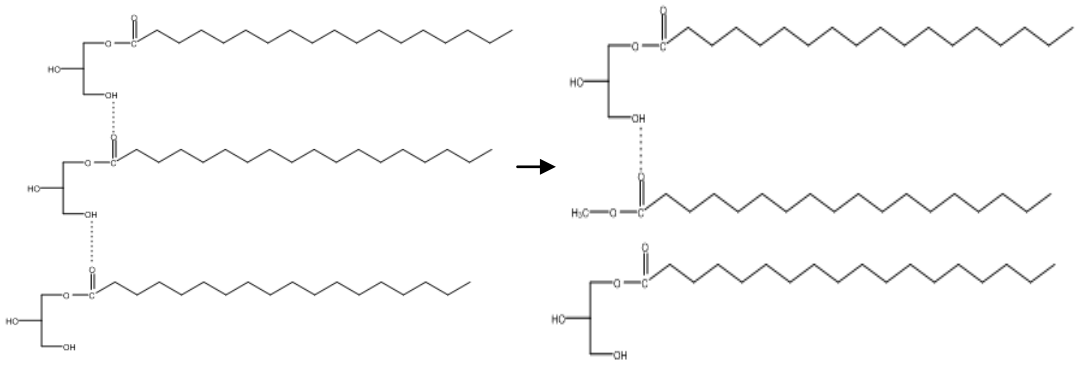

Figure 51 Schematic graph of metyl stearate weakens the interaction between monostearin molecules

In addition to facilitating the formation of amorphous monostearin, the extent of aggregation is reduced in methyl stearate NLC. It is possible that methyl stearate preventing aggregation by retarding polymorphic transition of lipid crystals. The presence of particle aggregation, could be attributed to the sintering effect.

Effect of oleic acid

Thermogram shows the presence of sub α monostearin and β methyl stearate in methyl stearate NLC (Figure 40). The addition of spatial incompatible unsaturated fatty acid should be able to 1. Inhibit crystallization of solid lipids and form amorphous structure; 2. Act as plasticizer and surfactant to stabilize lipid nanoparticles.

Research results suggest that oleic acid has a complex effect on crystallinity and morphology of NLCs. Show by DSC (Figure 41), up to 10% oleic acid inhibits the formation crystallized monostearin even in the presence of curcumin. Since raman spectra shows no oleic acid specific peak. Therefore, it is possible that during solidification process, oleic acid is incorporated into hot emulsion oil droplet, in between monostearin crystals. For methyl stearate, incorporation of oleic acid does not significantly change the

crystallographic structure of methyl stearate. However, it induces slight change in methyl stearate molecular arrangement since peak intensity of different increases disproportionally in oleic acid NLCs. Therefore, it is reasonable to believe that oleic acid is able to disrupt crystallization process of both lipids to different extent.

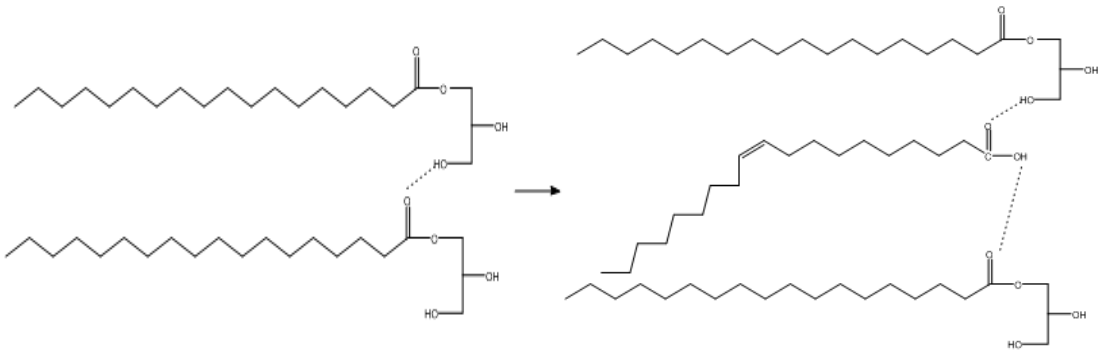

Figure 52 Schematic graph of oleic acid blocks the interaction between monostearin molecules

In addition, Raman spectra of oleic acid NLC shows 1.no specific peaks for oleic acid can be found even when 10% oleic acid presence in the formulation; 2.Peaks in 1000 cm^{-1}-1500 cm^{-1} remain the same but become broader than NLC without oleic acid; 3. Chain mobility is increased with increasing amount of oleic acid. These findings suggest that a proportion of oleic acid in incorporated into the lipid nanoparticles during solidification process.

On the other hand, oleic acid should be in disassociate form at this pH=7.0. Therefore, it is reasonable to believe that small proportion of oleic acid should be arranged at the interface as surfactant and change surface morphology of NLC: Dynamic light scattering shows that for control NLC, increasing in oleic acid narrows down size distribution and decrease particle size. In the presence of curcumin, however, the effect seems complicate. DLS shows the presence of broad size distribution and peaks at several micros.

With 20% oleic acid, TEM study shows that smaller particles around 25-50nm are formed and large aggregation are detected. Raman spectroscopy shows that 20% oleic acid partially blocks the interaction between curcumin and Tween20, and lead to more curcumin on the surface layer (stronger intensity in curcumin specific peaks). Therefore it is possible oleic acid is initially incorporated into the imperfection or "micro leakage" of lipid crystals, and helps to stable the integrity of the particles. With the excessive amount, oleic acid begins to form layer around particles, between Tween 20 and lipid shell, leading to the formation of smaller particles with greater chain mobility. These small particles will then form aggregate and undergone polymorphic transition.

Effect of polyethylene glycol

Polyethylene glycol monostearate is added into the system to further suppress crystallization of monostearin and methyl stearate. However, the encapsulation PEG-SA reverses the effect of oleic acid and favors the crystallization of monostearin. From DSC thermogram, 10% PEG leads to endothermic peak at 55℃, suggesting that tighter packing pattern. X-ray study shows peaks become sharper, suggesting formation of perfect crystals. Therefore, PEG is not crystal inhibitor for lipids in used in this study. As for effect of size, it is possible that PEG reduces aggregation by introducing steric effect.

Conclusion

Nanostructured lipid carriers are fabricated via hot emulsification. Curcumin is successively encapsulated in different NLCs. For curcumin loaded methyl state NLC, 40% methyl stearate retards polymorphic transition of monostearin during storage. In addition, methyl stearate reduces particle sizes by preventing aggregation. Although oleic acid

(5%-20%), does not inhibit crystallization of β methyl state crystals, it leads to increasing number of imperfect methyl stearate crystals. What is more, oleic acid leads to the formation of amorphous monostearin. However, 20% oleic acid leads to formation of gel like pearl net work. Additionally, oleic acid modifies surface of NLC and narrows down particle size distribution. PEG is unable to inhibit crystallization of methyl stearate and monostearin, but it is able to reduces extend of aggregation induced by oleic acid. The best result obtained in this study is 60% methyl stearate with 5% oleic acid. Research with regards to the understanding mechanism of crystallization inhibition effect of methyl stearate and oleic acid to monostearin is still needed to be performed to provide guidance to better control polymorphic transition of lipid nanoparticles, which have profound impact on increasing loading capacity, manipulating release pattern and even improving long term stability of lipid nanoparticles.

References

Anand, P., A. B. Kunnumakkara, et al. (2007). "Bioavailability of Curcumin: Problems and Promises." Molecular Pharmaceutics **4**(6): 807-818.

ANON."Chronic Diseases and Health Promotion." from http://www.cdc.gov/chronicdisease/stats/index.htm.cited on 3/16/2011

ANON. (2010). Functional beverages-US.from "http://academic.mintel.com.proxy.libraries.rutgers.edu/sinatra/oxygen_academic/search_results/show&/display/id=482636/display/id=527020#hit1" cited on 3/16/2011

Attama, A. A. and C. C. Muller-Goymann (2008). "Effect of beeswax modification on the lipid matrix and solid lipid nanoparticle crystallinity." Colloids and Surfaces A: Physicochemical and Engineering Aspects **315**(1-3): 189-195.

Batte, H. D., A. J. Wright, et al. (2007). "Effect of processing conditions on the structure of monostearin-oil-water gels." Food Research International **40**(8): 982-988.

Bengmark, S. (2006). "Curcumin, an atoxic antioxidant and natural NFkappaB, cyclooxygenase-2, lipooxygenase, and inducible nitric oxide synthase inhibitor: a shield against acute and chronic diseases." JPEN J Parenter Enteral Nutr **30**(1): 45-51.

Bresson, S., M. El Marssi, et al. (2006). "Conformational influences of the polymorphic forms on the CO and C-H stretching modes of five saturated monoacid triglycerides studied by Raman spectroscopy at various temperatures." Vibrational Spectroscopy **40**(2): 263-269.

Bresson, S., M. E. Marssi, et al. (2005). "Raman spectroscopy investigation of various saturated monoacid triglycerides." Chemistry and Physics of Lipids **134**(2): 119-129.

Bunjes, H., M. H. J. Koch, et al. (2000). "Effect of Particle Size on Colloidal Solid Triglycerides." Langmuir **16**(12): 5234-5241.

Bunjes, H. and T. Unruh (2007). "Characterization of lipid nanoparticles by differential scanning calorimetry, X-ray and neutron scattering." Advanced Drug Delivery Reviews **59**(6): 379-402.

Bunjes, H., K. Westesen, et al. (1996). "Crystallization tendency and polymorphic transitions in triglyceride nanoparticles." International Journal of Pharmaceutics **129**(1-2): 159-173.

Bunow, M. R. and I. W. Levin (1980). "Molecular conformations of cerebrosides in bilayers determined by Raman spectroscopy." Biophysical Journal **32**(3): 1007-1021.

Casoli, P., A. Vacca, et al. "A numerical procedure for predicting the performance of high pressure homogenizing valves." Simulation Modelling Practice and Theory **18**(2): 125-138.

Chi-Tang Ho, M. M. R., and Geetha Ghai Bioactive Substances: Nutraceuticals and Toxiants. Fennema's Food Chemistry. K. L. P. Srinivasan Damodaran, Owen R.Fennema, CRC.

Corma, A., S. Iborra, et al. (1998). "Catalysts for the Production of Fine Chemicals: Production of Food Emulsifiers, Monoglycerides, by Glycerolysis of Fats with Solid Base Catalysts." Journal of Catalysis **173**(2): 315-321.

Da Silva, E., S. Bresson, et al. (2009). "Characterization of the three major polymorphic forms and liquid state of tristearin by Raman spectroscopy." Chemistry and Physics of Lipids **157**(2): 113-119.

Dunn, R. (2008). "Crystallization Behavior of Fatty Acid Methyl Esters." Journal of the American Oil Chemists' Society **85**(10): 961-972.

Esposito, E., M. Fantin, et al. (2008). "Solid Lipid Nanoparticles as Delivery Systems for Bromocriptine." Pharmaceutical Research **25**(7): 1521-1530.

Freitas, C. and R. H. Muller (1999). "Correlation between long-term stability of solid lipid nanoparticles (SLN(TM)) and crystallinity of the lipid phase." European Journal of Pharmaceutics and Biopharmaceutics **47**(2): 125-132.

Gaber, B. P., P. Yager, et al. (1978). "Interpretation of biomembrane structure by Raman difference spectroscopy. Nature of the endothermic transitions in phosphatidylcholines." Biophysical Journal **21**(2): 161-176.

Gugler, R., M. Leschik, et al. (1975). "Disposition of quercetin in man after single oral and intravenous doses." European Journal of Clinical Pharmacology **9**(2): 229-234.

Hakansson, A., C. Tragadh, et al. (2009). "Dynamic simulation of emulsion formation in a high pressure homogenizer." Chemical Engineering Science **64**(12): 2915-2925.

Han, F., S. Li, et al. (2008). "Effect of surfactants on the formation and characterization of a new type of colloidal drug delivery system: Nanostructured lipid carriers." Colloids and Surfaces A: Physicochemical and Engineering Aspects **315**(1-3): 210-216.

Helgason, T., T. Awad, et al. (2008). "Influence of Polymorphic Transformations on Gelation of Tripalmitin Solid Lipid Nanoparticle Suspensions." Journal of the American Oil Chemists' Society **85**(6): 501-511.

Helgason, T., T. S. Awad, et al. (2009). "Effect of surfactant surface coverage on formation of solid lipid nanoparticles (SLN)." Journal of Colloid and Interface Science **334**(1): 75-81.

Hertog, M. G., E. J. Feskens, et al. (1993). "Dietary antioxidant flavonoids and risk of coronary heart disease: the Zutphen Elderly Study." Lancet **342**(8878): 1007-1011.

Hikosaka, K. N. M. (2001). Crystallization Process of Fats and Lipids System. N. G. K. Sato, Marcel Dekker.

Hu, F.-Q., S.-P. Jiang, et al. (2006). "Preparation and characteristics of monostearin nanostructured lipid carriers." International Journal of Pharmaceutics **314**(1): 83-89.

Huang, C., J. T. Mason, et al. (1983). "Raman spectroscopic study of saturated mixed-chain phosphatidylcholine multilamellar dispersions." Biochemistry **22**(11): 2775-2780.

Hwang, J.-T., J. Ha, et al. (2007). "Apoptotic effect of EGCG in HT-29 colon cancer cells via AMPK signal pathway." Cancer Letters **247**(1): 115-121.

Ishii, T., T. Mori, et al. "Structural characteristics of green tea catechins for formation of protein carbonyl in human serum albumin." Bioorganic & Medicinal Chemistry **18**(14): 4892-4896.

Jain, A., A. Agarwal, et al. "Mannosylated solid lipid nanoparticles as vectors for site-specific delivery of an anti-cancer drug." Journal of Controlled Release **148**(3): 359-367.

Jee, J.-P., S.-J. Lim, et al. (2006). "Stabilization of all-trans retinol by loading lipophilic antioxidants in solid lipid nanoparticles." European Journal of Pharmaceutics and Biopharmaceutics **63**(2): 134-139.

Jenning, V., M. Schaer-Korting, et al. (2000). "Vitamin A-loaded solid lipid nanoparticles for topical use: drug release properties." Journal of Controlled Release **66**(2-3): 115-126.

Jores, K., W. Mehnert, et al. (2004). "Investigations on the structure of solid lipid nanoparticles (SLN) and oil-loaded solid lipid nanoparticles by photon correlation spectroscopy, field-flow fractionation and transmission electron microscopy." Journal of Controlled Release **95**(2): 217-227.

Junyaprasert, V. B., V. Teeranachaideekul, et al. (2009). "Q10-loaded NLC versus nanoemulsions: Stability, rheology and in vitro skin permeation." International Journal of Pharmaceutics **377**(1-2): 207-214.

Kris-Etherton, P. M., K. D. Hecker, et al. (2002). "Bioactive compounds in foods: their role in the prevention of cardiovascular disease and cancer." The American Journal of Medicine **113**(9, Supplement 2): 71-88.

Kushi, L. H., A. R. Folsom, et al. (1996). "Dietary Antioxidant Vitamins and Death from Coronary Heart Disease in Postmenopausal Women." New England Journal of Medicine **334**(18): 1156-1162.

Larsson, K. and R. P. Rand (1973). "Detection of changes in the environment of hydrocarbon chains by raman spectroscopy and its application to lipid-protein systems." Biochimica et Biophysica Acta (BBA) - Lipids and Lipid Metabolism **326**(2): 245-255.

Lee, D.-H., M. Szczepanski, et al. (2008). "Role of Bax in quercetin-induced apoptosis in human prostate cancer cells." Biochemical Pharmacology **75**(12): 2345-2355.

Lee, M.-K., S.-J. Lim, et al. (2007). "Preparation, characterization and in vitro cytotoxicity of paclitaxel-loaded sterically stabilized solid lipid nanoparticles." Biomaterials **28**(12): 2137-2146.

Lim, G. P., T. Chu, et al. (2001). "The curry spice curcumin reduces oxidative damage and amyloid pathology in an Alzheimer transgenic mouse." J Neurosci **21**(21): 8370-7.

Liu, C.-H. and C.-T. Wu "Optimization of nanostructured lipid carriers for lutein delivery." Colloids and Surfaces A: Physicochemical and Engineering Aspects **353**(2-3): 149-156.

Liu, R. H. (2004). "Potential Synergy of Phytochemicals in Cancer Prevention: Mechanism of Action." J. Nutr. **134**(12): 3479S-3485.

Lukowski, G., J. Kasbohm, et al. (2000). "Crystallographic investigation of cetylpalmitate solid lipid nanoparticles." International Journal of Pharmaceutics **196**(2): 201-205.

Lutton, E. S. and F. L. Jackson (1948). "The Polymorphism of 1-Monostearin and 1-Monopalmitin." Journal of the American Chemical Society **70**(7): 2445-2449.

Mandzuka, Z. and Z. Knez (2008). "Influence of temperature and pressure during PGSS(TM) micronization and storage time on degree of crystallinity and crystal

forms of monostearate and tristearate." The Journal of Supercritical Fluids **45**(1): 102-111.

McClements, D. J. and Y. Li "Structured emulsion-based delivery systems: Controlling the digestion and release of lipophilic food components." Advances in Colloid and Interface Science **159**(2): 213-228.

McSweeney, S. L., R. Healy, et al. (2008). "Effect of lecithin and monoglycerides on the heat stability of a model infant formula emulsion." Food Hydrocolloids **22**(5): 888-898.

Mehnert, W. and K. Muller (2001). "Solid lipid nanoparticles: Production, characterization and applications." Advanced Drug Delivery Reviews **47**(2-3): 165-196.

Mendelsohn, R. and D. J. Moore (1998). "Vibrational spectroscopic studies of lipid domains in biomembranes and model systems." Chemistry and Physics of Lipids **96**(1-2): 141-157.

Motterlini, R., R. Foresti, et al. (2000). "Curcumin, an antioxidant and anti-inflammatory agent, induces heme oxygenase-1 and protects endothelial cells against oxidative stress." Free Radic Biol Med **28**(8): 1303-12.

Muller, R. H., K. Mader, et al. (2000). "Solid lipid nanoparticles (SLN) for controlled drug delivery - a review of the state of the art." European Journal of Pharmaceutics and Biopharmaceutics **50**(1): 161-177.

Muller, R. H., K. Maer, et al. (2000). "Solid lipid nanoparticles (SLN) for controlled drug delivery - a review of the state of the art." European Journal of Pharmaceutics and Biopharmaceutics **50**(1): 161-177.

Muller, R. H., R. D. Petersen, et al. (2007). "Nanostructured lipid carriers (NLC) in cosmetic dermal products." Advanced Drug Delivery Reviews **59**(6): 522-530.

Muller, R. H., M. Radtke, et al. (2002). "Solid lipid nanoparticles (SLN) and nanostructured lipid carriers (NLC) in cosmetic and dermatological preparations." Advanced Drug Delivery Reviews **54**(Supplement 1): S131-S155.

Nayak, A. P., W. Tiyaboonchai, et al. "Curcuminoids-loaded lipid nanoparticles: Novel approach towards malaria treatment." Colloids and Surfaces B: Biointerfaces **81**(1): 263-273.

Nissim Garti, K. S., Ed. (2001). Crystallization process in fats and lipid, Marcel Dekkar. Inc.

Olbrich, C. and R. H. Muller (1999). "Enzymatic degradation of SLN--effect of surfactant and surfactant mixtures." International Journal of Pharmaceutics **180**(1): 31-39.

Orendorff, C. J., M. W. Ducey, et al. (2002). "Quantitative Correlation of Raman Spectral Indicators in Determining Conformational Order in Alkyl Chains." The Journal of Physical Chemistry A **106**(30): 6991-6998.

P.Klug, H. and L. E. Alexander (1974). X-Ray Diffraction Procedures For Polycrystalline and Amorphous Materials. New York, John wiley& sons.

Pardeike, J., A. Hommoss, et al. (2009). "Lipid nanoparticles (SLN, NLC) in cosmetic and pharmaceutical dermal products." International Journal of Pharmaceutics **366**(1-2): 170-184.

Paul Knekt, Jorma Kumpulainen, et al. (2002). "Flavonoid intake and risk of chronic diseases." *Am J Clin Nutr 2002;76:560–8.*(*76*): *560-8*.

Price, L. C. and R. W. Buescher (1996). "Decompostion of Turmeric Curcuminoinds as Affected by Light, Solvent And Oxygen." Journal of Food Biochemistry **20**(5): 125-133.

Price, L. C. and R. W. Busecher (1997). "Kinetics of Alkaline Degradation of the Food Pigments Curcumin and Curcuminoids." Journal of Food Science **62**(2): 267-269.

R.Pecora (2000). "Dynamic light scattering measurement of nanometer particles in liquids." Journal of nanoparticle research: 123-131.

Radomska-Soukharev, A. (2007). "Stability of lipid excipients in solid lipid nanoparticles." Advanced Drug Delivery Reviews **59**(6): 411-418.

Reddy, K. S. and M. B. Katan (2004). "Diet, nutrition and the prevention of hypertension and cardiovascular diseases." Public Health Nutrition **7**(1a): 167-186M3 - 10.1079/PHN2003587.

Richard K. Chang and Thomas E.Furtak (1982). Surface Enhanced Raman Scattering, Plenum press.

Ross, J. A. and C. M. Kasum (2002). "DIETARY FLAVONOIDS: Bioavailability, Metabolic Effects, and Safety." Annual Review of Nutrition **22**(1): 19-34.

Sagalowicz, L. and M. E. Leser "Delivery systems for liquid food products." Current Opinion in Colloid & Interface Science **15**(1-2): 61-72.

Sagalowicz, L., M. E. Leser, et al. (2006). "Monoglyceride self-assembly structures as delivery vehicles." Trends in Food Science & Technology **17**(5): 204-214.

Sarmento, B., S. Martins, et al. (2007). "Oral insulin delivery by means of solid lipid nanoparticles." Int J Nanomedicine **2**(4): 743-749

Saupe, A., K. C. Gordon, et al. (2006). "Structural investigations on nanoemulsions, solid lipid nanoparticles and nanostructured lipid carriers by cryo-field emission scanning electron microscopy and Raman spectroscopy." International Journal of Pharmaceutics **314**(1): 56-62.

Scalbert, A., C. Morand, et al. (2002). "Absorption and metabolism of polyphenols in the gut and impact on health." Biomedecine & Pharmacotherapy **56**(6): 276-282.

Shaikh, J., D. D. Ankola, et al. (2009). "Nanoparticle encapsulation improves oral bioavailability of curcumin by at least 9-fold when compared to curcumin administered with piperine as absorption enhancer." European Journal of Pharmaceutical Sciences **37**(3-4): 223-230.

Shegokar, R., K. K. Singh, et al. "Production & stability of stavudine solid lipid nanoparticles--From lab to industrial scale." International Journal of Pharmaceutics **In Press, Corrected Proof**.

Shen, Y., R. L. Powell, et al. (2008). "Interfacial and stability study of microbubbles coated with a monostearin/monopalmitin-rich food emulsifier and PEG40 stearate." Journal of Colloid and Interface Science **321**(1): 186-194.

Shimizu, M., A. Deguchi, et al. (2005). "EGCG inhibits activation of the insulin-like growth factor-1 receptor in human colon cancer cells." Biochemical and Biophysical Research Communications **334**(3): 947-953.

Siebert, K. J., A. Carrasco, et al. (1996). "Formation of Protein-olyphenol Haze in Beverages." Journal of Agricultural and Food Chemistry **44**(8): 1997-2005.

Siekmann, B. and K. Westesen (1994). "Thermoanalysis of the recrystallization process of melt-homogenized glyceride nanoparticles." Colloids and Surfaces B: Biointerfaces **3**(3): 159-175.

Souto, E. B., W. Mehnert, et al. (2006). Polymorphic behaviour of Compritol 888 ATO as bulk lipid and as SLN and NLC. Journal of Microencapsulation, Taylor & Francis Ltd. **23:** 417-433.

Sozer, N. and J. L. Kokini (2009). "Nanotechnology and its applications in the food sector." Trends in Biotechnology **27**(2): 82-89.

Stankovic, I. (2004). Curcumin, "Curcumin," from ftp://ftp.fao.org/es/esn/jecfa/cta/CTA_61_Curcumin.pdf. cited on 3/16/2011.

Steinmetz, K. A. and J. D. Potter (1996). "Vegetables, Fruit, and Cancer Prevention: A Review." Journal of the American Dietetic Association **96**(10): 1027-1039.

Subedi, R. K., K. W. Kang, et al. (2009). "Preparation and characterization of solid lipid nanoparticles loaded with doxorubicin." European Journal of Pharmaceutical Sciences **37**(3-4): 508-513.

Tal-Figiel, B. (2007). "The Formation of Stable W/O, O/W, W/O/W Cosmetic Emulsions in an Ultrasonic Field." Chemical Engineering Research and Design **85**(5): 730-734.

Teeranachaideekul, V., E. B. Souto, et al. (2007). "Cetyl palmitate-based NLC for topical delivery of Coenzyme Q10 - Development, physicochemical characterization and in vitro release studies." European Journal of Pharmaceutics and Biopharmaceutics **67**(1): 141-148.

Tonnesen, H. H. and J. Karlsen (1985). "Studies on curcumin and curcuminoids. V. Alkaline degradation of curcumin." Z Lebensm Unters Forsch **180**(5): 132-4.

Unruh, T., H. Bunjes, et al. (1999). "Observation of Size-Dependent Melting in Lipid Nanoparticles." The Journal of Physical Chemistry B **103**(47): 10373-10377.

Valko, M., C. J. Rhodes, et al. (2006). "Free radicals, metals and antioxidants in oxidative stress-induced cancer." Chemico-Biological Interactions **160**(1): 1-40.

Vereecken, J., W. Meeussen, et al. (2009). "Comparing the crystallization and polymorphic behaviour of saturated and unsaturated monoglycerides." Food Research International **42**(10): 1415-1425.

Walstra, P. (1993). "Principles of emulsion formation." Chemical Engineering Science **48**(2): 333-349.

Weiss, J., E. Decker, et al. (2008). "Solid Lipid Nanoparticles as Delivery Systems for Bioactive Food Components." Food Biophysics **3**(2): 146-154.

Weiss, J., P. Takhistov, et al. (2006). "Functional Materials in Food Nanotechnology." Journal of Food Science **71**(9): R107-R116.

Westesen, K., H. Bunjes, et al. (1997). "Physicochemical characterization of lipid nanoparticles and evaluation of their drug loading capacity and sustained release potential." Journal of Controlled Release **48**(2-3): 223-236.

Willcox, J. K., S. L. Ash, et al. (2004). Antioxidants and Prevention of Chronic Disease. Critical Reviews in Food Science & Nutrition, Taylor & Francis Ltd. **44:** 275-295.

Willett, W. C. (2000). "Diet and Cancer." Oncologist **5**(5): 393-404.

Wissing, S. A., O. Kayser, et al. (2004). "Solid lipid nanoparticles for parenteral drug delivery." Advanced Drug Delivery Reviews **56**(9): 1257-1272.

Xie, S., L. Zhu, et al. "Preparation, characterization and pharmacokinetics of enrofloxacin-loaded solid lipid nanoparticles: Influences of fatty acids." Colloids and Surfaces B: Biointerfaces **83**(2): 382-387.

Ying, X.-Y., D. Cui, et al. "Solid lipid nanoparticles modified with chitosan oligosaccharides for the controlled release of doxorubicin." Carbohydrate Polymers **In Press, Corrected Proof**.

Yuan, H., J. Miao, et al. (2008). "Cellular uptake of solid lipid nanoparticles and cytotoxicity of encapsulated paclitaxel in A549 cancer cells." International Journal of Pharmaceutics **348**(1-2): 137-145.

Zavalij, V. K. P. P. Y. (2008). Fundamentals of Powder Diffraction and Structural Characterization of Materials, Springer.

zur Muhlen, A., C. Schwarz, et al. (1998). "Solid lipid nanoparticles (SLN) for controlled drug delivery - Drug release and release mechanism." European Journal of Pharmaceutics and Biopharmaceutics **45**(2): 149-155.